Alma Mater Studiorum – Università di Bologna

DOTTORATO DI RICERCA IN

SCIENZE BIOCHIMICHE E BIOTECNOLOGICHE

Ciclo XXVI

Settore Concorsuale di afferenza: 05E1

Settore Scientifico disciplinare: B10/10

TITOLO TESI

"MITOCHONDRIAL RESPIRATORY SUPERCOMPLEX ASSOCIATION LIMITS PRODUCTION OF REACTIVE OXYGEN SPECIES FROM COMPLEX I"

Presentata da: **Dott.ssa. Evelina Susana Beatriz Maranzana**

Coordinatore Dottorato   **Relatore**

Prof. Santi Mario Spampinato   **Prof. Carlo Guarnieri**

Abstract

Evidence accumulated in the last ten years has demonstrated that a large proportion of the mitochondrial respiratory chain complexes in a variety of organisms is arranged in supramolecular assemblies called *supercomplexes* or *respirasomes*. Besides conferring a kinetic advantage (substrate channeling) and being required for the assembly and stability of Complex I, indirect considerations support the view that supercomplexes may also prevent excessive formation of reactive oxygen species (ROS) from the respiratory chain.

Following this line of thought we have decided to directly investigate ROS production by Complex I under conditions in which the complex is arranged as a component of the supercomplex I_1III_2 or it is dissociated as an individual enzyme. The study has been addressed both in bovine heart mitochondrial membranes and in reconstituted proteoliposomes composed of complexes I and III in which the supramolecular organization of the respiratory assemblies is impaired by: (i) treatment either of bovine heart mitochondria or liposome-reconstituted supercomplex I-III with dodecyl maltoside; (ii) reconstitution of Complexes I and III at high phospholipids to protein ratio.

The results of this investigation provide experimental evidence that the production of ROS is strongly increased in either model; supporting the view that disruption or prevention of the association between Complex I and Complex III by different means enhances the generation of superoxide from Complex I .

This is the first demonstration that dissociation of the supercomplex I_1III_2 in the mitochondrial membrane is a cause of oxidative stress from Complex I. Previous work in our laboratory demonstrated that lipid peroxidation can dissociate the supramolecular assemblies; thus, here we confirm that preliminary conclusion that primary causes of oxidative stress may perpetuate reactive oxygen species (ROS) generation by a vicious circle involving supercomplex dissociation as a major determinant.

It is easy to foresee the implications of these findings in human diseases and in aging, where oxidative stress plays a major etiologic and pathogenic role.

Contributors and Funding Sources

Contents

Contents

DISCUSSION 135

CONCLUSIONS 141

REFERENCES 144

List of Figures

List of Tables

Abbreviations

BHM   Bovine heart mitochondria

DDM   Dodecyl-β-D-maltoside

ROS   Reactive oxygen species

SDS   Sodium dodecylsulfate

SMP   Submitochondrial particles

R4B   Mitochondrial fraction enriched in Complex I and Complex III

CoQ   Ubiquinone, Coenzyme Q_{10}

Cyt *c*   Cytochrome c

INTRODUCTION

THE MITOCHONDRIAL RESPIRATORY CHAIN

Reducing equivalents (hydrogen atoms) released from mitochondrial oxidations of the tricarboxylic acid cycle, from pyruvate oxidation, fatty acid and amino acid catabolism and other oxidative reactions, are collected by a multi enzyme system, the electron transfer chain or respiratory chain that conveys them to molecular oxygen reducing it to water. The free energy decrease of this electron transfer generates an electrochemical proton gradient ($\Delta\mu_{H+}$) by proton translocation from the mitochondrial matrix, to the space existing between the inner and outer mitochondrial membranes. The proton gradient is then used as a source of energy to synthesize ATP from ADP and Pi by the ATPsynthase complex, or alternatively to drive other energy-linked reactions. The electron transfer chain consists of four major complexes designated as *NADH:ubiquinone oxireductase* (Complex I), *succinate-ubiquinone oxireductase* (Complex II), *ubiquinol- cytochrome c oxireductase* (Complex III) and *cytochrome c oxidase* (Complex IV) and two connecting redox-active molecules, *i.e.* a lipophilic quinone, designated ubiquinone (Coenzyme Q or CoQ) embedded in the membrane lipid bilayer ,and a hydrophilic hemeprotein, cytochrome *c*, localized on the external surface of the inner membrane (Figure 1.1).
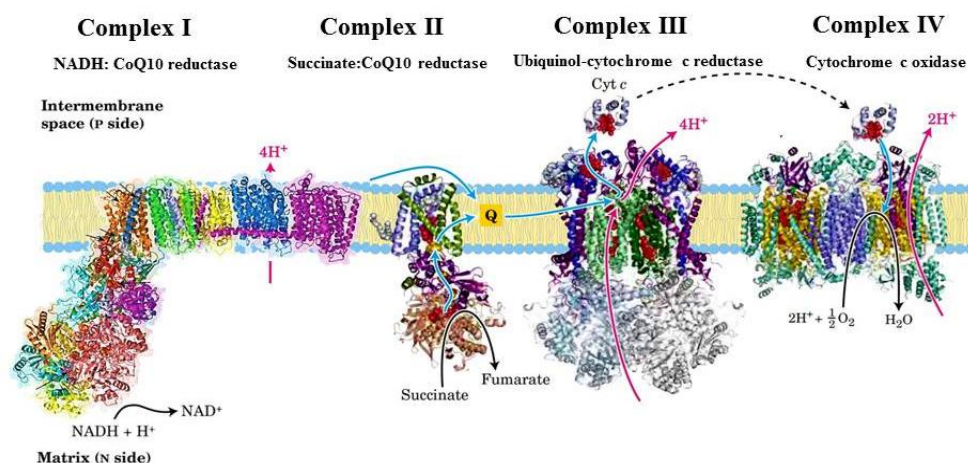
Figure 1.1: The mitochondrial respiratory chain. Textbook description of the respiratory chain. The transmembrane protein complexes of the elec- tron transport chain generate an electrochemical gradient over the mitochondrial inner membrane. NADH is oxidized to NAD$^+$. Electrons are transferred from NADH via Complex I and ubiquinone (Q) to Complex III. From there they pass through the peripheral electron carrier cytochrome *c* and complex IV to the terminal acceptor, molecular oxygen, which is reduced to water. [modified from Lehningher Principles of Biochemistry 5th edition (Nelson, D.L. and Fox, M.M)]

STRUCTURAL ORGANIZATION OF THE RESPIRATORY CHAIN

Since the early 1950s an important part of mitochondrial research has been concerned to elucidate the mechanism and structural organization of electron transport and oxidative phosphorylation. Since then, different models have been suggested for the way in which components of the electron-transfer chain interact to accomplish efficient, energy-conserving electron transfer.

When only the structural aspects of the membrane are considered, two limiting-cases which are loosely termed '*liquid-state*' and '*solid-state*' can be proposed [Rich, 1984. Lenaz, 1988] (Figure 1.2)

(i)   In a *solid-state* model, the components of the respiratory chain are present as supramolecular aggregates, with the respiratory complexes I-IV arranged in an orderly sequence (Chance and Williams, 1956. Schägger and Pfeiffer, 2000).

(ii)   Alternatively, in a *liquid-state* configuration, the respiratory multiprotein complexes, ubiquinone, and cytochrome *c* are randomly distributed in the membrane where they freely move by lateral diffusion. Interactions between respiratory components occur by collisional processes and the electron transport is a diffusion-coupled kinetic process (Hackenbrock et al, 1986).

The main difference between these two models concerns the mechanism of electron transfer: in a liquid random model, the diffusion of ubiquinone and cytochrome *c* between respiratory complexes ensure electron transfer at any effective collision with them, whereas in the solid supramolecular model, all redox reactions take place by direct electron transfer (substrate channeling) within the aggregate framework .

However, these two cases described above are clearly extreme examples and an intermediate organization is feasible. This view postulates that a dynamic equilibrium exists between complete aggregates, partial aggregates, and freely diffusing components of the respiratory chain, all active in electron transfer. The possibility of transitory functional aggregates (dynamic aggregates) among the electron transfer chain components where the efficiency of electron transfer may be increased by formation of specific associations between respiratory components would reconcile the apparently inconsistent empirical evidences between the two extreme models. [Acín-Pérez et al, 2008] (Figure 1.3)
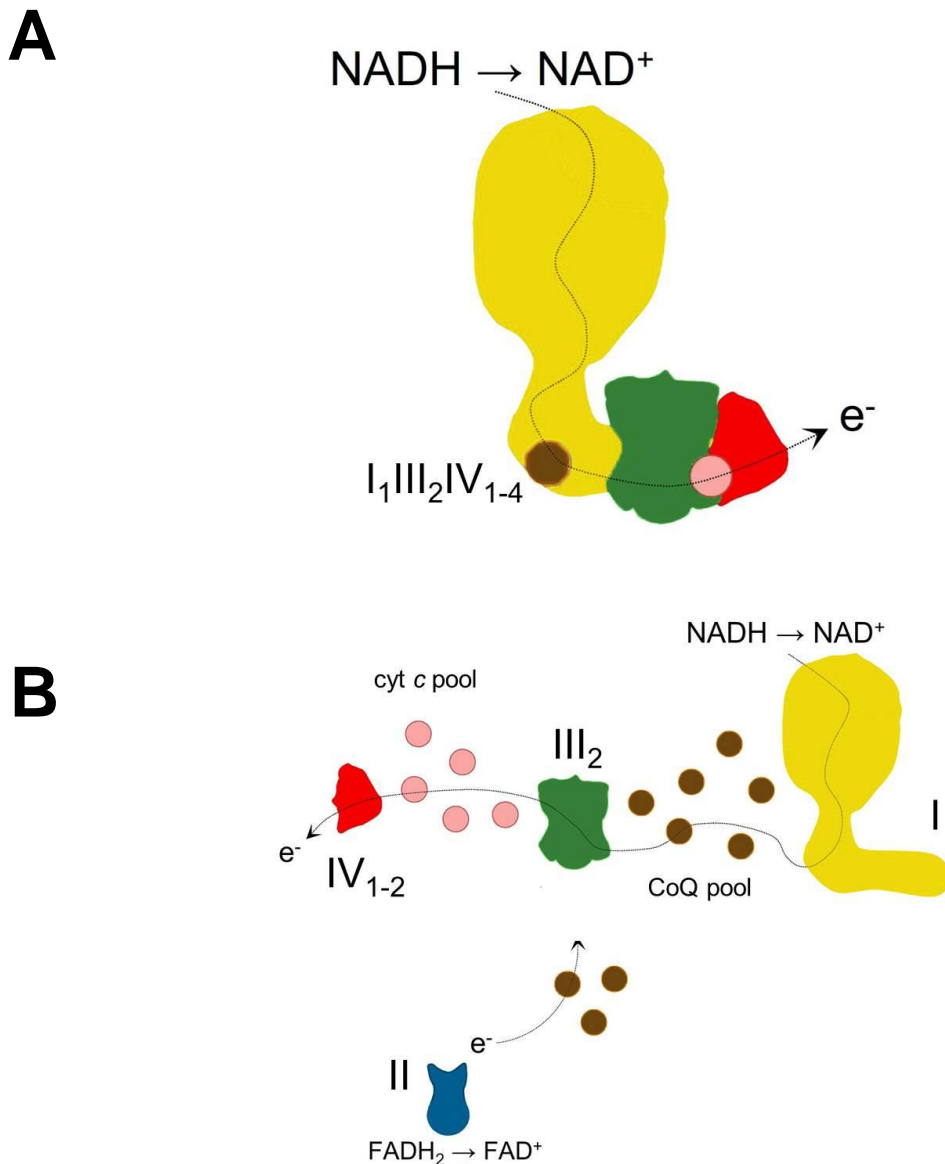
Figure 1.2: Structural Organization of Mitochondrial Respiratory Complexes. A) Solid-model (*Respirasomes*) of the mitochondrial electron transport chain in which complexes I–IV are organized into supramolecular aggregates (respirasomes). The substrate (cyt *c* or CoQ) is channeled directly from one enzyme to the next, within the respiratory complexes assembled into a huge supramolecular energy-converting machine, except for Complex II, which feeds electrons via ubiquinone to Complex III non-bound to Complex I. **B) Liquid-model (*Random collision model*)** all components of the respiratory chain diffuse individually in the membrane, and electron transfer depends on the random, transient encounter of the four individual protein complexes and the two smaller mobile electron carriers, CoQ and cytochrome c; are assumed to diffuse laterally in the membrane as an individual entity and/or as homo-oligomers.

Black arrows show electron pathways. Complex I (I) in yellow. Complex II (II) in blue, dimeric Complex III (III$_2$) in red, Complex IV (IV) in green. The cytochrome *c*; (cyt c) in pink, ubiquinol (Q), in brown. The positions of the matrix (M), the intermembrane space (IMS) and cristae or inner membrane (IM) are indicated.
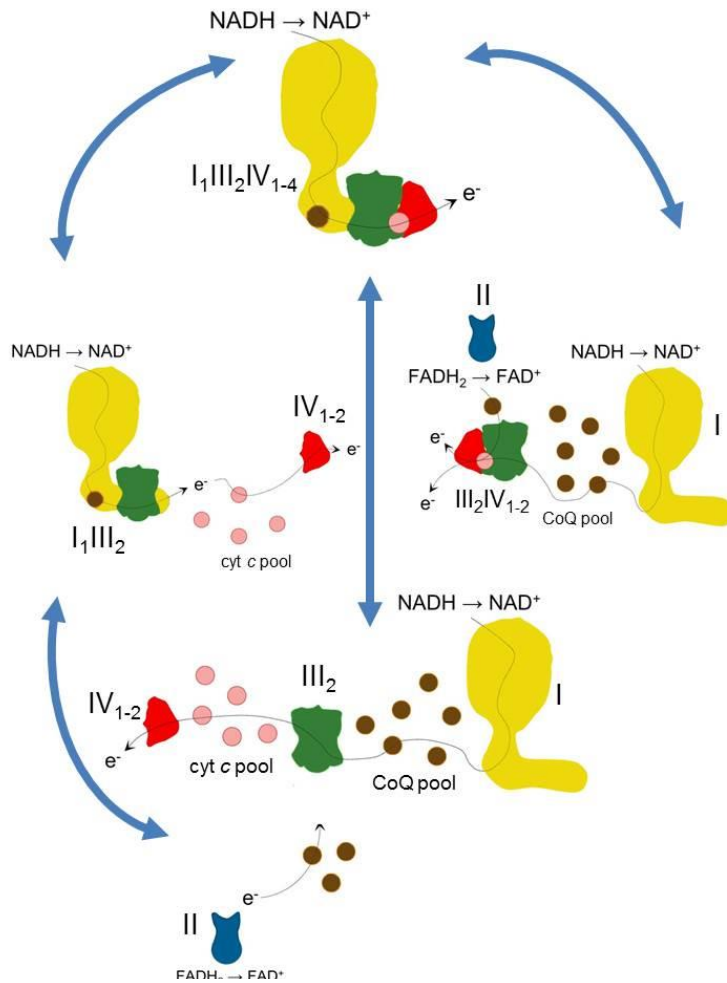
Figure 1.3: Dynamic Organization of Mitochondrial Respiratory Complexes. Plasticity model. The supramolecular organization of the mitochondrial respiratory chain has been proposed to confer kinetic advantages on electron transfer through substrate channeling, to prevent ROS production, and to aid the assembly and stabilization of Complex I. Recently it has been reported a new functional role for the dynamic association/dissociation of mitochondrial respiratory complexes and supercomplexes, which defines dedicated CoQ and cyt c pools in order to organize electron flux to optimize the use of available substrates through the respiratory chain. These dynamic rearrangements range from all-bound to all-free respiratory complexes, and they open the possibility that different modes of organization are switched on/switched off to regulate diverse physiological functions through, i.e., ROS signaling or turnover of respiratory enzymes. $I_1III_2IV_{1-4}$ ers to the respirasomes or supercomplexes formed by the association of one Complex I (I), a homodimer Complex III (III_2), and one to four copies of Complex IV (IV_{1-4}). Intermediate supercomplex species can be found in nature, in combination with free Complex II (II), dimers of Complex III, and Complex IV in different stoichiometries (IV_{1-2}). Complex I requires to be associated in supercomplexes to minimize destabilization and ROS generation.

Solid-state organization

In [Chance and Williams, 1955], a method based on the use of dual-beam, dual-wavelength spectrophotometer in combination with an oxygen electrode for the study of oxidative phosphorylation is published. The redox states of various respiratory-chain components were determined by spectrophotometry, simultaneously with the polarographic measurement of oxygen uptake. This method made possible the first quantitative study of the concentrations and kinetics of electron-transport enzymes not only in intact mitochondria but also in intact cells and tissues allowing depicting the respiratory chain as a solid-state assembly of flavins and cytochromes in a protein matrix.

From these studies, Chance and Williams have also determined the sequence of enzymatic steps in the mitochondrial respiratory chain and hypothesized two alternative mechanisms for electron transfer from one protein carrier to another along the solid-state array [Chance and Williams, 1956] (Figure 1.4).

For the first mechanism, there are restricted rotations in the protein carriers to permit collision of the prosthetic groups. In the second, the molecules are completely fixed, and electrons then must pass through the protein moieties to the prosthetic groups. This intra-protein electron transfer mechanism through the insulating protein medium today is well described as *electron tunnelling* transfer where the maximal distances allowing for physiological electron transfer between the interacting centres should not exceed 13–14 Å [Moser et al, 2005].

Contemporaneously, a comprehensive study of large-scale preparation of beef heart mitochondria was begun in Green's laboratory [Crane et al, 1956]. Mitochondria from beef heart proved to possess a remarkably high degree of stability; they were capable of withstanding preparation procedure involving disruption of the tissue by relatively harsh mechanical means, and subsequent storage of the mitochondria in the frozen state for long periods of time. These preparations thus became the material of choice for future studies that aimed at a resolution and reconstitution of the respiratory chain and the phosphorylating system.

Shortly after the discovery of ubiquinone (coenzyme Q, CoQ) [Crane et al, 1957] and of its participation in electron transfer [Crane et al, 1959. Hatefi *et al*, 1959] the resolution of the four respiratory complexes functionally active: *NADH:ubiquinone reductase* (Complex I) [Hatefi et al, 1961], *succinate:ubiquinone reductase* (Complex II) [Ziegler and Doeg, 1961], *ubiquinol:cytochrome c reductase* (Complex III) [Hatefi et al, 1962a], and *cytochrome c oxidase* (Complex IV) [Fowler et al, 1962] from bovine heart mitochondria was possible.

In 1962 Hatefi *et al* [Hatefi et al, 1962b] succeeded in reconstituting NADH oxidase and succinoxidase by combining complexes I, III, and IV and complexes II, III, and IV, respectively, in the presence of cytochrome *c*. In both cases, the reconstitution required high concentrations of the complexes and resulted in a particulate preparation which did not dissociate upon subsequent dilution.

These results gave rise to the concept that the components of the respiratory chain exist in mitochondria as a fixed assembly ("*elementary particles*") [Ernster and Schatz, 1981]. Indeed, it was found that cytochrome *c* can form stable complexes with complex III and complex IV [Kuboyama et al, 1962] and that mitochondria contain the cytochromes in near stoichiometric amounts. Thus, it was assumed that the respiratory complexes formed a single functional unit in the mitochondria and were present in an orderly sequence which could be disrupted by appropriate reagents [Blair, 1967].

These early ideas concerning the structure of the respiratory chain where the possibility that electron-transport chain might exist as a structural unit (*solid-model*) has been considered also in [Lehninger, 1959] and, in the following years, Chance extended this concept to include direct communication with the ATP-synthesizing machinery [Boyer et al, 1977. Chance, 1977].

A $$O_2 \longrightarrow a_3 \longrightarrow a \longrightarrow c \longrightarrow b \longrightarrow \text{fp} \longrightarrow \text{DPN} \longrightarrow \text{substrate}$$

B
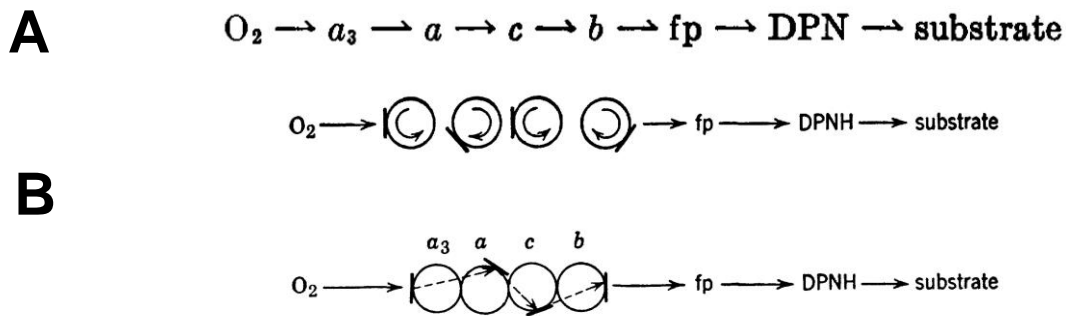
Figure 1.4: Solid-model of Chance and Williams (1955). A) Sequence of respiratory components in solid-array determined spectrophotometrically [Chance and Williams, 1955] **B)** Hypotesized models of electron transfer mechanisms along the chain of fixed electron carriers in the respiratory chain. The first sequence depicts restricted rotations of protein carriers to allow electron collisions with prosthetic groups. The second sequence describes electron transport through proteins moieties towards prosthetic groups (*electron tunneling*). [Chance and Williams, 1956]. a_3, a, c, b: cytochromes a_3, a, c, and b respectively. *fp*: flavoprotein. DPN or DPNH: diphosphopyridine nucleotide (NADH)

Liquid-state organization. Random collision model

On the other hand, on the basis of the isolation of the functional individual respiratory complexes Green and Tzagoloff [Green and Tzagoloff, 1966] postulated that the overall respiratory activity is the result of both intracomplex electron transfer in *solid-state* between redox components having fixed steric relations and, in addition, of intercomplex electron transfer ensured by rapid diffusion of the mobile components acting as co-substrates (*i.e.*, ubiquinone and cytochrome *c*). This proposal was supported by the kinetic analysis of Kröger and Klingenberg [Kröger and Klingenberg, 1973a. Kröger and Klingenberg, 1973b] showing that the ubiquinone behaves kinetically as a homogeneous pool in submitochondrial particles from beef heart.

Over the following years, this model was substantially confirmed by several lines of evidences leading Hackenbrock *et al* to the postulation of the *Random Diffusion Model of Electron Transfer* [Hackenbrock et al, 1986] (reviewed in [Lenaz and Genova, 2007. Lenaz and Genova, 2009a]) (Figure 1.5).

According with this model, the respiratory complexes are randomly distributed in the plane of the membrane, where they freely move by lateral diffusion. Ubiquinone and cytochrome *c* are also mobile electron carriers, whose diffusion rates are faster than those of the respiratory complexes. The electron-transferring reactions between all redox components and their respective redox partners occur via a long-range diffusional process, where their diffusion-coupled collision frequencies may be either higher or lower than any given reaction step within the complexes. Consequently electron transfer is rate limited by the diffusion of ubiquinone and cytochrome *c*.
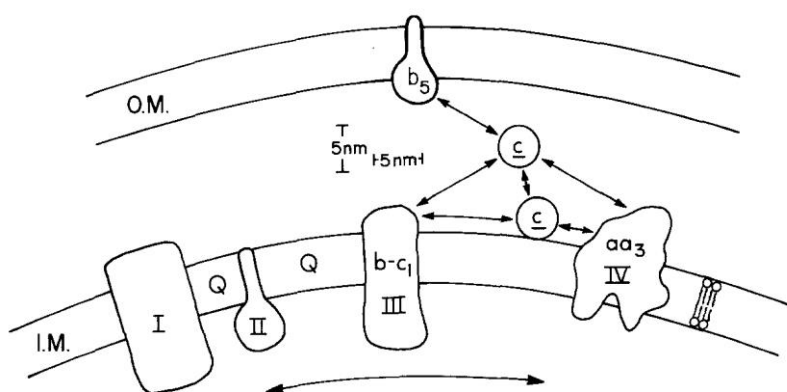
Figure 1.5: Random collision model of Hackenbrock (1986). Structural arrangement of mitochondrial respiratory components [Hackenbrock et al, 1986]. O.M: outer membrane, I.M.: inner membrane, b_5: cytochrome b_5, c: cytochrome *c*, Q: ubiquinone, I, II, III, IV: complexes I, II, III, and IV, respectively

Evidences for supramolecular organization

Structural evidences

Despite the wide acceptance of the *Random Collision Model* during the following twenty years, circumstantial evidences of supramolecular organization of the respiratory complexes come from the pioneering isolation of bovine respiratory complexes where NADH:cytochrome *c* reductase (complex I+III) [Hatefi and Rieske, 1967] and succinate:cytochrome *c* reductase (complex II+III) [Tisdale, 1967] were purified, and interaction between complexes II and III in yeast [Bruel et al, 1996] was demonstrated.

Stable supercomplexes of complexes III and IV were also isolated from some bacteria [Berry and Trumpower, 1985. Sone et al, 1987. Keefe and Maier, 1993. Iwasaki et al, 1995] indicating that such enzymes may be perentially associated in native membrane. Nevertheless, these reports could not challenge the prevalent view and have been overlooked.

The paradigm of how the respiratory chain is structurally organized drastically changed in 2000 when direct evidences for the existence of higher-order stoichiometric assemblies of respiratory complexes came from the development of the *blue-native polyacrylamide gel electrophoresis* (BN-PAGE) by Hermann Schägger and colleagues [Schägger and von Jagow, 1991. Schägger et al, 1994. Schägger, 1995].

Mitochondrial membranes solubilized with very mild non-ionic detergents like digitonin which preserve the respiratory complexes activities as well as protein interactions are used in BN-PAGE. This methodology is able to separate the largest stable and functional protein complexes that can withstand solubilization.

The complex stoichiometric composition is then determined by an orthogonal second dimension BN-PAGE (2D BN/BN-PAGE) with a relatively stronger non-ionic detergent as dodecylmaltoside or Triton X-100, to dissociate supercomplexes, or by the subunit composition with a denaturing second dimension (2D BN/SDS-PAGE). This approach allowed the separation and stoichiometric characterization of high molecular weight supramolecular aggregates of respiratory complexes first in mitochondria of bovine heart and of the yeast *Saccharomyces cerevisiae* [Cruciat et al, 2000. Schägger and Pfeiffer, 2000. Schägger and Pfeiffer, 2001] which remain the best characterized species (Figure 1.6)

The introduction of the BN-PAGE methodology marked the beginning of the study of the higher level of structural organization for the OXPHOS system.

After the first characterizations of supercomplexes by BN-PAGE direct structural insights in the architecture of the supercomplexes were provided more recently by the application of electron microscopy and single particle analysis [Dudkina et al, 2008. Vonck and Schäfer, 2009].

The respiratory supercomplexes are either separated by centrifugation in sucrose density gradients or electroeluted directly from preparative BN-gels, and then imaged by negative stain electron microscopy and subjected to single particle analysis. Several supercomplexes of yeast, plants and mammals have been studied.

Since then, respiratory supercomplexes have been found both in *Bacteria*, *Achaea* and in organisms belonging to different kingdoms of eukaryotes. Despite their phylogenetic distances from each other, all of them have in common that their respiratory chain share similar ultrastructure in their respiratory membranes. At this stage, one could consider that a supramolecular organization of the respiratory chain is an evolutionary-conserved trait for which selective advantages remain to be established [Chaban et al, 2013. Magalon et al, 2012].
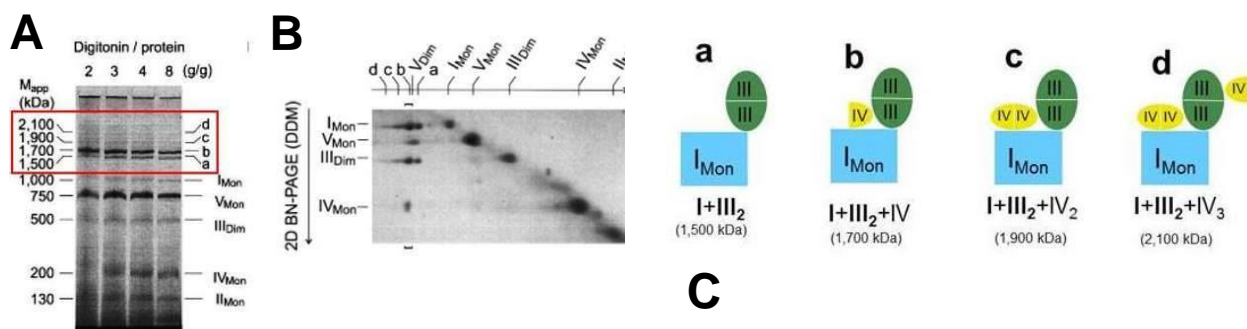
Figure 1.6: Characterization of bovine respiratory chain supercomplexes and dimeric complex V by BN-PAGE. **A)** BN-PAGE of bovine heart mitochondria after solubilization by digitonin. Most Complex I and Complex III was found assembled into two major supercomplexes *a* and *b*, and two minor supercomplexes *c* and *d*. The 200 kDa mass differences indicate the presence of varying copy numbers of monomeric Complex V [Schägger and Pfeiffer; 2000] **B)** Supercomplexes a-d and dimeric ATP synthase (Vdim) from the BN-PAGE were dissociated by 2D BN-PAGE using addition of dodecylmaltoside to the cathode buffer. Direct interaction of complexes I and III was apparent from the dissociation of supercomplex a (I_1III_2) into monomeric Complex I and dimeric Complex III. Superomplexes b-d comprised Complex IV in addition [Schägger and Pfeiffer; 2000]. **C)** Organization of bovine heart mitochondrial respirasomes according to Schägger [Schägger, 2001]. Supercomplexes (a–d) characterized by BN-PAGE; they all contain a complex I monomer, a complex III dimer, and a variable copy number of monomeric complex IV, as indicated by the 200-kDa mass differences. Only 14–16% of total complex I was found in free form in the presence of digitonin.

Functional evidences

When Chance and Williams have proposed their pioneering *solid-state* model to describe the respiratory chain organization, they also hypothesized that electron transfer between the protein components in the solid array occurs along predefined pathways [Chance and Williams, 1956].

Thus, the assumption that respirasome has a major function conferring a more efficient transfer of substrates is an inherent consequence if respiratory components are arranged in a sequentially-ordered supramacromolecular assembly.

Considering the two extreme models, the rate of electron transfer between respiratory components depends on their structural arrangement in the membrane:

For the liquid random model view, if two redox enzymes are connected by a mobile redox carrier undergoing long-range diffusion in the membrane, the overall reaction rate would be governed by the frequency of effective collisions between the mobile carrier and its two redox partners [Gupte et al, 1984. Gupte and Hackenbrock, 1988a. Gupte and Hackenbrock, 1988b]. According with this model, the mobile electron carriers components, ubiquinone and cytochrome *c*, constitute intermediate pools diffusing into the bulk framework of the mitochondrial inner membrane (*substrate pools*), then if diffusion of the quinone and quinol species is much faster than the chemical reactions of CoQ reduction and oxidation, the quinone behaves kinetically as a homogeneous pool (*pool behavior*).

On the other hand, if respiratory components are arranged in a solid-array configuration, the frequency of effective collisions will be determined only by the proximity between the redox components. In the case of the respiratory chain, this means direct transfer of electrons between two active sites of two enzymes that are physically adjacent by successive reduction and oxidation of the intermediate with restricted diffusion into the surrounding milieu (*substrate channeling*) [Ovandi, 1991].

These two models in the case of the organization of the respiratory chain are kinetically distinguishable:

Pool behavior

Kröger and Klingenberg [Kröger and Klingenberg 1973a, 1973b], based on the assumption that quinone behaves as a homogenous pool, postulated that the overall electron flux observed (V_{obs}) between two enzymes will follow a hyperbolic relation with the rate of ubiquinol oxidation (v_{ox}) and the rate of ubiquinone reduction (v_{red}):

$$v_{obs} = \frac{v_{red} \cdot v_{ox}}{v_{red} + v_{ox}}$$

Where CoQ is the mobile electron carrier between a first enzyme reducing ubiquinone and the second oxidizing ubiquinol. They showed this hyperbolic relation in steady-state respiration in bovine submitochondrial particles using either NADH or succinate as electron donors.

Further experimental evidences validated this pool behavior in a variety of mitochondrial systems establishing that CoQ distributes electrons randomly among the dehydrogenases and Complex III, behaving indeed as a freely diffusible intermediate. But most available data concern succinate oxidation (Complex II) in submitochondrial particles, whereas fewer data are available for NADH oxidation (Complex I).

Then, kinetics analysis changing V_{red} or V_{ox} on inhibitor titration curves (*e.g.* titration of Complex III by antimycin) allows to distinguish between CoQ pool behavior (random model) or CoQ channeling (supercomplexes). Pool behavior is kinetically characterized by a convex hyperbolic relationship between the integrated oxidation rate and the inhibitor concentration, whereas a linear relationship is expected by a stoichiometric association (supercomplexes) between the two enzymes.

Direct Transfer of Substrates (Channeling)

Early evidences about substrate channeling in respiratory complexes came from [Ragan and Heron, 1978]. They demonstrated that Complex I-Complex III binary complex is formed in a 1:1 molar ratio after reconstitution of in lipid vesicles. They also showed that this binary complex contains CoQ_{10}, and equimolar quantities of FMN and cytochrome c_1.

This study also described for the first time the stoichiometric behavior for the activity of NADH:cytochrome *c* reductase, ascribable to the formation of a Complex I-Complex IIII supercomplex. In addition, they showed that CoQ-pool behavior could be restored if adding additional amounts of phospholipid and ubiquinone in the concentrated mixture. Under these conditions they demonstrated that Complex I and Complex III activities were independent of each other.

Heron and co-workers [Heron et al, 1978] have also reported that endogenous CoQ_{10} leaks out of the Complex I–III unit when extra phospholipid is present, causing a decrease in activity that could be alleviated by adding more ubiquinone.

A more direct comparison of the effect of channeling with respect to CoQ-pool behavior was performed in a simpler experimental condition in our laboratory.

A system, obtained by reconstitution of a crude mitochondrial fraction (R4B) [Hatefi et al, 1962b] enriched in Complex I and Complex III with different amounts of phospholipids and CoQ_{10} [Lenaz *et al*, 1999] was used to discriminate whether the reconstituted protein fraction behaves as individual enzymes (CoQ-pool behavior) or as assembled supercomplexes depending on the experimental distances between the intramembrane particles.

The comparison of the experimentally determined NADH:cytochrome *c* reductase activity with the values expected by theoretical calculation applying the pool equation showed overlapping results at phospholipid dilutions (w:w) from 1:10 on, *i.e.* for theoretical distances > 50 nm. On the contrary, pool behavior was not effective and the observed rates of NADH:cytochrome *c* reductase activity were higher than the theoretical values [Lenaz et al, 1999. Bianchi et al, 2003. Genova et al, 2008] at a low protein:lipid dilution of 1:1 (w:w), resembling the mean nearest neighbor distance between respiratory complexes in mitochondria [Vanderkooi, 1978].

Flux Control Analysis

The first functional demonstration of the existence of supercomplexes was given by kinetic analysis of the pool function of Coenzyme Q and cytochrome *c* in mitochondria from *Saccharomyces cerevisiae* [Boumans et al, 1998]. The finding that these mitochondria did not follow pool behaviour unless treated with chaotropic agents was considered a peculiarity of this organism, because pool behaviour had been widely accepted after the kinetic studies of [Kröger and Klingenberg, 1973b].

Later on, the existence of functional supercomplexes in mammalian and plant mitochondria were confirmed flux control analysis [Bianchi et al, 2003. Bianchi et al, 2004].

In bovine heart mitochondria, Bianchi *et al* found that both Complex I and Complex III have flux control coefficients approaching 1, suggesting that they behave as a single enzymatic unit, so that electron transfer through Coenzyme Q is accomplished by channelling between the two complexes

In addition, flux control analysis using cyanide inhibition [Bianchi et al, 2004], showed that Complex IV appears to be randomly distributed, or in other words that a large excess of active enzyme exists in free form in the pathway from NADH to oxygen.

Respiratory supercomplexes in eukaryotes

In regards to eukaryotes, the first experimental evidences of supramolecular organization came from the pioneering breakthroughs achieved by Hatefi and his collaborators in the 1960s. Starting from beef heart, mitochondria were isolated and purified in large amounts and subjected to systematic solubilization and fractionation. The devised scheme allowed the isolation of all five complexes from the same batch of mitochondria while at the same time was possible to isolate NADH:cytochrome *c* reductase (complex I+III) and succinate:cytochrome *c* reductase (complex II+III). However, even this evidence for a supramolecular arrangement for respiratory complexes was unseen by the subsequent studies that supported its random distribution in the inner mitochondrial membrane.

Bovine heart mitochondria have been the model for respiratory chain studies from the earliest studies, and they were also the first mammalian source where supercomplexes were detected and characterized by BN-PAGE [Schägger and Pfeiffer, 2000] and later studied by direct structural methods in the 2000's [Schäfer et al, 2006. Schäfer et al, 2007. Althoff et al, 2011 . Dudkina et al, 2011]. (Table 1.1)

The three major complexes involved in proton translocation (complexes I, III, and IV) are found mainly assembled in supercomplexes in fungi, plant as well as mammalian mitochondria [Eubel et al, 2003. Muster et al, 2010].

The evidence for higher associations of other respiratory enzymes is negative or ambiguous. Complex II is mostly found in a free, non-associated form although Acín-Pérez *et al* reported Complex II associated with other respiratory complexes [Acín-Pérez et al, 2008], however this was not supported by any other structural studies [Chaban et al, 2013]. By the other side, complex V (ATP synthase) forms dimers which constitute oligomeric chains in cristae [Arnold et al, 1998. Chaban et al, 2013]. Based on their composition, respiratory supercomplexes can be classified into three main groups which relative abundance varies from organism to organism:

Table 1.1: Supramolecular organization of eukaryotic respiratory complexes (mitochondrial respiratory supercomplexes)

Organism	I_1III_2	III_2IV_{1-2}	$I_1III_2IV_{1-4}$	V_2	References
Protista					
Chlamydomas reinhardtii				B	[Van Lis et al, 2003]
Polytomella sp.	B			B	[Atteia et al, 2003, Dudkina et al, 2005]
Tetrahymena thermophila	B			B	[Balaskaran et al, 2010]
Plasmodium falciparum				B	[Balaskaran et al, 2011]
Fungi					
*Saccharomyces cerevisiae**		B,EM		B	[Arnold et al, 1998 . Schägger and Pfeiffer, 2000]
Podospora anserina	B	B	B	B	[Krause et al, 2004a . Maas et al, 2009]
Neurospora crassa			B	B	[Marques et al, 2007]
Yarrowia lipolytica	B	B	B	B	[Nubel et al, 2009, Davies et al, 2011]
Plantae					
Arabidopsis thaliana	EM			B	[Eubel et al 2003]
Hordeum vulgare	B				[Eubel et al 2003]
Phaseolus vulgare	B				[Eubel et al 2003]
Solanum tuberosum	B	B	B	B	[Eubel et al 2003,Eubel et al 2004]
Spinacia oleracea	B	B	B	B	[Krause et al, 2004b]
Nicotiana sylvestris	B				[Pineau et al, 2005]
Pisum sativum	B				[Taylor et al, 2005]
Helianthus annuus			B		[Sabar et al, 2005]
Zea mays	B,EM			B	[Dudkina et al 2008]
Asparagus officinalis	B	B			[Dudkina et al, 2006]
Arum macalatum	B	B	B	B	[Sunderhaus et al, 2010]
Animalia					
Bos taurus	B,EM		B,EM	B	[Schägger and Pfeiffer, 2000. Althoff et al, 2011]
Homo sapiens	B		B	B	[Schägger et al, 2004, De los Rios Castillo et al, 2011]
Canis lupus familiaris	B		B	B	[Rosca et al, 2008]
Mus musculus	B		B	B	[Acín-Pérez et al, 2004]
Rattus norvegicus	B		B	B	[Dencher et al, 2007]

*In contrast to most eukaryotes, *S.cerevisiae* instead of complex I, it contains three NADH dehydrogenases that are associated with the inner mitochondrial membrane but are not involved in proton translocation. Thus the respiratory chain consists of complexes II, III, and IV. B: found by BN-PAGE or CN-PAGE. EM: identified by electron microscopy

Supercomplex I$_1$III$_2$

Supercomplexes consisting of one copy of Complex I associated with dimeric Complex III (supercomplex I$_1$III$_2$) have been found in mammals and plants [Schägger and Pfeiffer 2001. Eubel et al 2003 and, 2004. Krause 2004a] (Figure 1.7). Based on BN-PAGE, this supercomplex has an estimated molecular mass ~1,500 kDa.

In plants, this is the most abundant supercomplex. Structural characterization by single-particle electron microscopy revealed that III$_2$ is laterally attached to the membrane arm of Complex I in its concave portion [Dudkina et al, 2005a. Dudkina et al, 2005b. Peters et al, 2008; Bultema et al 2009]. In all species studied, the complex III homodimer is associated laterally with the membrane arm of Complex I, but the interaction between the two complexes differs. In the bovine supercomplex, the interaction surface appears to be more extensive and Complex III is attached to the middle of the Complex I membrane arm, whereas in the plant Complex III attaches to the end of the membrane arm.

Supercomplexes III$_2$IV$_{1-2}$

In some organisms, dimeric Complex III was found to associate with one or two copies of Complex IV [Heinemeyer et al, 2007. Bultema et al, 2009. Krause et al, 2004a. Dudkina et al, 2006] (Figure 1.7). The III$_2$+IV$_1$ (~750 kDa) and III$_2$+IV$_2$ (~1,000 kDa) supercomplexes are the most stable in *Saccharomyces cerevisiae*, which in contrast to most eukaryotes, instead of Complex I, in the inner mitochondrial membrane contains three NADH dehydrogenases that are not involved in proton translocation.

Single-particle analysis at 15 Å resolution obtained by electron microscopy with docking of x-ray structures for Complex III and IV allowed to obtain a pseudo atomic model of the 3D structure which revealed that dimeric Complex III is flanked from both sides by monomeric Complexes IV, and that these monomeric complexes IV are attached to dimeric Complex III at two alternate sides with their convex sides facing the Complex III$_2$ [Heinemeyer et al, 2007]. From the recent and more detailed 3D cryo-EM map of the III$_2$+IV$_2$ supercomplex, authors also concluded that the distance between cytochrome *c* binding sites in complexes III and IV is about 6 nm, which supports the proposed channeling of cytochrome *c* between the individual complexes. The purified yeast III$_2$IV$_2$ supercomplex, by the other side, also contained bound cytochrome *c* and catalyzed electron transfer from reduced ubiquinone (QH$_2$) to oxygen [Mileykovskaya et al, 2012].
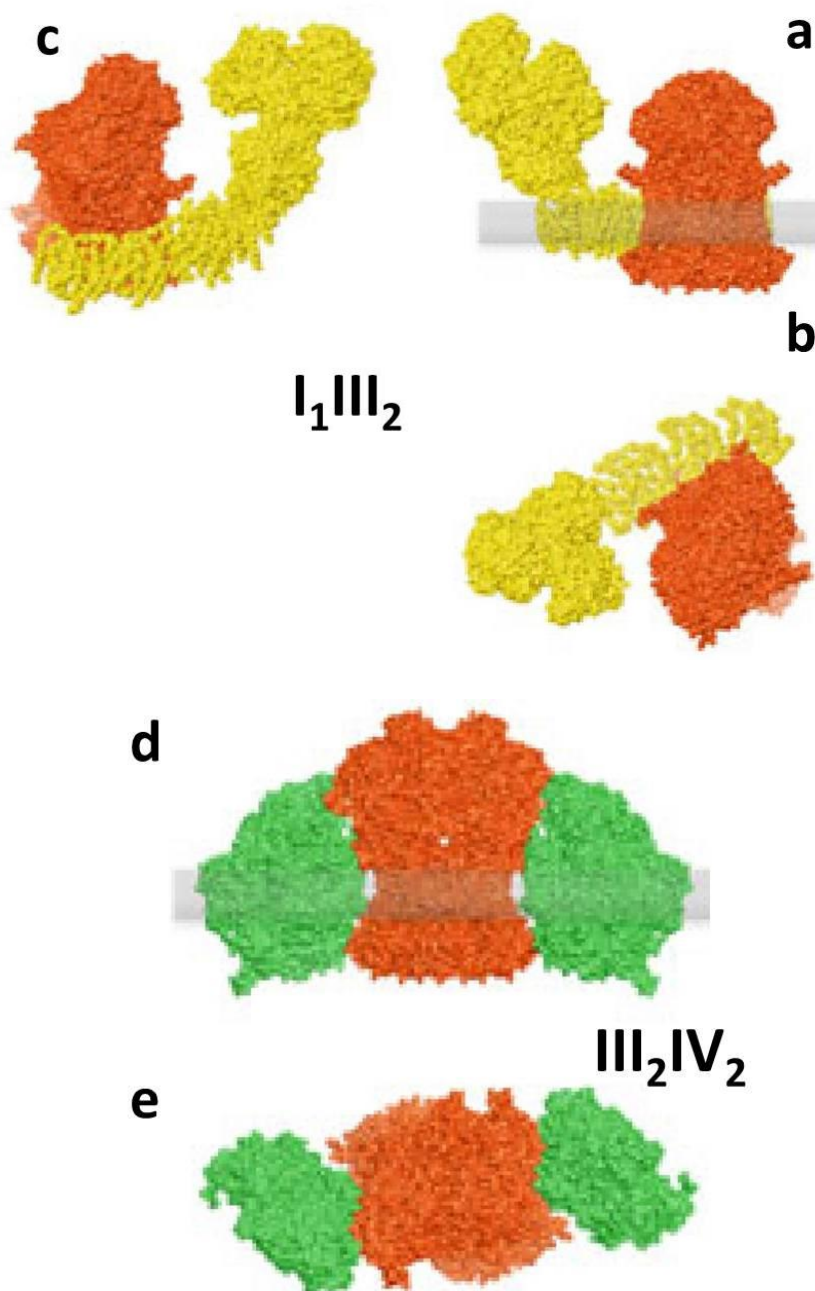
Figure 1.7: Models of respiratory supercomplexes. (a,b) Models for the bovine I_1III_2 supercomplex based on data in [Schäfer *et al* 2006, Schäfer *et al* 2007]. Complex III (red) is attached to the middlde of Complex I (yellow) membrane arm. **(c)** Bovine I_1III_2 supercomplex rotated 40° along the Complex I membrane arm to shows dimeric Complex III attached to the end of the membrane arm, as observed in plant I_1III_2 supercomplexes [Heinemeyer et al, 2007. Bultena et al 2009]. **(d,e)** Model for the yeast III_2IV_2 supercomplex [Heinemeyer et al 2007]. Two copies of Complex IV (green) are attached to dimeric Complex III (red) with the convex face. **(a, d)** The models in the plane of the membrane (grey). **(b, e)** the models as seem from the mitochondrial matrix. The models are built from bovine heart Complex III (pdb code 1BGY) and Complex IV (1IOC) and *Thermus thermophilus* Complex I (3M9S). The figure was made using UCSF Chimera software (University of California, San Francisco)

Supercomplexes $I_1III_2IV_{1-4}$

The terms *respirasome* and *respiratory supercomplex* are synonyms for the largest stoichiometric associations of respiratory chain complexes which contain monomeric Complex I, dimeric Complex III, and up to four copies of Complex IV (Figure 1.8). The $I_1III_2IV_1$ supercomplex is denominated respirasome because it is considered the minimal unit to perform complete respiration from NADH to oxygen. The role of respirasome as functional NADH oxidase was reported by Acín-Pérez *et al* [Acín-Pérez et al, 2008] for a respirasome isolated from mammalian mitochondria.

They demonstrated that mouse repirasomes isolated by elution of protein bands separated by BN-PAGE contained both ubiquinone and cytochrome *c*. These supercomplexes showed complete NADH oxidase activity, as oxygen consumption was measured using a Clark electrode after addition of NADH. This study demonstrated that supercomplexes not only are real entities, but are competent in respiration.

Recently, three-dimensional (3D) density maps of the bovine heart $I+III_2+IV_1$ respirasome (~1,700 kDa) were determined by two different single-particle electron microscopy methods: cryoelectron tomography of digitonin-solubilized respirasomes [Dudkina et al, 2011] and cryoelectron microscopy of amphipol-solubilized respirasomes [Althoff et al, 2011] (Figure 1.9).

Docking of available crystal structures of the individual complexes [Hunte et al, 2010 . Huang et al, 2005 . Solmaz and Hunte, 2008] both 3D density maps generated very similar pseudo-atomic models.

These 3D-structures demonstrated that the Complex III_2 sits in the arc of the membrane arm of Complex I while Complex IV is present adjacent to dimeric Complex III at the distal tip of the membrane arm of Complex I. Additionally, the 3D structure reported by Althoff *et al.* shows distances of 13 nm between ubiquinol-binding sites of complexes I and III, and of 10-11 nm between cytochrome *c* binding sites of complexes III and IV (Figure 1.9). This model indicates the pathways along which ubiquinone and cytochrome *c* can travel to shuttle electrons between their respective protein partners.

Althoff and coworkers in addition reported the presence of significant amounts of bound phospholipids in the purified respirasome and demonstrated that cardiolipin is enriched in the surpercomplex compared with mitochondria total lipids. Moreover, analysis of lipid extracts by HPLC indicated that each respirasome contains at least one molecule of ubiquinol, and immunodetection analysis confirmed the presence of cytochrome *c* [Althoff et al, 2011].

Interestingly, mutual orientation of Complex IV and III in the bovine respirasome differs significantly from their orientation in the structure of the yeast supercomplex III_2IV_2 [Heinemeyer et al, 2007. Mileykovskaya et al, 2012]. These differences between the organization of the bovine and yeast respirasomes might be partly explained by the necessity of Complex III to interact with both Complex I and Complex IV in mammalian mitochondria. Nevertheless, considering the interaction between Complex I and Complex III homodimer there is no spatial restriction in the bovine respirasome for the dimeric Complex III and Complex IV to interact in the same way as in yeast [Chaban et al 2013]. Another possible explanation would be a string-like association between respirasomes via complexes IV [Wittig et al, 2006a].

The abundance of the supercomplexes with different compositions varies from organism to organism. Thus, $I+III_2$ supercomplex is the most abundant in plants [Eubel et al, 2003], III_2+IV_2 supercomplex in fungi [Schägger and Pfeiffer, 2000. Heinemeyer et al, 2007], and $I+III_2+IV_{1-4}$ supercomplex is higher in abundance in mammals [Schägger and Pfeiffer, 2000]
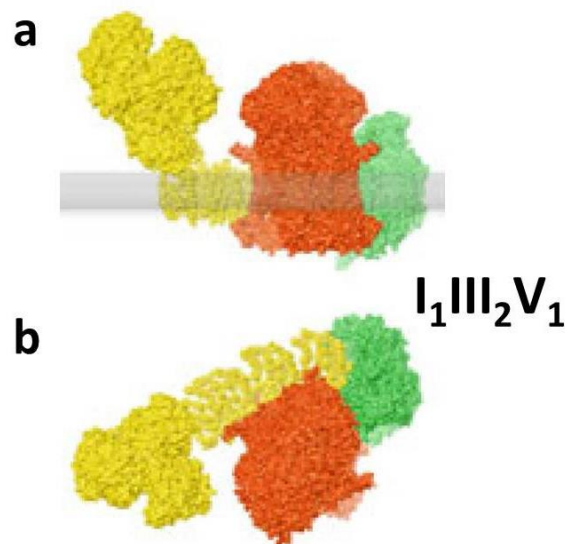
Figure1.8: Model for the bovine $I_1III_2IV_1$ supercomplex (respirasome) [Schäfer et al 2006, 2007]. Complex IV (green) is attached at the ende of the Complex I membrane arm (yellow) via its concave face. **(a)** The model in the plane of the membrane (grey). **(b)** The model as seen from the mitochondrial matrix. The models are built from bovine heart Complex III (pdb code 1BGY) and Complex IV (1IOC) and *Thermus thermophilus* Complex I (3M9S). The figure was made using UCSF Chimera software (University of California, San Francisco)
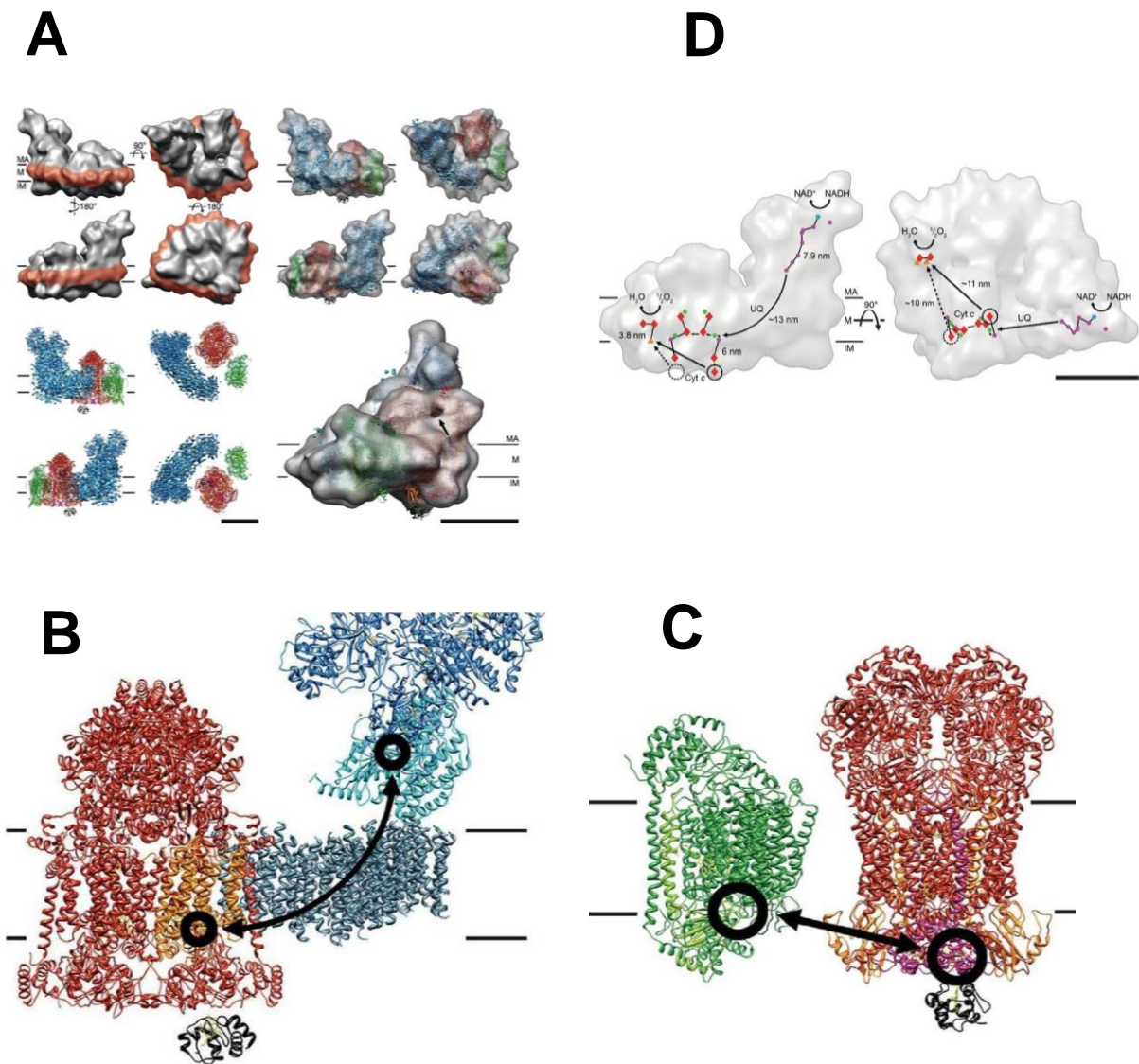
Figure 1.9: Cryo-EM 3D map and fitted X-ray structures of bovine I₁III₂IV₁ supercomplex (respirasome) and Electron transfer pathway **A)**. Cryo-EM 3D at 19 Å resolution [Althoff et al 2011] with docked X-ray structure of Complex I (blue), Complex III (red), Complex IV (green), and cytochrome *c* (black). MA: mitochondrial matrix, M: membrane, IM: intermembrane space. Scale bars 10 nm. **B)** Ubiquinol binding sites are located between the 49 kDa and the PSST subunits near the first Fe-S cluster above the membrane in Complex I and the cytochrome *b* subunit in Complex III (orange). View from the mitochondrial membrane. **C)** Cytochrome *c* binding sites are circled and the shortest cytochrome c trajectories are marked with arrows.Dashed circles mark the unoccupied distal cytochrome c binding site. Side view. **D)** Electron transfer pathways in the respirasome. Outline of the supercomplex with factors active in electron transport marked in blue (FMN), purple (Fe-S clusters), green (quinol), red (hemes), and orange (copper atoms). On the left, view from the membrane.On the right, electron trajectories marked in black. The dashed circle masks the distal cytochrome c binding site, which is unoccupied in the supercomplex. Staight arrow on the left indicate the shortest distances from the cytochrome c binding side on Complex III to the site of cytochrome c oxidation in Complex IV. The shorter, proximal branch may be perred for electron transport. MA: mitochondrial matrix. M: membrane. IM intermembrane space. UQ, ubiquinol. Cyt, c, cytochrome c. Scale bar 10 nm. ,

Respiratory strings

It has been also postulated that the assembly of respiratory complexes into supercomplexes is the first step in the formation of much larger supramolecular structures called *respiratory strings*.

The model of respiratory strings proposed by Wittig *et al* [Wittig et al 2006] envisions a linear aggregate of alternating Complex III homodimers and Complex IV tetramers, with Complex I bound to some of these units. This model takes into account also the occurrence of $I_1III_2IV_4$, III_2IV_4, and IV_4 supercomplexes and the ratio of respiratory complexes I:III:IV that was determined as 1:3:6 in bovine heart mitochondria [Schägger and Pfeiffer 2001]. The existence of these assemblies was demonstrated as the isolation in large pore BN-PAGE of larger assemblies of Complex I, III, and IV in bovine hearth mitochondria with apparent masses of 35 - 45 MDa [Strecker et al 2010]. These higher assemblies are possible to split into individual Complex I, III, and IV under 2D BN/BN-PAGE with dodecylmaltoside, allowing also the identification of tetrameric Complex IV and showing the lack of oligomeric Complex I and Complex III. According these authors, this evidence suggests a specific and ordered association of these complexes as core pieces of respiratory strings and not random aggregates of respiratory supercomplexes (Figure 1.10).

By the other side, Bultema *et al* [Bultema et al, 2009] postulated a model based on a single-particle electron microscopy study of potato mitochondria where among others (I_1III_2, III_2IV_1, $I_1III_2IV_1$) supercomplexes I_2III_2 consisting of two copies of Complex I bound to both sides of a Complex III homodimer were found. In that model the string would have a basic unit of Complex III dimer with a Complex I and Complex IV bound to either side, and the contacts would be formed by Complex IV dimers (Figure 1.10).
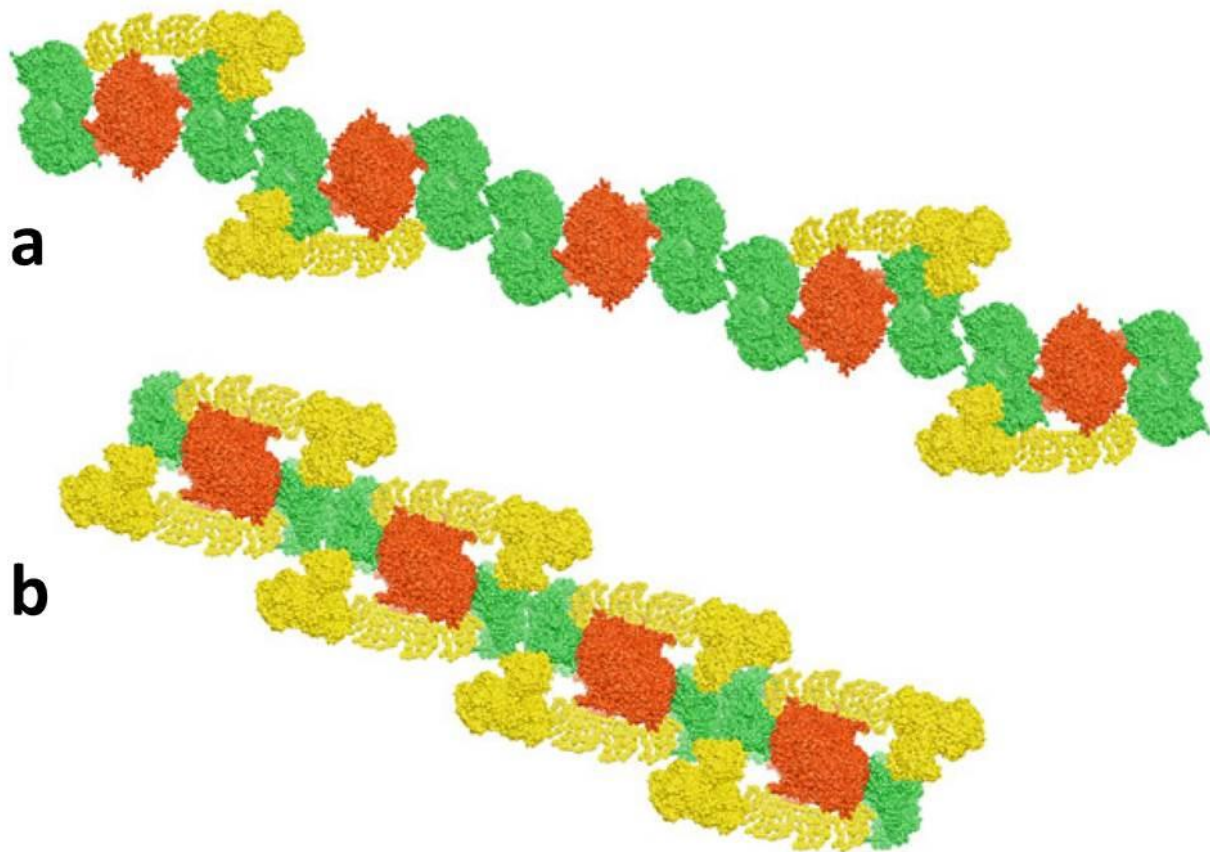
Figure 1.10: Hypothetical models for a higher organization of respiratory chain complexes (respiratory strings). (a) Model for bovine heart mitochondria respiratory string according to [Wittig et al 2006] and built from a linear combination of $I_1III_2IV_4$ and III_2IV_4 supercomplexes, connected via Complex IV tetramers. **(b)** Model for potato mitochondrial respiratory string based on Bultema *et al* 2009 which consists of $I_2III_2IV_2$ supercomplexes, connected via Complex IV dimers. Complex I (yellow), Complex III (red), Complex IV (green). The models are built from bovine heart Complex III (pdb code 1BGY) and Complex IV (1IOC) and *Thermus thermophilus* Complex I (3M9S). The figure was made using UCSF Chimera software (University of California, San Francisco)

Respiratory supercomplexes in prokaryotes

The organization of the respiratory chain in many prokaryotes is very complex. Respiratory flexibility in both electron input and output can be found at its most extreme, leading to a branched character of their respiratory chains.

Prokaryotes contain alternative terminal oxidases that, besides oxygen, enable them to use multiple alternative electron acceptors. This metabolic characteristic allow these microorganisms to colonize multiple and very diverse environments adapting their oxidative phosphorylation efficiency upon environmental changing conditions [Richardson 2000].

In regards to the exceptional diversity in respiratory complexes in *Archeae* or *Bacteria*, supramolecular organization of respiratory complexes has been reported covering only a part of their respective existing phyla in a yet restricted number of prokaryotes (Table 1.2). Interestingly, most of the reported supercomplexes of the aerobic respiratory chain in prokaryotes include the highly conserved complexes III and IV. A supramolecular organization of complexes III and IV has also been shown in eukaryotic mitochondria. Hence, ubiquinol:oxygen oxidoreductase supercomplexes were detected in all branches of the tree of life supporting the idea that this highly organized state is a general feature of living organisms [Magalon et al, 2012].

Table 1.2: Supramolecular organization of prokaryotic respiratory complexes (Aerobic respiratory supercomplexes)

Organism	Quinol:O_2 OR					NADH:O_2 OR	H$_2$S:O_2 OR	Fe(II):O_2 OR	References
	bc_1-aa_3	bcc-aa_3	bc_1-ba_3	bc_1-$cbb3$	ACIII-cbb_3	CI-bc_1-aa_3	SQR-bc_1-ba_3	cyc_2-cyc_1-RcY-aa_3	
Archaea									
Sulfolobus sp.	X								[Iwasaki et al, 1995]
Bacteria (Gram-positive)									
Mycobacterium smegmatis		X							[Megehee et al, 2006]
Corynebacterium glutamicum		X							[Niebisch and Bott, 2003]
Bacillus sp. PS3	X								[Sone et al 1987]
Bacillus subtilis		B Bc-caa3 supercomplexes							[Garcia Montes de Oca et al, 2012. Souza et al, 2013a]
Bacteria (Gram-negative)									
Aquifex aeolicus	B		B				B		[Guiral et al, 2009. Gao et al, 2012. Prunetti et al, 2010]
Paracoccus denitrificans	X					B			[Berry and Trumpower, 1985. Stroh et al, 2004]
Bradyrhizobium japonicum				X					[Keefe and Maier, 1993]
Rhodothermus marinus					B				[Refojo et al, 2010a. Refojo et al, 2010b]
Acidithiobacillus ferroxidans								B	[Castelle et al, 2008]
Escherichia coli		B Formate-oxygen oxidoreductase							[Souza et al, 2012. Souza et al, 2013b]

The enzymatic composition and overall activity of each supercomplex are indicated as well as in which microorganism it has been isolated. Small italic letters refer to the cytochromes, CI for the NADH dehydrogenase, ACIII for alternative complex III, SQR for sulfide quinone reductase, HYD for hydrogenase, SR for sulfur reductase. OR refers to oxidoreductase activity of the different supercomplex

Factors that affect supramolecular associations

In the last years, research efforts have been also placed into the search for factors responsible for gluing together the respirasome components. These aspects were extensively analyzed in a previous reviews (Lenaz and Genova, 2007; Chaban 2013) and will be briefly summarized in the following section.

Lipid content

The role of non-bilayer-forming phospholipids, cardiolipin and phosphatidylethanolamine in the formation and stability of supercomplexes is generally accepted.

These phospholipids have a relative small head group and a bulky fatty acid moiety, which results in a conical shape of the phospholipid molecule. This structural characteristic is responsible for their tendency to form hexagonal-phase structures and thus to increase the tension within a bilayer, which is important for the function of membrane proteins [Osman et al 2011].

Cardiolipin (1,3-bis(*sn*-3'-phosphatidyl)-*sn*-glycerol), an anionic phospholipid, is uniquely found in energy-transducing membranes, as the mitochondrial inner membrane. A decrease in cardiolipin content Niebisch and Bott 2003s found to be associated with decreased membrane potential, ATP synthesis, and overall mitochondrial dysfunction [Santiago et al 1973].

Phosphatidylethanolamine, by the other side, is the most abundant non-bilayer-forming phospholipid in the mitochondrial inner membrane [Bednarz-Prashad and Mize, 1978. Böttinger et al 2012]; it also binds to respiratory chain complexes [Shinzawa-Itho et al 2007. Palsdottir and Hunte, 2004], and *in vivo* data indicate an important role of this phospholipid for mitochondrial functions [Birner et al 2001. Kuroda et al 2011. Joshi et al 2012].

Cardiolipin and phosphatidylethanolamine were shown to bind to the cytochrome bc_1 complex and cytochrome c oxidase, likely including the interface of both complexes [Shinzawa-Itho et al 2007. Palsdottir and Hunte 2004 .Wenz et al 2009]. The requirement of cardiolipin for the activity of Complex I, Complex III, and Complex IV as well as for that of several mitochondrial carriers, suggests that this phospholipid plays a crucial role in the coupled electron transfer process of these enzymes [Fry and Green, 1981].

Recently, some structural evidences seem also to indicate that cardiolipin stabilizes respiratory chain supercomplexes as well as the individual complexes.

The cryo-EM maps of the yeast III_2IV_2 supercomplex and bovine $I_1III_2IV_1$ respirasome clearly showed that the Complexes I, Complex III homodimer, and Complex IV are at some distance within the supercomplex in the lipid bilayer and these gaps between complexes appear as a lower density material in the electron microscopy maps. [Mileykovskaya et al, 2012. Althoff et al, 2011. Dudkina et al, 2011]. Consistent with these observations, about 50 cardiolipin molecules per yeast supercomplex III_2IV_2 were determined by mass spectrometry analysis [Mileykovskaya et al, 2012] and about 200 cardiolipins molecules were estimated to be present in the purified bovine respirasome $I_1III_2IV_1$ [Althoff et al 2011], which is much larger due to the presence of Complex I. Due to larger distances between complexes, the bovine respirasome can potentially accommodate several times more cardiolipin molecules.

Mutations in the *taz1* gene which encodes and acyltransferase involved in the metabolism of cardiolipin result in Barth syndrome, a X-linked cardiomyopathy with neutropenia and growth retardation in humans, characterized by respiratory chain dysfunction [Barth et al 1983]. Barth syndrome patient mitochondria showed a cardiolipin-dependent respirasome organization with lower cardiolipin content and polydispersity in acyl chain composition of cardiolipin molecules [Schalame and Ren, 2006]. McKenzie *et al* [McKenzie et al 2006] demonstrated that cardiolipin defect in Barth syndrome results in destabilization of the supercomplexes by

weakening the interactions between respiratory complexes as BN-PAGE revealed a decrease in the $I_1III_2IV_1$ supercomplexes and increase of free Complex IV.

Tafazzin is found in the inner membrane in a complex including ATP synthase and the adenine nucleotide carrier; the absence of this complex due to *taz1* mutations also induces altered cristae morphology [Claypool et al 2008].

Additionally, Gonzalvez and co-workers [Gonzalvez et al 2013] observed an increase in mitochondrial content, which compensates for the decrease in the level of respiratory complexes and supercomplexes. Mutants in the homologous yeast gene [Ma et al 2004] also have reduced supercomplex and complex IV contents [Brandner et al, 2005 . Li et al, 2007a].

Thus, evidences from yeast to humans actually support a role for cardiolipin in the higher organization of respiratory complexes. It has been shown that reduced formation of individual respiratory complexes and supercomplexes is also correlated with lowered cardiolipin levels due to oxidative stress and cardiolipin peroxidation in aging [Gomez and Hagen, 2012], neurodegenerative diseases [Paradies et al, 2011], and cancer [Gasparre et al, 2013].

In regards to phosphatidylethanolamine, Böttinger *et al* [Böttinger et al 2012], recently have demonstrated that protein transport into and across the mitochondrial inner membrane is impaired in phosphatidylethanolamine-depleted mitochondria.

Though both phosphatidylethanolamine and cardiolipin are required for respiratory activity and efficient generation of $\Delta\psi$ by mitochondria, they play opposing roles in the stabilization of respiratory complexes. Their opposite effects on protein complex stability may be explained by the fact that cardiolipin has a negatively charged head group, whereas phosphatidylethanolamine is a zwitterionic phospholipid of neutral charge.

Functional and Structural Consequences for Supramolecular Association

Kinetic Advantage: Channeling

The functional consequence of supercomplex assemblies in the respiratory chain is substrate channeling between. Substrate channeling is the direct transfer of an intermediate between the active sites of two enzymes catalyzing consecutive reactions [Ovàdi, 1991]; in the case of electron transfer, this means direct transfer of electrons between two consecutive enzymes by successive reduction and reoxidation of the intermediate without its diffusion in the medium milieu. In such a case, inter-complex electron transfer becomes indistinguishable from intra-complex electron transfer, so that the so-called mobile intermediates, predicted to exhibit substrate-like behavior in the classic view of the random collision model [Hackenbrock et al 1986], would rather be buried in the interface between the two consecutive complexes.

Structural Advantage: Protein stability and Assembly Scaffold

The interdependency of supercomplexes formation and complex stability has been shown in several genetic models, in which low levels or respirasomes are detected in the absence of Complex III [Schägger et al, 2004. Acin-Perez et al, 2004], Complex IV [Diaz et al, 2006], or cytochrome *c*. These experimental observations lead to the proposal that the formation of respirasomes may be essential for the assembly / stability of Complex I.

Schägger and collaborators [Schägger et al, 2004], demonstrated that respirasomes is required to stabilize bacterial Complex I since mutant strains of *Paracoccus denitrificans* lacking Complex III or Complex IV showed complete disassembling of Complex I from supercomplexes. Reduced stability of Complex I in those mutant strains was also corroborated from an almost complete loss of NADH:ubiquinone reductase activity.

The necessity of stably assembled human Complex III for the stability of Complex I was later demonstrated using muscle biopsies and cultured patient cells with isolated deficiencies of single complexes. Human Complex I was almost completely lacking in the absence of assembled Complex III. Genetic alternations leading to a loss of Complex III prevented respirasome formation and led to secondary loss of Complex I; seen as Complex III/Complex I defects. Conversely, Complex III stability was not influenced by the absence of Complex I [Schägger et al, 2004. Acin-Perez et al, 2004].

Animal models with mutations on Complex I proved to be useful to evaluate its effects on Complex III and Complex IV and understand their role in supercomplex assembly. Several works have demonstrated that Complex I assembly also depends on Complex IV [Diaz et al, 2006. Li et al, 2007b. D'Aurelio et al, 2006]. While Complex I was found to be unstable in the absence of Complex III, lack of Complex IV totally abrogated assembly of Complex I [Li et al, 2007b].

Suthammark *et al* [Suthammarak et al, 2009] have shown that Complex I activity is dependent on the presence of Complex IV, despite no overall decrease in the intrinsic amount of Complex I. Then, Complex III defects inhibit Complex IV activity by several different mechanisms involving supercomplex destabilization. These mechanisms included also inhibition of Complex I function by weakening its interaction into the respirasome or by decreasing the amount of Complex I, or its assembly within the respirasome [Suthammarak et al, 2010].

By the other side, mutations of Complex I showed controversial results, since in some studies they did not affect the amount of other respiratory complexes [Schägger et al, 2004. Pineau et al, 2005], while in others they significantly reduced the amounts of respiratory complexes III and IV [Acín-Pérez et al, 2009. Ugalde et al, 2004a. Grad and Lemire, 2004. Grad and Lemire, 2006].

The reason for this discrepancy is still unknown, but one reasonable hypothesis is that these controversial results might be related with the specificity of these

mutations that would be affecting (or not) subunits of Complex I involved in direct interactions with other complexes within the respirasome [Genova and Lenaz, 2013].

Because Complex I stability was found to be dependent on the assembly of supercomplexes, it was hypothesized that respirasome assembly follows the assembly of individual respiratory complexes. Several works addressing the pathway for respirasome formation suggest that these supercomplexes are assembled in stages.

Acín-Pérez *et al* [Acin-Perez et al, 2008] studies of pulse-chase labeling of mitochondrial translational products indicated that there is sequential incorporation of mtDNA encoded subunits into respective complexes followed by supercomplex assembly. Thus there seemed to be a temporal delay in the complete assembly of individual complexes and the following assembling into supercomplex.

However, a more extensive study showed that Complex I assembly and synthesis was very closely linked with supercomplex formation as the formation of Complex I/III supercomplex was observed to occur before Complex I was entirely formed [Marques et al, 2007].

Recently, it has been shown that Complex III and IV appear to be assembled independent of each other. In contrast, complex I is assembled in stages [Mimaki et al, 2012].

Moreno-Lastres *et al* [Moreno-Lastres et al, 2012], have shown that assembly and not just stability of Complex I may require an association with Complex III and IV indicating that supercomplex assembly precedes the assembly of individual respiratory complexes as association of Complex IV and Complex III is required for the incorporation of the remaining Complex I subunits such as NDUFS4 and NDUFV1 and supercomplex formation occurs prior to the final stage in maturation, namely, the addition of the NADH dehydrogenase N module. This early supercomplex assembly intermediate lacks respirasome activity. The final addition of the N module catalytic subunits of Complex I appears to occur on this supercomplex intermediate.

One proposed function of the respirasome is as a platform for the sequential assembly of Complex I [Moreno-Lastres et al, 2012]. This observation provides an alternative interpretation of the presentation of multicomplex deficiencies in patients with mutations within a single respiratory complex. The interpretation of the candidate stabilizing interactions' interconnections between the complexes given above under composite nature of respiratory supercomplexes may not be the major answer. Defects in Complex III or Complex IV may result in Complex I deficiency through impaired Complex I assembly.

Supercomplex intermediates can also form in cells stalled in the maturation of Complex III or Complex IV. The final step in Complex III biogenesis is the addition of the Rieske Fe/S catalytic subunit, and cells impaired in Rieske maturation form supercomplexes [Fernandez-Vizarra et al, 2007. Moreno-Lastres et al, 2012]. The last step in the maturation of both Complex I and Complex III is the addition of a key catalytic subunit or module. This may ensure that the supercomplex intermediates are not activated until all components are present.

DYNAMIC ORGANIZATION: PLASTICITY MODEL

As seen in the previous sections, during the past decade significant experimental evidence supports the organization of the mitochondrial respiratory chain into higher order "respirasome" structures.

Although the functional significance of mitochondrial supercomplexes has been questioned after their discovery, recent evidences indirectly support the view that in mammalian cells $I_1III_2IV_1$, respirasomes and I_1III_2, III_2IV_1 supercomplexes in physiological conditions coexist in dynamic in equilibrium with individual respiratory complexes randomly dispersed in the mitochondria membrane.

Acin-Perez *et al.* in 2008 proposed a *"Plasticity model"* where both random collision and supercomplex models coexist, depending on the different mitochondrial systems and on the particular physiological states (Figure 2).

The plasticity model well suits the information obtained by flux control analysis suggesting that electron transfer between Complex I and Complex III is effected *only* by CoQ channelling (at least in beef heart and rat liver mitochondria) whereas that between Complex II and Complex III and between Complex III and Complex IV seems to occur *mostly* by the pools of CoQ and cytochrome *c*, respectively [Bianchi et al. 2004; Genova et al. 2008].

CoQ compartmentalization

Recently, Lapuente-Braun and coworkers [Lapuente-Braun et al 2013;] demonstrated that electron flux from Complex I to Complex III proceeds essentially within supercomplexes, whereas electron flow from Complex II preferentially occurs trough Complex I-unbound Complex III

By genetic modulation of the relative levels of complexes I and III, which alter the ratios of supercomplexes and individual complexes, they were able to demonstrate that electron transfer occurs by a mixture of direct substrate channeling of CoQ/cyt c within supercomplexes and through random collision of CoQ/cytochrome c and individual respiratory complexes dependent on the metabolic state of the cell and substrate availability.

This compartametalization of CoQ molecules between NADH oxidation (Complex I-dependent) and succinate oxidation (Complex II-dependent) implies that those Complex III molecules physically associated with Complex I (I_1III_2 and $I_1III_2IV_1$ supercomplexes) are also exclusively dedicated to NADH oxidation ($CIII_{NADH}$) while those Complex III molecules that are not bound to Complex I are mainly responsible for oxidation of succinate and other substrates using the free CoQ pool.

In addition, they concluded that Complex I has a very high affinity for Complex III, so that this association is preferred to the free state of either Complex I or Complex III when a partial loss of Complex III occurs. In this situation NADH oxidation is preferentially maintained despite the risk of compromising the oxidation of FAD-linked substrates [Lapuente-Brun et al, 2013]

These evidences would reconciliate the pool behavior of CoQ from the random model with the structructural and functional evidences that supports the existence of supercomplexes.

COMPLEX I

Complex I (*NADH: ubiquinone oxidoreductase*, E.C. 1.6.5.3) is a main entry-point for electrons to the respiratory chain of mitochondria and several bacteria. Complex I catalyzes the reversible oxidation of the NADH that is produced predominantly by the tricarboxylic acid (Krebs) cycle and the β-oxidation of fatty acids, regenerating the NAD^+ pool in the mitochondrial matrix (in eukaryotes) or cytoplasm (in prokaryotes). [Walker, 1992. Yagi and Matsuno-Yagi, 2003. Brandt, 2006].

The exergonic transfer of two electrons from NADH to reduce ubiquinone is coupled to the vectorial transport of four protons across the mitochondrial membrane (in eukaryotes) or cytoplasmic membrane (in bacteria), contributing to the proton-motive force (Δp) that supports ATP synthesis and the mitochondrial import and export of metabolites and proteins:

$$NADH + H^+ + Q + 4H^+_{in} \rightarrow NAD^+ + QH_2 + 4H^+_{out}$$
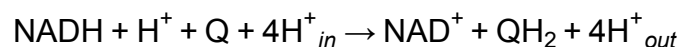
Complex I is present in many bacteria and in the mitochondria of most eukaryotes, including animals, plants and fungi. Modified versions of the enzyme, utilizing different electron inputs and reducing various ubiquinone analogues, have an even broader spread, encompassing chloroplasts and archaea [Moparthi and Hagerhall, 2011].

Complex I is also considered as the main source of reactive oxygen species (ROS) in mitochondria, which cause oxidative stress, damage to mtDNA and energetic decline [Ozawa, 1997]. Complex I-related diseases, aging and age-related degenerative diseases arise from both decreased Complex I activity or increased ROS production [Lin and Beal, 2006. Balaban et al, 2005. Wallace, 2005]. Mutations in nucleus and mitochondria encoded Complex I subunits have been associated with several neurodegenerative diseases [Schapira, 1998].

Structure

Complex I is one of the largest known membrane proteins. The total molecular weight is close to 1 MDa for the mitochondrial enzyme and about 550 kDa for the prokaryotic version. The mammalian mitochondrial enzyme consists of 44 subunits [Carroll et al, 2006a, Balsa et al, 2012], while bacterial Complex I is composed of at least 14 subunits usually encoded in the same operon [Yagi et al, 1998]. Sequence analysis of these 14 subunits reveals homologues in eukaryote Complex I [Fearnley and Walker, 1992]. Thus, those 14 'core subunits' are sufficient for energy transduction and theore regarded as a minimal structure of Complex I. [Walker, 1992. Yagi and Matsuno-Yagi, 2003].

For historic reasons, no unified nomenclature has been established for the subunits of Complex I. Theore, regardless of the species concerned, the names established for bovine Complex I, the first studied and best characterized enzyme [Carroll et al, 2006a. Balsa et al, 2012], are used in this thesis for all central subunits and those accessory subunits. Table 1.3 presents the nomenclatures of other relevant species for convenience.

The core subunits comprise two distinct categories. The seven predominantly hydrophilic subunits that bear all binding motifs for redox prosthetic groups (Fe-S clusters and FMN). The remaining seven subunits are highly hydrophobic proteins folded into several transmembrane helices embedded in the membrane [Efremov et al, 2010].

In addition to these core subunits, the mammalian Complex I contains 31 additional, supranumerary or 'accessory' subunits [Brandt, 2006] (Table 1.4). These subunits mostly form a protective shell around the core [Brandt, 2006. Angerer et al, 2011], although some are presumed to participate in the regulation of the enzyme as suggested by the fact that some of these subunits can be phosphorylated [Chen et al, 2004. Palmisano et al, 2007. Schilling et al, 2005 Ugalde et al, 2004b]. Other subunits seem to be associated with enzymatic functions (apoptosis [Fearnley et al, 2001] or biosynthesis of lipoic acid [Cronan et al, 2005]). Some of these accessory subunits might also play a role in the regulation of the assembly and stability of Complex I [Gabaldon et al, 2005. Abdrakhmanova et al, 2006].

In eukaryotes, the hydrophobic subunits are encoded by the mitochondrial genome [Chomyn et al, 1986], whereas the hydrophilic and all the supernumerary subunits are encoded by the nuclear genome and imported to the mitochondrion [Yagi and Matsuno-Yagi, 2003. Carroll et al, 2003].

The 14 core subunits of the bacterial enzyme thus, are consider that represent the minimal form that began acquiring the supernumerary subunits before the endosymbiotic event that lead to the origin of mitochondria and creation of eukaryotic cell [Yip et al, 2011].

Electron microscopic reconstructions of the Complex I structure established its overall *L*-shaped appearance in all organisms studied consisting of a membrane-embedded part in addition to a promontory peripheral arm protruding and pointing toward the mitochondrial matrix side (or bacterial cytoplasm), which stands more or less perpendicular on one end of the membrane [Sazanov, 2007 . Efremov et al, 2010. Hofhaus et al, 1991. Guenebaut et al, 1998. Grigorieff, 1998. Djafarzadeh et al, 2000. Peng et al, 2003].

The current knowledge about the structure of Complex I comes from the structural studies in bacteria as crystallization of the mitochondrial Complex I, generally more stable than bacterial enzyme, is complicated by a number of post translational modifications and compositional heterogeneity [Hunte et al, 2010]. A molecular structure with 3.3 Å resolution from the entire enzyme of *T. thermophilus* has been recently published [Baradaran et al, 2013] (Figure 1.11).

Table 1.3: Nomenclature for the 14 core subunits of Complex I and prosthetic cofactors bound by the hydrophilic subunits.

Domain	Module	*B. taurus*	*T.thermophilus*	*H. sapiens*	*E. coli*	Prosthetic groups
Peripheral (hydrophilic)[a]	**N**	51 kDa	Nqo1	NDUFV1	NuoF	FMN and 1 tetranuclear Fe-S cluster (N3)
		24 kDa	Nqo2	NDUFV2	NuoE	1 binuclear Fe-S cluster (N1a)
		75 kDa	Nqo3	NDUFS1	NuoG	1 binuclear Fe-S cluster (N1b) and 2 tetranuclear Fe-S clusters (N4 and N5)
	Q	49 kDa	Nqo4	NDUFS2	NuoCD	
		30 kDa	Nqo5	NDUFS3	NuoC	
		TYKY	Nqo9	NDUFS8	NuoI	2 tetranuclear Fe-S clusters (N6a and N6b)
		PSST	Nqo6	NDUFS7	NuoB	1 tetranuclear Fe-S cluster (N2)
Membrane (hydrophobic)[b]	**(NuoH)**	ND1	Nqo8	ND1	NuoH	
	P	ND2	Nqo14	ND2	NuoN	
		ND3	Nqo7	ND3	NuoA	
		ND4	Nqo13	ND4	NuoM	
		ND4L	Nqo11	ND4L	NuoK	
		Nqo12	ND5	ND5	NuoL	
		Nqo10	ND6	ND6	NuoJ	

(a) nDNA-encoded subunits in eukaryotes
(b) mt DNA-encoded subunits in eukaryotes

Table 1.4: Nomenclature for the supranumerary subunits of mammalian Complex I

B. taurus	H. sapiens	B. taurus	H. sapiens
10 kDa	NDUFV3	B17.2	NDUFA12
30 kDa	NDUFS3	B16.6	NDUFA13
18 kDa (AQDQ)	NDUFS4	MNLL	NDUFB1
15 kDa	NDUFS5	AGGG	NDUFB2
13 kDa	NDUFS6	B12	NDUFB3
MWFE	NDUFA1	B15	NDUFB4
B8	NDUFA2	SGHD	NDUFB5
B9	NDUFA3	B17	NDUFB6
MLRQ*	NDUFA4*	B18	NDUFB7
B13	NDUFA5	ASHI	NDUFB8
B14	NDUFA6	B22	NDUFB9
B14.5a	NDUFA7	PDSW	NDUFB10
PGIV	NDUFA8	ESSS	NDUFB11
39 kDa	NDUFA9	SDAP	NDUFAB1
42 kDa	BDUFA10	KFY1	NDUFC1
B14.7	NDUFA11	B.14.5	NDUFC2

*Recently it has been demonstrated that NDUFA4 is a subunit of complex IV [Balsa et al, 2012]
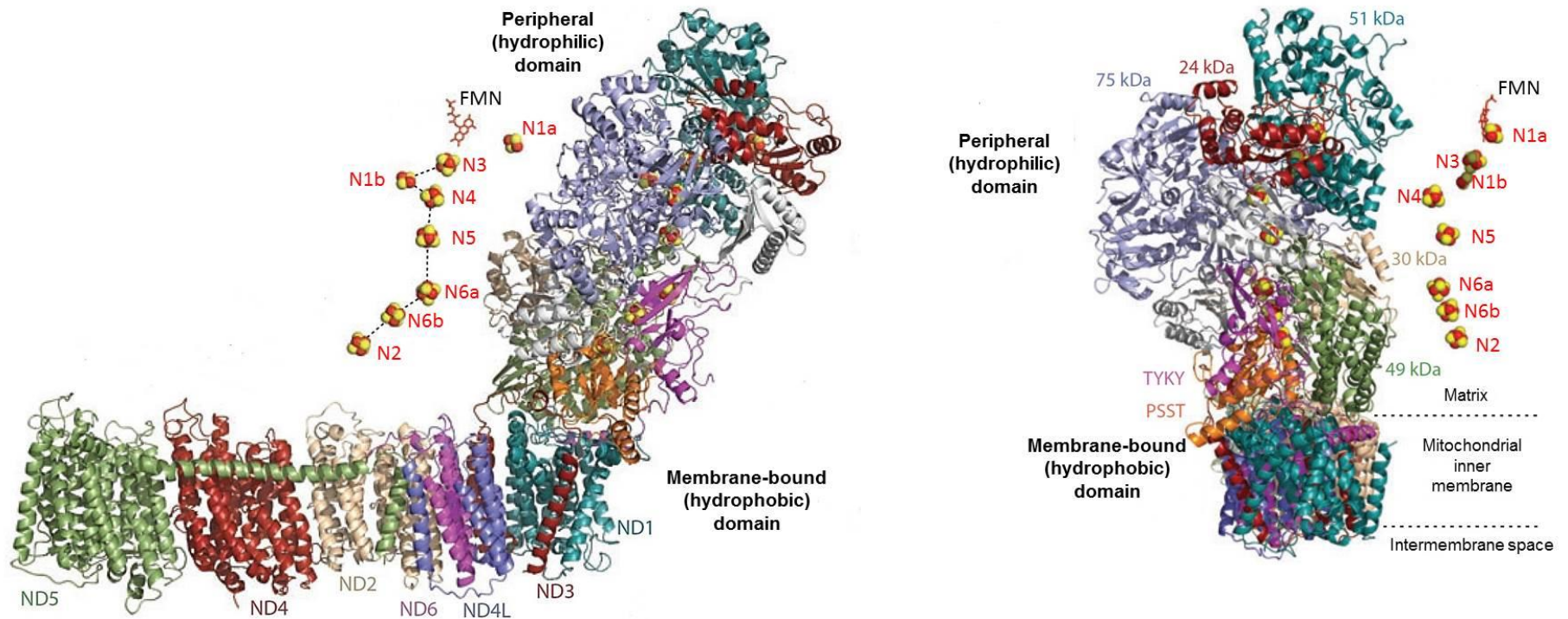
Figure 1.11: Structure of complex I from *Thermus thermophilus*. The structural model of the entire 536 kDA complex I (Protein Data Bank identifier 4HEA) at 3.3 Å resolution which comprises the 14 core subunits. *B. taurus* nomenclature is used for the subunits.The flavin (FMN) and FeS clusters are shown to the side of the structure. The [4Fe-4S] cluster N7, which is particular to *T. thermophilus* and a few other organisms, is not shown. The *B. taurus* subunits nomenclature is according to their apparent size in SDS-PAGE analysis (the 75, 51, 49, 30, and 24 kDa subunits), for the first four amino acids of the mature protein sequences (PSST and TYKY subunits), and for the NADH dehydrogenase products of the mitochondrial DNA (ND1 to ND6 and ND4L).

Peripheral arm. The peripheral hydrophilic domain contains the NADH-binding site, a part of quinone binding site, and all redox centres, including a non-covalently bound flavin mononuclotide (FMN), eight iron-sulfur (Fe-S) clusters conserved between all enzymes, and an additional Fe-S cluster found in some bacterial Complex I [Berrisford and Sazanov, 2009].

The 51 kDa, 24 kDa and the 75 kDa subunits form the dehydrogenase domain at the uppermost part of the peripheral arm. By the other side, the lower part formed by the 49 kDa, 30 kDa, TYKY, and PSST subunits, contains a part of the ubiquinone-binding site (Q site) and forms the interface with the membrane domain. [Sazanov and Hinchliffe, 2006].

FMN is bound by an unusual Rossman fold-like domain in the 51 kDa subunit [Fearnley and Walker, 1992. Sazanov and Hinchliffe, 2006]. This atypical Rossmann fold domain of Complex I, which evolved to bind both flavin and the substrate nicotinamide by the addition of an extra glycine-rich loop has so far not been detected in any other enzyme [Berrisford and Sazanov, 2009]. All of the residues involved in interactions with these cofactors and most residues lining the binding cavity are very well conserved suggesting that the mechanism of dehydrogenation by Complex I is conserved throughout the species from bacteria to humans [Berrisford and Sazanov, 2009].

A tetranuclear cluster (N3) is bound near the C-terminus of the 51 kDa [Ohnishi, 1998. Yano et al, 1996. Fecke et al, 1994]. The remaining clusters are the tetranuclear N4 and N5 clusters, and the binuclear cluster N1b, all of them bound in the 75 kDa subunit. By the other side, the tetranuclear clusters N6a and N6b, which follow cluster N5 in the redox chain, are localized in the TYKY subunit [Ohnishi, 1998].

The tetranuclear N2, bound in the PSST subunit, [Duarte et al, 2002. Flemming et al, 2003. Ahlers et al, 2000. Garofano et al, 2003], is the last redox center in the chain. This cluster donates electrons to the bound ubiquinone substrate [Ohnishi, 1998. Vinogradov et al, 1995]. Notably, this cluster is ~25-30 Å away from the membrane surface suggesting that the ubiquinone has to move out of the membrane to accept electrons [Baradaran et al, 2013. Hunte et al, 2010]. The distances between neighbouring redox centres in the chain are within 14 Å, the maximal distance of physiological electron transfer [Page et al, 1999] (Figure 1.12).

With the exception of cluster N2, all active Fe-S centers (clusters N3, N1b, N5, N4, N6a, and N6b) have a midpoint potential of about −250 mV [Ohnishi 1998. Rasmussen et al, 2001] and are, theore, also named the isopotential Fe-S clusters of Complex I. Cluster N2 has a more positive and pH-dependent midpoint potential of –100 mV [Ohnishi 1998 . Ingledew and Ohnishi, 1980].

There are two additional Fe-S clusters that are not part of the main redox chain: the prokaryotic-specific tetranuclear cluster N7 bound to the 75 kDa subunit which is separated by more than 20 Å from the chain of redox active clusters, and hence is not involved in electron transport. This cluster likely represents an evolutionary remnant [Finel, 1998. Leif et al, 1995. Yano et al, 2003].

By the other side, the binuclear cluster N1a, coordinated by subunit 24 kDa, is conserved in Complex I from all species, which suggest it has a functional role [Yano et al, 1996]. Found in an hydrophobic environment, cluster N1a is 12.3 Å away from FMN, has a one-electron potential of −370 mV and can thus reduce flavosemiquinone (FSQ) efficiently [Sazanov and Hinchliffe, 2006]. It was suggested that N1a plays an important role in reducing ROS production by Complex I [Sazanov 2007. Sazanov and Hinchliffe, 2006].

Thus, the NADH – FMN – N3 – N1b – N4 – N5 – N6a – N6b – N2 – ubiquinone sequence in Complex I, is likely to be the main route for electron transfer within the enzyme [Sazanov and Hinchliffe, 2006].
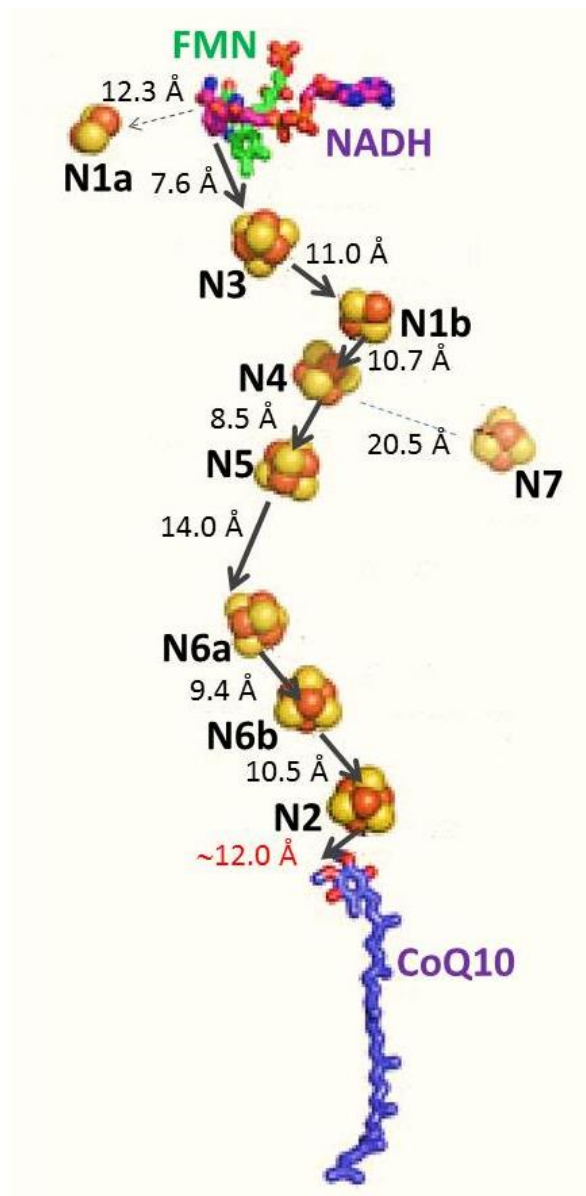
Figure 1.12: Scheme of the electron pathway in the peripheral arm of Complex I. Spatial arrangement of the cofactors within the peripheral arm of Complex I. The edge-to-edge distances between the cofactors are deduced from the crystal structure [Sazanov and Hinchliffe, 2006] are given. The distance between N2 and the headgroup of ubiquinone was determined from electron density corresponding to bound decylubiquinone [Baradaran et al, 2013]. Grey arrows shows the main electron transfer pathway between FMN and ubiquinone-10.

Interface domain. Most of the interactions between the peripheral and membrane domains involve subunit ND1, which forms many salt bridges and hydrogen bonds to hydrophilic subunits 49 kDa, PSST, and TYKY [Baradaran et al, 2013].

ND1 subunit is the most conserved membrane subunit of Complex I and participates in the interface with the hydrophilic domain contributing to the Q site [Sekiguchi et al, 2009]. ND1 emerged only once during evolution, joining hydrogenase and antiporter modules of Complex I – related proteins.

The Q site is found at the interface of 49 kDa, TYKY, PSST, and ND1 subunits supported by the stabilizing interactions of the ND3 subunit that keeps the peripheral and membrane domains together [Baradaran et al, 2013].

The structural studies of Complex I from *T. thermophilus* co-crystallized with ubiquinone analogues [Baradaran et al, 2013] showed that the ubiquinone headgroup interacts with conserved and essential residues. It is ~12 Å from the cluster N2 and ~15 Å above the membrane surface [Baradaran et al, 2013]. Hence, it is located at an appropriate distance for electron exchange with the Fe-S chain [Page et al, 1999], but must move a significant distance out of the membrane [Baradaran et al, 2013].

A 30-Å long chamber, framed by helices of ND1 and ND3 subunits, is completely enclosed from the solvent and leads from a narrow entry point in the membrane toward cluster N2. This quinone chamber is long and narrow enough to restrict the quinone tail to an extended conformation (Figure 1.13 and 1.14).

It has been proposed that only the last one to three isoprenoid units from ubiquinone-10 will protrude out of the cavity into the lipid, as the entrance of the quinone chamber is narrower that the rest of the cavity, so that the quinone tail will block solvent access to the cavity, sealing this reaction chamber. Consequently, slight structural re-arragements are necessary to allow the quinone headgroup to move in and out the cavity.

The polar residues lining this chamber are highly conserved and mutations in many of these residues lead to human diseases and loss of Complex I activity [Baradaran et al, 2013. Sazanov, 2007].

Membrane arm. The membrane-spanning part of the enzyme lacks covalently bound prosthetic groups [Carroll et al, 2006b]. The structure analyses revealed that ND2, ND4, and ND5 subunits are related to the Mrp family of Na+/H+ antiporters [Moparthi et al, 2011]. They each exhibits a conserved 14 transmembrane helices structure, comprising two inverted-symmetry half-channels motifs. These half-channels are linked into a single full proton-translocation channel by charged residues (Figure 1.15 and 1.16).

By the other side, a discontinuous and long α-helix from the C-terminal region of ND5 runs orthogonal to the transmembrane helices (HL) [Efremov and Sazanov, 2010. Baradaran et al, 2013]. Beneath the membrane domain, β-hairpin connecting elements (βH), contribute further interactions between antiporter subunits. These two elements, HL and βH have been proposed as the coupling elements in Complex I [Baradaran et al, 2013].

The core fold of ND1 is structurally similar to the half-channel motif of the three antiporter subunits. Together with transmembrane helices from ND6 and ND4L form a second half-channel, this motif constitutes a fourth proton-transfer pathway and it is erred as the E-channel owing to abundance of glutamates in its centre. Many of these residues are conserved and essential for activity (Figure 1.15).

The four related pairs of half-channels identified in the membrane domain of Complex I provide a structural basis for the mechanistic understanding of the proton stoichiometry and proton-transfer mechanism [Baradaran et al, 2013].

These subunits are at a significant distances away from the N2 cluster and the ubiquinone binding site, so the coupling process of the redox and transport activities requires long-range energy transfer through Complex I.
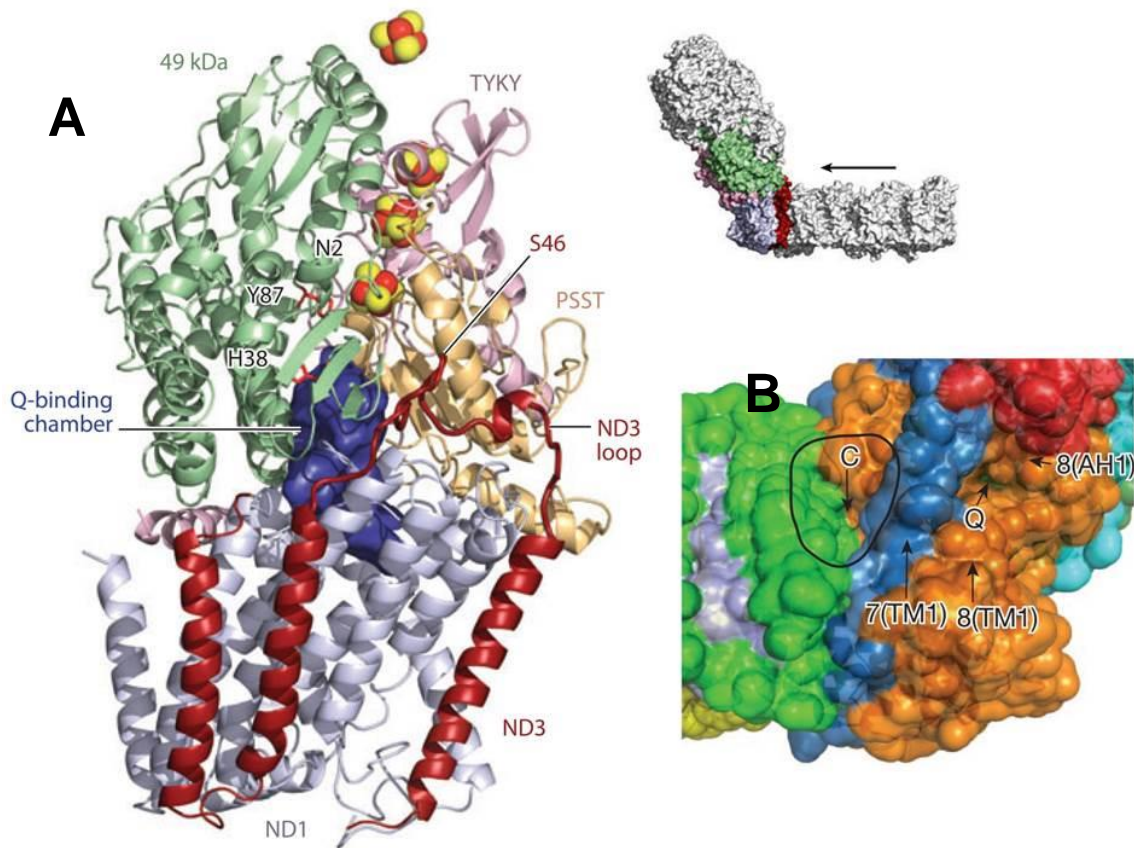
Figure 1.13: Quinone-reaction chamber of Complex I. Cartoon representation of the atomic model (Protein Data Bank identifier 4HEA) at 3.3 Å resolution from *T. thermophilus*. **A)** The five subunits that form the interface between the hydrophilic and hydrophobic domains are viewed along the membrane domain as indicated in the inset. *B. taurus* nomenclature is used for the subunits. The 49 kDa, PSST, and TYKY subunits at the bottom of the hydrophilic domain sit on top of ND1 and interact extensively with its interhelical loops. One loop of ND3 reaches up to connect with the 49 kDa and PSST subunits on the front of the hydrophilic domain. The cavity of the quinone-reaction chamber proposed from structural analyses is shown in dark blue and two residues that form hydrogen bonds with the ubiquinone headgroup are marked, residues are numbered according to the *Thermus thermophilus* structure (His92 and Tyr141 in *B. taurus*). **B)** Surface (solvent-accessible) representation of the interface between hydrophilic and hydrophobic domains. The empty crevice (C, circled) between ND6 (green), ND1 (orange) and ND3 (blue) subunits, as well as helices framing the entry point to the quinone site (Q) are indicated. This empty crevice may provide space for conformational changes during the catalytic cycle, since the central helices of the ND1 half-channel tilt into this crevice. 7(TM1) = transmembrane helix from Nqo7 subunit of *T. thermophilus* (ND3 in *B. taurus*). 8(AH1) = amphipathic helix and 8(TM1) = transmembrane helix from Nqo8 subunit of *T. thermophilus* (ND1 in *B. taurus*). [from Baradaran et al, 2013]
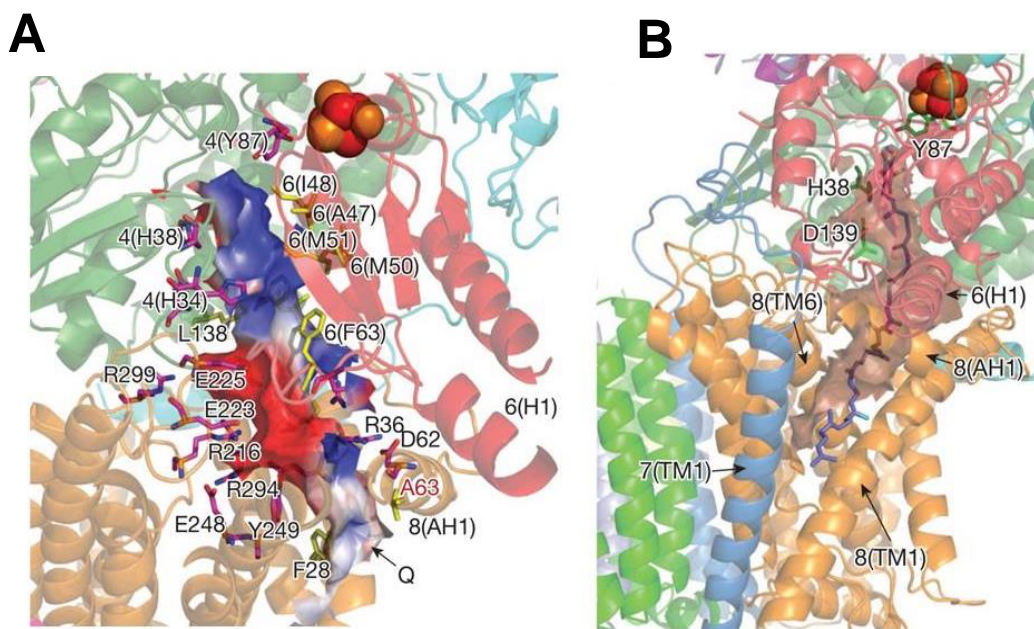
Figure 1.14: Ubiquinone binding site of Complex I. Cartoon representation of the atomic model (Protein Data Bank identifier 4HEA) at 3.3 Å resolution from *T. thermophilus*. **A)** The internal solvent-accessible surface colored red for negative, white for neutral and blue for positive surface charges. Charged residues lining the cavity are shown with carbon in magenta and hydrophobic residues in yellow. Ala63, the site of the primary Leber's hereditary optic neuropathy disease mutation, is labelled in red. Residues are numbered according to the *Thermus thermophilus* structure [Nqo8 subunit of *T.thermophilus* (ND1 subunit in *B. taurus*): Phe28 (Val17), Arg36 (Arg25), Asp62 (Asp51), Ala63 (Ala52), Leu138 (Trp118), Arg216 (Arg195), Glu223 (Glu202), Glu225 (Glu204), Glu248 (Glu227), Tyr249 (Tyr228), Arg294 (Arg273), Arg299 (Arg278)]; [Nqo6 subunit of *T. thermophilus* (PSST subunit in *B. taurus*): Ala47 (Ala93), Ile48 (Val94), Met50 (Met96), Met51 (Met97), Phe63 (Phe109)]; [Nqo4 subunit of *T. thermophilus* (49 kDa subunit in *B. taurus*): His34 (His88), His38 (His92), Tyr87 (Tyr141), Asp139 (Asp193)]. **B)** Theoretical model of bound ubiquinone-10. Carbon atom in cyan indicates the eighth isoprenoid unit. Residues of Nqo4 subunit (49 kDa subunit in *B. taurus*) interacting with the headgroup are indicated: His38 (His92), Tyr87 (Tyr141), Asp139 (Asp193). The quinone chamber is shown with surface in brown and helices framing its entry point are indicated. Movable hydrophobic helix 6(H1) (Nqo6 subunit in *T. thermophilus*, PSST subunit in *B. taurus*] interacting with the amphipathic 8 (AH1) helix [Nqo8 subunit of *T. thermophilus*, ND1 subunit in *B. taurus*] are labelled. [from Baradaran et al, 2013]
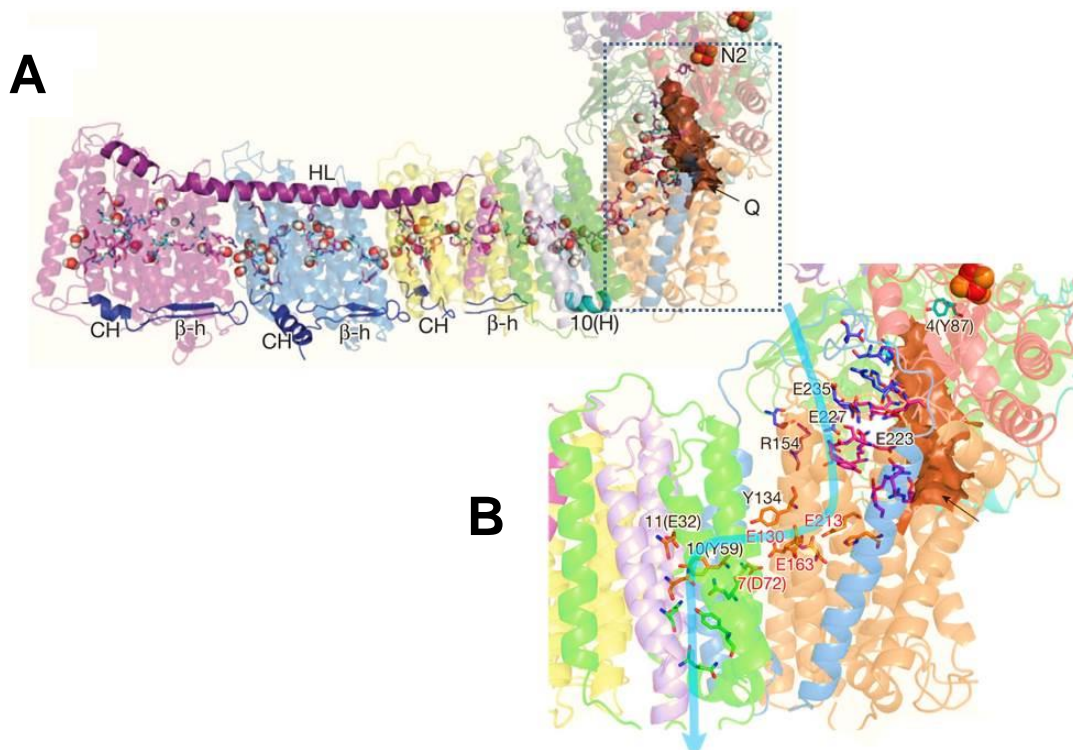
Figure 1.15: E-channel and central hydrophilic axis of Complex I. Cartoon representation of the atomic model (Protein Data Bank identifier 4HEA) at 3.3 Å resolution from *T. thermophilus*. **A)** Central axis of charged and polar residues (charged residues have carbon in magenta, polar in cyan). Residues shown are either central to half-channels or are forming the connection between them. Predicted waters nearby are shown as spheres. Connecting elements are shown in solid colors: helix HL in magenta and the βH element in blue, with the C-terminal helix CH and the β-harping (β-h) from each antiporter labelled. **B)** Charged and polar residues constituting the channel are shown as sticks. Quinone cavity is shown with surface in brown and approximate proton translocation path is indicated by blue arrow. Key residues are labelled, with the Glu/Asp quartet in red. Residues are numbered according to the *Thermus thermophilus* structure [Nqo8 subunit of *T.thermophilus* (ND1 subunit in *B. taurus*): Glu130 (Ser110), Tyr134 (Tyr114), Arg154 (Arg134), Glu213 (Glu192), Glu223 (Glu202), Glu227 (Glu216), Glu235 (Glu224)]; [Nqo7 subunit of *T. thermophilus* (ND3 subunit in *B. taurus*): Asp72 (Asp66)]; [Nqo10 subunit of *T. thermophilus* (ND6 subunit in *B. taurus*): Tyr59 (Tyr60)]. [from Baradaran et al, 2013]
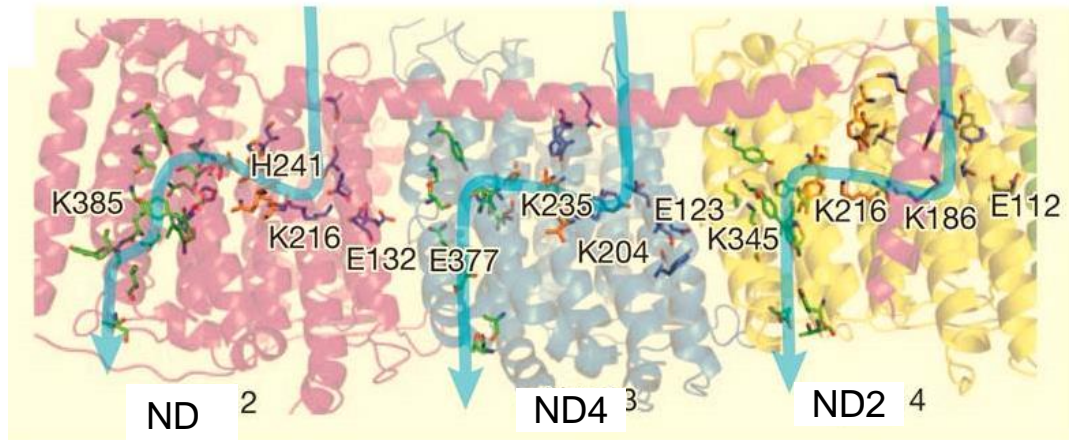
Figure 1.16: Putative proton-translocation channels in the antiporter-like subunits. Cartoon representation of the atomic model (Protein Data Bank identifier 4HEA) at 3.3 Å resolution from *T. thermophilus*. Polar residues lining the channels are shown as sticks with carbon in dark blue for the first (N-terminal) half-channel, in green for the second (C-terminal) half-channel and in orange for connecting residues. Key residues –Glu and Lys- from the first half-channel, Lys/His from the connection and Lys/Glu from the second half-channel, are labelled. [Nqo14 subunit of *T. thermophilus* (ND2 subunit in *B. taurus*): Lys186 (Lys105), Lys216 (Lys135), Lys345 (Lys213)]; [Nqo13 subunit of *T. thermophilus* (ND4 subunit in *B. taurus*): Glu123 (Glu123), Lys204 (Lys206), Lys235 (Lys237), Glu377 (Lys378)]; [Nqo12 subunit of *T. thermophilus* (ND5 subunit in *B. taurus*): Glu132 (Glu145), Lys216 (Lys223), His241 (His248), Lys385 (Lys392)]. Approximate proton-translocation paths are indicated by blue arrows. [from Baradaran et al, 2013]

The crystal structures of bacterial Complex I have given much insight into the structure and how subunits are arranged within these complexes. In higher eukaryotes the most detailed topological structure of subunits within complex I is obtained from experiments using mild chaiotropic salts to break up complex I into subcomplexes. First studies performed by Hatefi and colleagues enabled to fractionate complex I into a flavoprotein part, a hydrogenase part and a membrane part [Galante and Hatefi, 1978]. This approach was later ined with mildly detergents, thus intact bovine Complex I has been resolved into various subcomplexes (Iα, Iβ, Iλ, Iγ fragments) that have subsequently been subjected to extensive analysis [Carroll et al, 2003] (Figure 1.17).

Subcomplex Iλ represents the peripheral arm of the complex, subcomplex Iα consists of subcomplex Iλ plus part of the membrane arm and subcomplex Iβ forms the major part of the membrane arm. Subunits that do not associate with the Iα or Iβ subcomplexes are grouped as the Iγ 'subcomplex', a fraction for which it is not clear whether it represents a true fragment of Complex I.
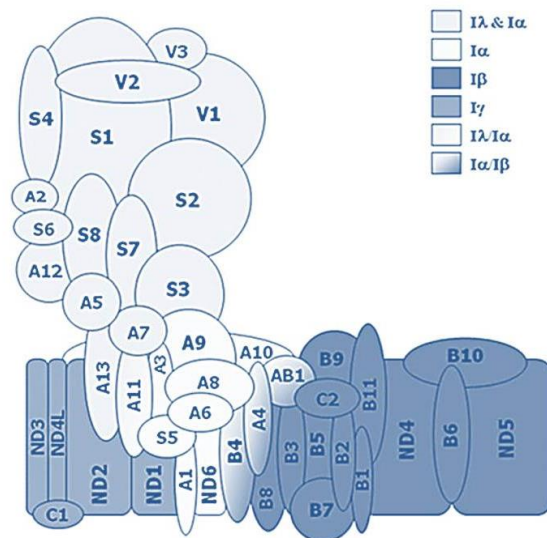
Figure 1.17: Topology model of subunits in mammalian Complex I.
The L-shaped Complex I can be dissected into fragments Iα, Iβ, Iλ, and Iγ, whose composition allows a basic arrangement of the 44 subunits currently described for mammalian complex (*H. sapiens* nomenclature)

Evolution and modular organization of Complex I

Phylogenetic analyses revealed that the two arms of Complex I are evolutionary independent of each other representing a chimera of hydrogenases and cation-proton antiporter [Friedrich, 2001. Moparthi and Hagerhall 2011. Efremov and Sazanov, 2012. Friedrich and Scheide, 2000. Böhm et al, 1990. Albracht, 1993. Friedrich and Weiss, 1997. Finel, 1998].

The intricate evolutionary history of Complex I is intimately related to energy metabolism and the oxygen concentration levels in the early atmosphere.

Of particular interest is the modular evolution of complex I proposed by Friedrich and Weiss (Friedrich and Weiss 1997). Based on homologies with bacterial enzymes, this theory postulates that Complex I originates from fusion of distinct pre-existing protein assemblies, which have combined their activities in one complex. Thus, the initial step has been the association of a soluble heterodimeric reversible [NiFe]-hydrogenase with membrane-bound K^+/H^+ or Na^+ antiporters [Friedrich and Weiss, 1997. Friedrich and Scheide, 2000]. Mathiesen and Hägerhäll, 2002]. Subsequent acquisition of subunits with additional redox would have transformed this ancestral enzyme in a proton-pumping hydrogen:quinone oxidoreductase. Subsequently the multiplication and/or recruitment of antiporter genes plus the addition of other subunits, along with loss of hydrogenase activity and gain of diaphorase activity, would have given rise to Complex I (Figure 1.19)

The association of a soluble [NiFe]-hydrogenase with membrane-bound antiporter subunits may have been caused by the need of highly reducing electrons. It has been postulated that hydrogen may have been very abundant in the primordial atmosphere [Tian et al, 2005] explaining the early appearance of soluble [NiFe]-hydrogenases. However, this gas can easily escape to space and its atmospheric concentration may have dropped rather rapidly at the geological scale.

Reverse electron transport coupled to CO_2 reduction may have been the selective advantage that favored the formation of the hydrogenase:antiporter complex.

The evolutionary relationships established by phylogenetic studies are consistent with a plethora of structural and functional evidence and define three functional modules of Complex I: the NADH oxidizing or *N-module* serving for electron input

from NADH, the *Q-module* or output module which conducts electrons that reduces ubiquinone, and the *P-module* that translocates the protons (Figure 1.18).

The N - module

The NADH dehydrogenase module (N-module) of Complex I consists of the 24 kDa, 51 kDa, and 75 kDa subunits, are homologous to the α subunit and in part from the γ subunit of NAD^+-reducing hydrogenases of *Alcaligenes eutrophus* [Tran-Betcke et al, 1990].

This module harbor the NADH binding site and have FMN and iron-sulfur clusters as prosthetic groups [Yano et al, 1996].

The Q - module

The quinone module (*Q-module*) is composed of 49 kDa, 30 kDa, TYKY, and PSST subunits. The 49 kDa and part of the PSST subunit are homologous to the large and small subunits of water-soluble [NiFe] hydrogenases, respectively [Böhm et al, 1990. Albracht, 1993]. The 30 kDa subunit has no prosthetic group and seems to be unique for Complex I [Brandt, 2006].

The P – module

This *P-module* comprises the seven membrane-embedded subunits, which are encoded by the mitochondrial genome in most eucaryotes [Brandt, 2006]. Subunits ND2, ND4, and ND5 are homologous to each other, and one representative of this family has been acquired together with an ND1 homologue at the level of membrane-bound type-3 [NiFe] hydrogenases found in *Escherichia coli* [Fearnley and Walker, 1992] or the archaeon *Methanosarcina barkeri* [Hedderich, 2004]. Remarkably, the ND2/ND4/ND5 subunits seems to have evolved from Na^+/H^+ antiporters [Fearnley and Walker, 1992. Mathiesen and Hägerhäll, 2002], and are particularly homologous with proteins encoded by the *mrp* (multiple resistance and pH adaptation) operon of *Bacillus subtilis* .This type of antiporter is built up by seven proteins, MrpABCDEFG [Swartz et al, 2005], of which MrpA was shown to have higher sequence similarity to ND5 whereas MrpD showed more similarity to ND4 and ND2 [Mathiesen and Hägerhäll, 2002]. The small ND4L is homologous to MrpC [Mathiesen and Hägerhäll, 2003].

In an alternative module terminology [Friedrich and Scheide 2000; Friedrich 2001], the *hydrogenase module* is formed from the Q-module and two additional membrane-spanning proteins, ND1 and one of the homologous Mrp antiporter-derived proteins. The composition of this module is thereby equivalent to the protein subunit composition of present day Ech and Hyc hydrogenases [Hedderich, 2004. Vignais et al, 2001]. The remaining five membrane-spanning proteins comprise the *transporter module* [Friedrich and Scheide, 2000. Friedrich, 2001].
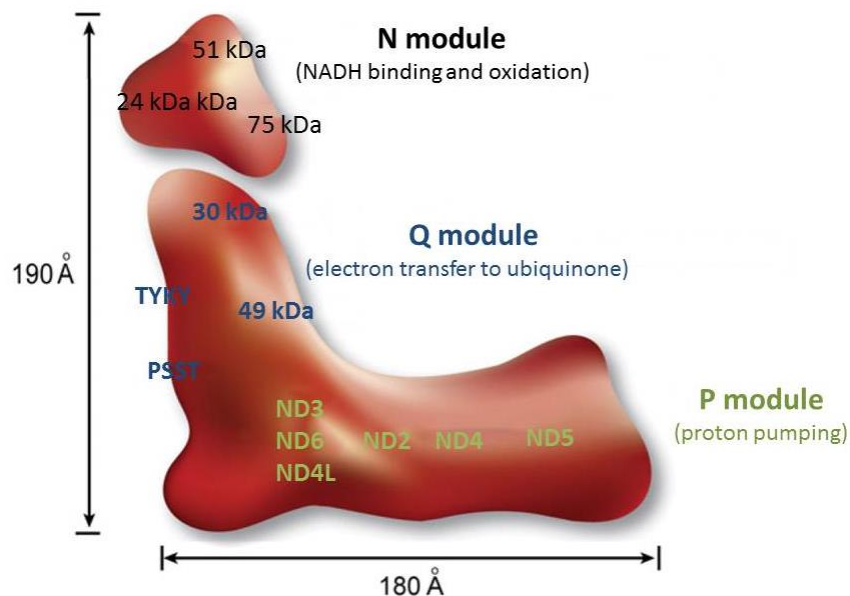
Figure 1.18: Modular organization of Complex I core subunits. Schematic graph of bovine mitochondrial Complex I structure. The matrix arm and membrane arm form an L-shaped structure, with an angle of 100°. It is composed of three conserved functional modules: the NADH dehydrogenase module (N module), the electron transfer module (Q module) and the proton translocation module (P module). The positions of the 14 core subunits are indicated, all of which are highly conserved from prokaryotes to eukaryotes. [modified from Mimaki et al 2012].
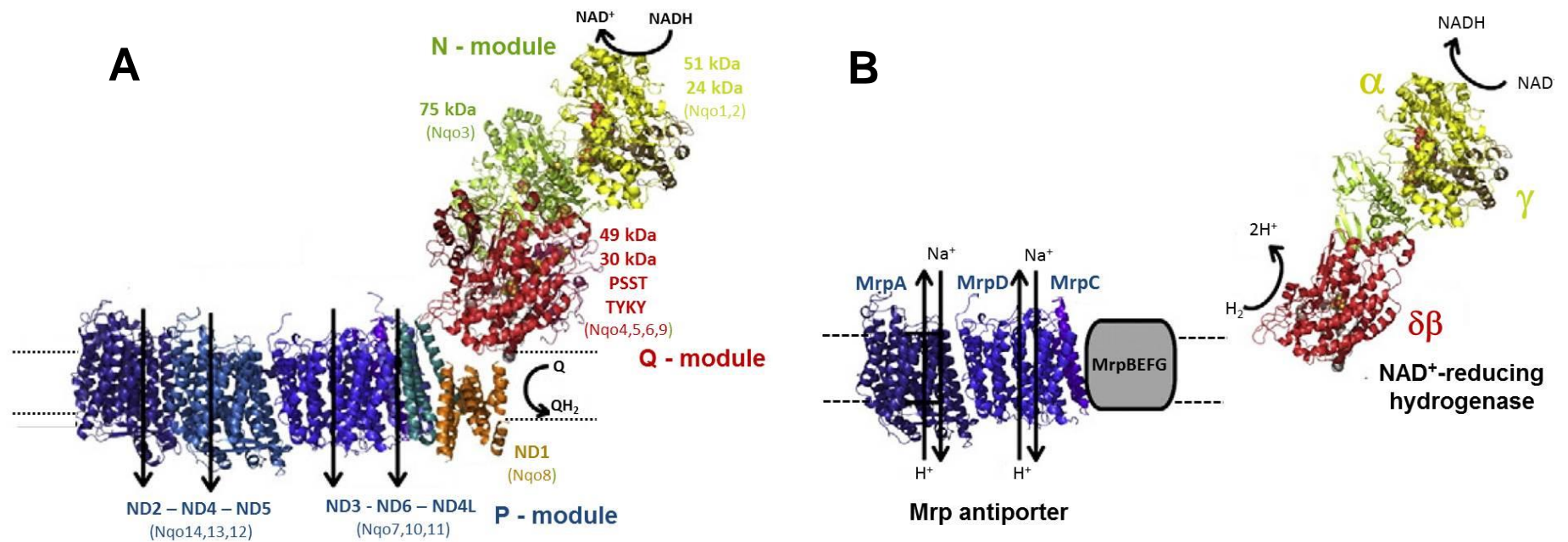
Figure 1.19: Evolutionary modules of Complex I. A) The structure of Complex I from *Thermus thermophilus* is shown with color-coded modules: yellow and green, N-module; red, Q-module; orange, NuoH-like subunits; blue, P-module. *B. taurus* nomenclature is used for the subunits, *T. thermopilus* nomenclature in round brackets. **B) Modular evolution hypothesis of Complex I.** Two separate origins of Complex I: Mrp (*multiple resistance and pH adaptation*) cation/H^+ antiporters of *Bacillus subtilis* are homologous to the P-module of Complex I and the N- and Q-module of Complex I are related to bidirectional NAD^+-reducing Ni-Fe hydrogenase from *Alcaligenes eutrophus* which uses NADH or NADPH to reversibly oxidize hydrogen [modified from . Efremov and Sazanov, 2012]

Mammalian Complex I Assembly

The mammalian Complex I is the most intricate structure of NADH:oxidoreductases, as it requires the combination of 44 protein subunits, encoded by two genomes, and at least nine cofactors. The nDNA-encoded subunits must assemble in coordination with the hydrophobic mtDNA-encoded subunits to form the functioning mature holocomplex.

Thus, the assembly of these subunits into a functional holoenzyme is a very complicate process to characterize due to the large size and numerous subunits of the enzyme, lack of a detailed crystal structure, and its dual genomic control.

It has been extensively demonstrated that Complex I assembly is disturbed if one of the structural subunits or assembly factors is altered [Janssen et al, 2006]. Since isolated Complex I deficiency is the main form of defective oxidative phosphorylation, the assembly of this enzyme is being elucidated by the characterization of intermediate subcomplexes and assembly factors from samples of patients with mutations in one of the subunits or with cybrid cell line models (cells depleted of mitochondrial DNA that can be repopulated with mutant DNA to study specific mutations in a control background) [Mimaki et al, 2012].

In the last years several models for the assembly of mammalian Complex I have been proposed [Antonicka et al, 2000. Lazarou et al, 2007. Ugalde et al, 2004b. Vogel et al, 2007]. Although these models show some differences, the recent consensus agrees that an early assembly intermediate is anchored to the membrane prior to its extension with additional membrane and peripheral subunits [McKenzie and Ryan, 2010] (Figure 1.20).

The early assembly stage starts with the preassembling of hydrogenase subcomplex, where core subunits 49 kDa and 30 kDa (NDUFS2 and NDUFS3 human nomenclature) form a small hydrophilic assembly complex. [Vogel et al, 2007]. This intermediate subcomplex further expands by the incorporation of hydrophilic subunits, PSST, TYKY, and 39 kDa (NDUFS7, NDUFS8, and NDUFA9), the connective module between the peripheral and membrane arms [Wessels et al, 2009. Ugalde et al, 2004a. Bourges et al, 2004]. This intermediate is further

anchored to the membrane by assembly chaperones [Saada et al, 2009]. The mtDNA encoded ND1 subunit thus, anchors peripheral arm to the inner mitochondrial membrane [Yano, 2002], forming an intermediate of ~400-kDa [Lazarou et al, 2007].

By the other side, independently N2, ND3, and ND4L are assembled into a ~460-kDa membrane intermediate. The incorporation of ND6 brings together both ~460-kDa membrane subcomplex and the~400-kDa module at a later stage and this is the last entry point of the mitochondrially encoded subunits [Perales-Clemente et al, 2010].

The binding of these subcomplexes form the ~650-kDa intermediate under the presence of several assembly factors [Sugiana et al, 2008.Nouws et al, 2010]. With the association of another membrane complex containing ND4, ND5, and possibly subunit B14.5 (NDUFC2), a ~830 kDa assembly intermediate is formed [Gershoni et al, 2010].

Meanwhile, the hydrophilic NADH: dehydrogenase module containing 51 kDa, 24 kDa, and 75 kDa (NDUFV1, NDUFV2, and NDUFS1) subunits, is assembled independently with several nDNA-encoded subunits that are directly or indirectly involved in binding and oxidizing NADH [Lazarou et al, 2007].

With the addition of the NADH: dehydrogenase module and the remaining subunits, the mature holoenzyme is assembled. In this concerted and elaborate assembly process, several assembly factors with unknown functions and undiscovered proteins are involved [Carilla-Latorre et al, 2010. Calvo et al, 2010].
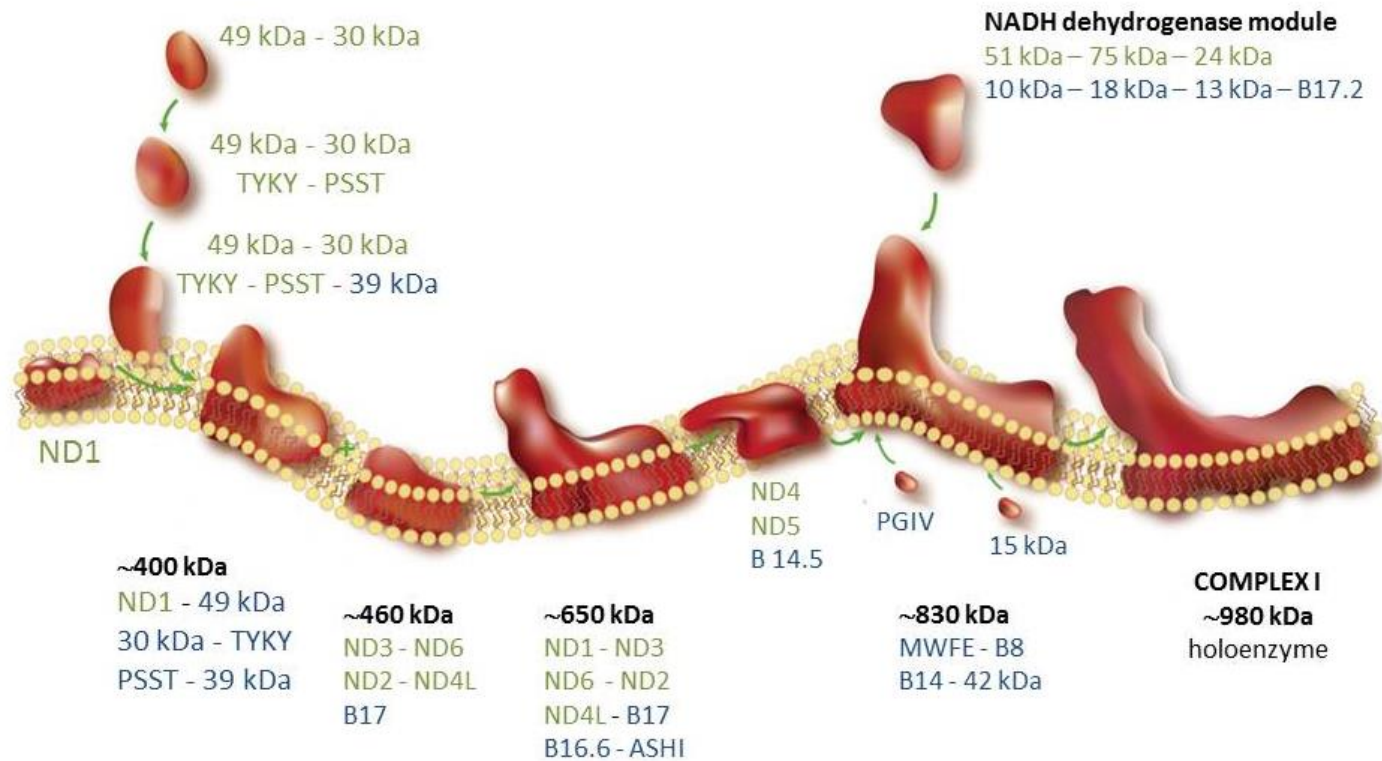
Figure 1.20: The assembly model of mammalian Complex I biogenesis. In the early assembly stages, the core subunits 49 kDa and 30 kDa form a small hydrophilic assembly complex, which further expands by the incorporation of hydrophilic subunits such as TKYK, PSST and later 39 kDa. This peripheral complex, together with a small membrane complex containing mtDNA-encoded subunit ND1, forms a ~400 kDa assembly intermediate. This ~400 kDa complex incorporates with a ~460 kDa membrane complex containing ND3, ND6, ND2, ND4L and B17 subunits to form a ~650 kDa complex. With the association of another membrane complex having ND4, ND5 and probably subunit B14.5, a ~830 kDa assembly intermediate is formed. Meanwhile, a hydrophilic complex, NADH: dehydrogenase module (N module) is assembled by some nDNA-encoded subunits directly or indirectly involved in binding and oxidizing NADH. With the addition of the N module and remaining subunits (such as the intermembrane space subunits PGIV and 15 kDa), mature complex I is assembled. The nDNA-encoded subunits are colored with blue. The mtDNA-encoded-subunits are in green. [modified from Mimaki et al, 2012]

Catalytic activity of Complex I

NADH oxidation and intramolecular electron transfer

The physiological activity of Complex I is the electron transfer from NADH (E_{m7} = −320 mV) to ubiquinone ($E_{m7} \cong$ +90 mV), this process is coupled to the formation of an electrochemical membrane potential. Despite a difference in the substrate redox potentials of about 400 mV, the reaction catalyzed by Complex I is fully reversible. It was demonstrated that in the presence of a protonmotive force mitochondria can transfer electrons from succinate onto NAD^+ [Klingenberg and Slenczka, 1959. Chance and Hollunger, 1960].

During the catalytic cycle two electrons are transferred from NADH to the non-covalently bound FMN as a hydride ion. Upon binding, the nicotinamide ring of NADH forms stacking interactions with the isoalloxazine ring of FMN, thus providing a favorable geometry for efficient hydride transfer between C^{4N} of NADH and N^5 of FMN [Berrisford and Sazanov, 2009]. The distance between these two atoms (3.2 Å) is slightly shorter than average for flavoenzymes [Fraaije and Mattevi, 2000], consistent with fast rates of hydride transfer in Complex I [Verkhovskaya et al, 2008].

The midpoint redox potential of the $FMN/FMNH_2$ couple was determined to −320 mV [Sled et al, 1994. Bungert et al, 1999. Kohlstädt et al, 2008]. Electrons are passed from the reduced FMN though the seven active Fe-S clusters (N3, N1b, N4, N5, N6a, N6b and N2) to the ubiquinone binding site at the interface between the two arms.

Cluster N3, represents the entrance of the electron transfer chain. The edge-to-edge distances between the clusters of the chain vary from 8.5 to 14 Å. Thus, all distances are compatible with the physiological electron transfer rate [Moser et al, 2006] (Figure 1.12).
The short distances between the individual Fe-S guarantee an electron transfer rate faster than the physiological turnover.

Cluster N2, the last redox center in the chain, transfer electrons to ubiquinone. The reduction of ubiquinone to ubiquinol is a two electron process, and so one-electron reduced semiquinone intermediates may be formed during turnover.

It has been demonstrated that N2 [Ohnishi 1998. Ingledew and Ohnishi, 1980], interacts paramagnetically with two semiquinone species that accumulate during steady-state turnover and differ in their spin relaxation behavior [Vinogradov et al, 1995. Yano et al, 2005]. The fast-relaxing species Q_{Nf} is only detected in the presence of a membrane potential, whereas the slow-relaxing species Q_{Ns} is also observed in both the absence and presence of membrane potential. It was shown that N2 interacts with the semiquinone radicals [Ohnishi and Salerno, 2005].

The interaction distance between N2 and Q_{Nf} was determined to 12 Å, while that between N2 and Q_{Ns} might be larger than 30 Å [Ohnishi et al 2010a. Ohnishi et al 2010b].

Ubiquinone reduction and coupling mechanism

The midpoint redox potential of NADH is about -320 mV and of the Q/QH2 pair ~ +100 mV (for ubiquinone) [Efremov and Sazanov, 2012]. Theore, most of the redox energy in Complex I is released during quinone reduction. Some of it would be also released upon reduction of cluster N2, resulting in the observed conformational changes [Berrisford and Sazanov, 2009].

Sazanov and co-workers, recently have proposed that the catalytic cycle of Complex I is likely to proceed via a negatively charged ubiquinol intermediate Q^{2-} [Efremov and Sazanov, 2012]. Either Q^{2-} or key charged residues nearby are likely to remain unprotonated in order to drive conformational.

The design of the enclosed Q-site is well suited for this purpose: the binding of the quinone at the deep end of sealed cavity, with protein tightly packed around the headgroup, will prevent solvent access and quinone protonation by means other than coordinating residues Tyr87 (Tyr141 in *B. taurus*) and His38 (His34 in *B. taurus*).

The charged residues can exist in this chamber because it is relatively hydrophilic and distal from the membrane. The Q-site is linked to the centre of the E-channel by a hydrophilic funnel (Figure 1.21).

Thus, the negatively charged ubiquinol (or adjacent charged residues) can interact electrostatically with these negatively charged residues driving conformational changes in this channel.

Additional driving force is probably provided by conformational movements of 49 kDa and PSST subunits upon N2 reduction, which directly interact with flexible parts of ND1 [Berrisford and Sazanov, 2009.Berrisford et al, 2008].

The flexible hydrophilic axis connects the half-channels in the middle of the membrane domain, linking membrane subunits in an overall conformational cycle that probably involve both helix HL and βH (coupling elements) [Efremov and Sazanov, 2011].

Tight coupling observed between proton translocation and quinone chemistry [Efremov and Sazanov, 2011] can be explained if opening of the Q-site entrance to allow quinone in and out forms a part of this cycle.

According to this *conformational switch model*, the electrostatically and N2-driven E-channel drives conformational changes first in the neighbouring antiporter ND2, which in its turn drives distal subunits ND4 and ND5. All through the hydrophilic central axis. The extent of the movement of the two coupling elements during the catalytic cycle is currently unclear, but authors hypothesize that these elements probably contribute at least to the coordination between the three antiporters. These concerted conformational changes would lead to changes in pKa and solvent exposure of key residues, resulting in proton translocation [Baradaran et al, 2013] (Figure 1.21).

Complex I inhibitors

Complex I is inhibited by a variety of compounds [Friedrich et al, 1994] from rotenone, to a number of synthetic insecticides/acaricides [Lümmen, 1998]. With the exception of a few inhibitors that inhibit electron input into Complex I such as rhein [Kean et al, 1971] and diphenyleneiodonium [Majander et al, 1994], all inhibitors act at the terminal electron transfer step of this enzyme [Friedrich et al. 1994] and it is commonly accepted that act at the ubiquinone reduction site [Fendel et al, 2008]. Complex I inhibitors have been grouped into three classes [Degli Esposti, 1998] (Table 1.5).
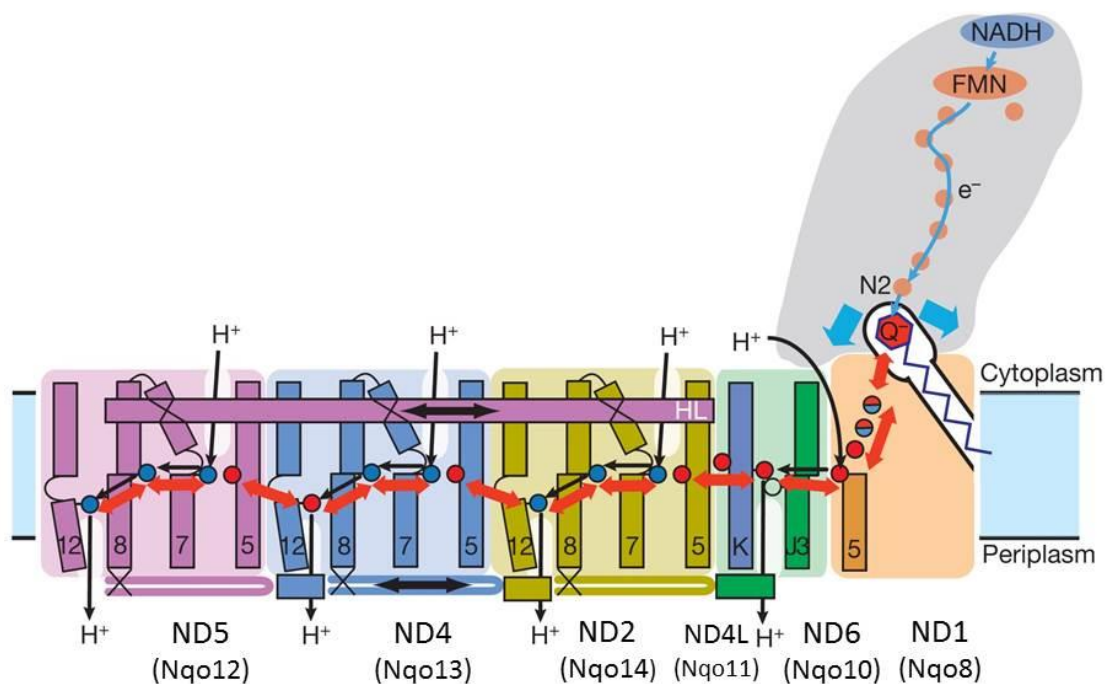
Figure 1.21: Proposed coupling mechanism of Complex I. Scheme showing key helices and residues. Upon electron transfer from cluster N2, negatively charged ubiquinol initiates a cascade of conformational changes, propagating from the E-channel (ND1, ND6, ND4L subunits) to the antiporters throught the central axis (red arrows) of charged and polar residues located around flexible breaks in key transmembrane helices (TM). Cluster-N2-driven shifts of 49 kDa and PSST helices (blue arrows) probably assit overall conformational changes. Helix HL and the βH element help to coordinate conformational changes by linking discontinuous TM helices between antiporters. In the antiporters, residues of Lys from the first half-channel are assumed to be protoned in the oxidized state. Upon reduction of ubiquinone and subsequent conformational change, the first half-channel closes to the mitochondrial matrix (or cytoplasm), a Glu residue of TM5 moves out and Lys residue of TM7 donates its proton to the connecting Lys/His TM8 and then onto Lys/Glu TM12 from the second half-channel. Lys/Glu TM12 ejects its proton into the intermembrane space (or periplasm) upon return from reduced to oxidized state. A fourth proton per cycle is translocated in the E-channel in a similar manner. TM helices are numbered (GluTM5, LysTM7, Lys/GluTM12, Lys/HisTM8 from ND5, ND4, and ND2. Glu67, Glu32 from ND4L). Key charged residues and some residues from the connection to Q cavity are indicated by red circles for Glu and blu circles for Lys/His. [from Baradaran et al, 2013]

Table 1.5: Functional classification of Complex I inhibitors

Inhibitor class	Representative compounds
Type A: quinone antagonists	Rolliniastin-2
	Piericidin A
	Idebenone
Type B: semiquinone antagonists	Rotenone
	Piericidin A
	Piercidin B
	Amytal
	4-alkyl-acridones
	4'-alkyl-MPP+analogues
	Phenoxan
Type C: quinol antagonists	Quinol products
	Reduced ubiquinone-2
	Myxothiazol
	Stigmatellin

Data from [Lenaz and Genova, 2010]

ROS PRODUCTION IN COMPLEX I

ROS is an acronym for *reactive oxygen species*, and this phrase is used to describe a variety of molecules and chemical species with one unpaired electron derived from molecular oxygen.

Molecular oxygen O_2 in ground state is a bi-radical, containing two unpaired electrons with the same spin (triplet state). These electrons, make molecular oxygen a not very reactive molecule. However, inverting the spin of one of the unpaired electrons by an energy input converts O_2 into a much more reactive molecule (singlet state, $^1O_2$). The resulting species become a powerful oxidant as the two electrons with opposing spins can quickly react with other pairs of electrons.

The univalent reduction of molecular oxygen produces intermediates relatively stable. If a single electron is supplied to O_2 it enters one of its two degenerate molecular orbitals (π^* orbitals) forming an electron pair, thus leaving only one unpaired electron and negative charge: superoxide anion radical ($O_2^{\bullet-}$) (equation1.1).

The addition of another electron gives the *peroxide* ion, which is a weaker acid and is protonated to hydrogen peroxide H_2O_2 (equation 1.2). This last molecule, can be reduced producing water (equation 1.4)

If H_2O_2 is reduced by metal ions (*e.g.* Fe^{2+}), the hydroxyl radical $OH\bullet$ is produced (*Fenton reaction*) (1.5). The hydroxyl radical is extremely reactive.

$$O_2 + 1e^- \ \rightarrow \ O_2\bullet^- \tag{1.1}$$

$$O_2\bullet^- + 1e^- + 2H^+ \ \rightarrow \ H_2O_2 \tag{1.2}$$

$$O_2 + 2e^- + 2H^+ \ \rightarrow \ H_2O_2 \tag{1.3}$$

$$H_2O_2 + 2e^- + 2H^+ \ \rightarrow \ 2H_2O \tag{1.4}$$

$$Fe^{2+} + H_2O_2 \ \rightarrow \ Fe^{3+} + OH\bullet + x \ (\text{Fenton reaction}) \tag{1.5}$$
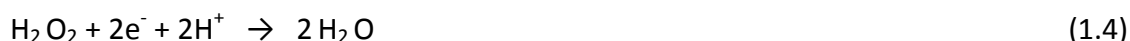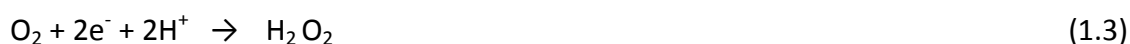
Mitochondria are an important source of ROS (reactive oxygen species) within most mammalian cells with the oxygen superoxide anion ($O_2^{\bullet-}$) being the primary mitochondrial ROS that is generated mainly by Complex III and Complex I [Lenaz, 2012]

ROS contributes to mitochondrial damage of proteins, lipids and DNA (oxidative stress) and is also important in in many signaling pathways (Figure 1.22 and 1.23). Therefore, only excessive ROS production (or defect of protective systems) leads to oxidative stress and pathological conditions. Whether cells will suffer from oxidative stress, depends on the balance between the continuous production of ROS and their removal by endogenous detoxification systems.
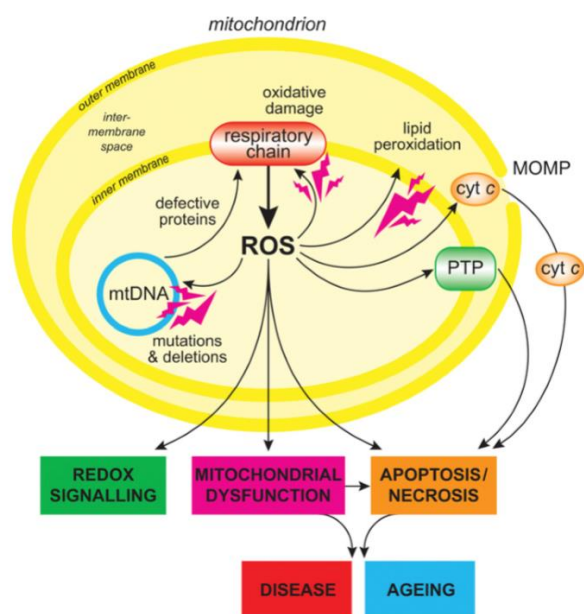
Figure 1:22: Overview of mitochondrial ROS production. ROS production by mitochondria can lead to oxidative damage to mitochondrial proteins, membranes and DNA (oxidative stress), impairing the ability of mitochondria to synthesize ATP and to carry out their wide range of metabolic functions, including the tricarboxylic acid cycle, fatty acid oxidation, the urea cycle, amino acid metabolism, haem synthesis and FeS centre assembly that are central to the normal operation of most cells (energetic failure). Mitochondrial oxidative damage can also increase the tendency of mitochondria to release intermembrane space proteins such as cytochrome *c* (cyt *c*) to the cytosol by mitochondrial outer membrane permeabilization (MOMP) and there by activate the cell's apoptotic machinery. In addition, mitochondrial ROS production leads to induction of the mitochondrial permeability transition pore (PTP), which renders the inner membrane permeable to small molecules in situations such as ischaemia/reperfusion injury. Consequently, it is unsurprising that mitochondrial oxidative damage contributes to a wide range of pathologies. In addition, mitochondrial ROS may act as a modulatable redox signal, reversibly affecting the activity of a range of functions in the mitochondria, cytosol and nucleus. [From Murphy, 2009]
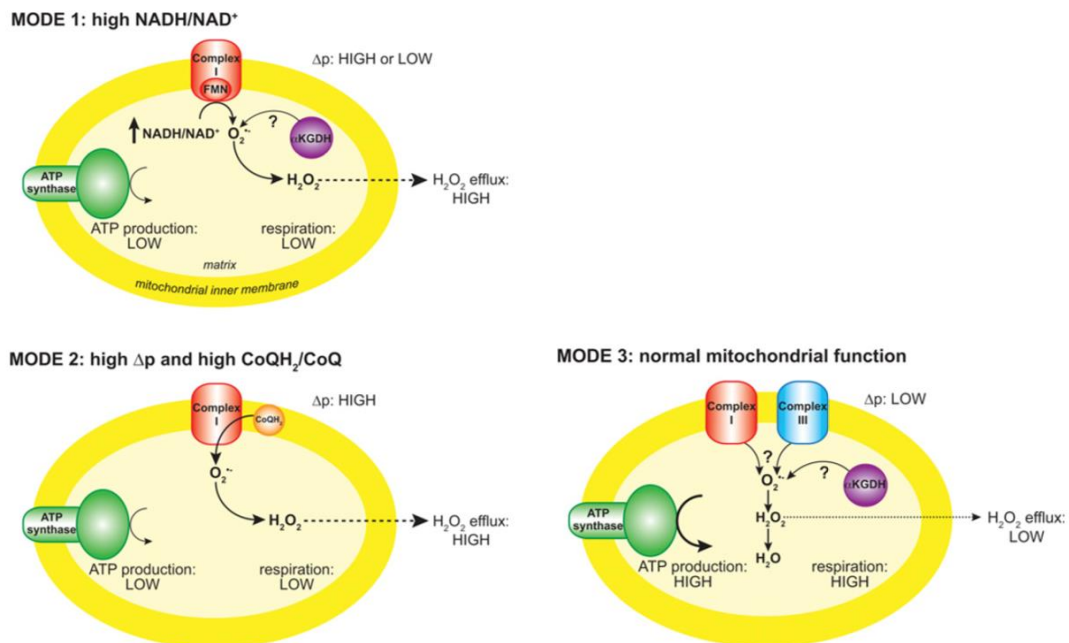
Figure 1.23: Modes of mitochondrial operation that lead to $O_2^{\bullet-}$ production. There are three modes of mitochondrial operation that are associated with $O_2^{\bullet-}$ production. In mode 1, the NADH pool is reduced, for example by damage to the respiratory chain, loss of cytochrome c during apoptosis or low ATP demand. This leads to a rate of $O_2^{\bullet-}$ formation at the FMN of complex I that is determined by the extent of FMN reduction which is in turn set by the NADH/NAD+ ratio. Other sites such as αKGDH may also contribute. In mode 2, there is no ATP production and there is a high Δp and a reduced CoQ pool which leads to RET through Complex I, producing large amounts of $O_2^{\bullet-}$. In mode 3, mitochondria are actively making ATP and consequently have a lower Δp than in mode 2 and a more oxidized NADH pool than in mode 1. Under these conditions, the flux of $O_2^{\bullet-}$ within mitochondria is far lower than in modes 1 and 2, and the $O_2^{\bullet-}$ sources are unclear. [From Murphy, 2009]

The midpoint redox potential of mitochondrial superoxide production is between 100 – 250 mV, and a low oxygen concentrations is 68 mV. [Murphy, 2009].

Therefore, *in vivo*, the one-electron reduction of O_2 to $O_2 \bullet^-$ is thermodynamically favored, even by relatively oxidizing redox couples, and a wide range of electron donors within mitochondria could potentially carry out this reaction.

However, only a small proportion of mitochondrial electron carriers with the thermodynamic potential to reduce O_2 to $O_2 \bullet^-$.

Early experiments proved the involvement of Complex I in ROS production [Takeshige and Minakami, 1979. More recent studies confirmed that Complex I is a major source of superoxide production in mitochondria [Lenaz, 2012]

The superoxide production by Complex I is higher during the reverse electron transport (RET) from succinate to NAD^+, whereas during the forward electron transport it is much lower [Turrens 2003].

In addition, it has been demonstrated that rotenone enhances ROS formation during forward electron transfer [Herrero and Barja, 2000. Genova et al. 2001] and inhibits it during reverse electron transfer.

The identification of the oxygen reducing site has been the subject of extensive investigation, and debate as several prosthetic groups in the enzyme have been suggested to be the direct reductants of oxygen (Figure 1.24).

These include FMN, ubisemiquinone, and iron sulphur cluster N2 [Fato et al, 2009].

In isolated Complex I, fully reduced FMN is considered the major electron donor to oxygen to form superoxide anion [Galkin and Brandt, 2005. Kussmaul and Hirst, 2006]

In mitochondrial membranes, however, the identification of flavin as the site of oxygen reduction is incompatible with the finding that two classes of inhibitors both acting downstream of the iron sulphur clusters in the enzyme have opposite effects, in that rotenone enhances superoxide production whereas stigmatellin inhibits it [Fato et al, 2009]

However, Hirst *et al* (208) admit the possible presence of two oxygen-reacting sites at the two ends of the cofactor chain, ascribing the distal one to ROS generation during reverse electron transfer. The superoxide production by Complex I is maximal during reverse electron transfer, however the site of oxygen reduction in this instance is even less well defined [Murphy, 2009].

The electron donor to ubiquinone in the Complex is FeS cluster N2 [Ohnishi et al, 1998]. It is likely that this centre is also the electron donor to oxygen both directly and via one-electron reduction of several exogenous quinones.

Ohnishi *et al*. [Ohnishi et al, 2010c] presented a new hypothesis that the generation of superoxide reflects a dynamic balance between the flavosemiquinone (semiflavin or S_F) and the CoQ semiquinone (S_Q). In a purified preparation of Complex I, during catalytic electron transfer from NADH to decyl ubiquinone, the superoxide generation site was mostly shifted to the S_Q. A quinone-pocket binding inhibitor (rotenone or piericidin A) inhibits the catalytic formation of the SQ, and it enhances the formation of SF and increases the overall superoxide generation. This suggests that if electron transfer was inhibited under pathological conditions, superoxide generation from the SF would be increased. The identification of SQ rather than N2 as the electron donor to oxygen is however in contrast with the findings reported in the previous section showing that when SQ reduction to QH_2 is blocked by stigmatellin no superoxide is produced [Fato et al, 2009].
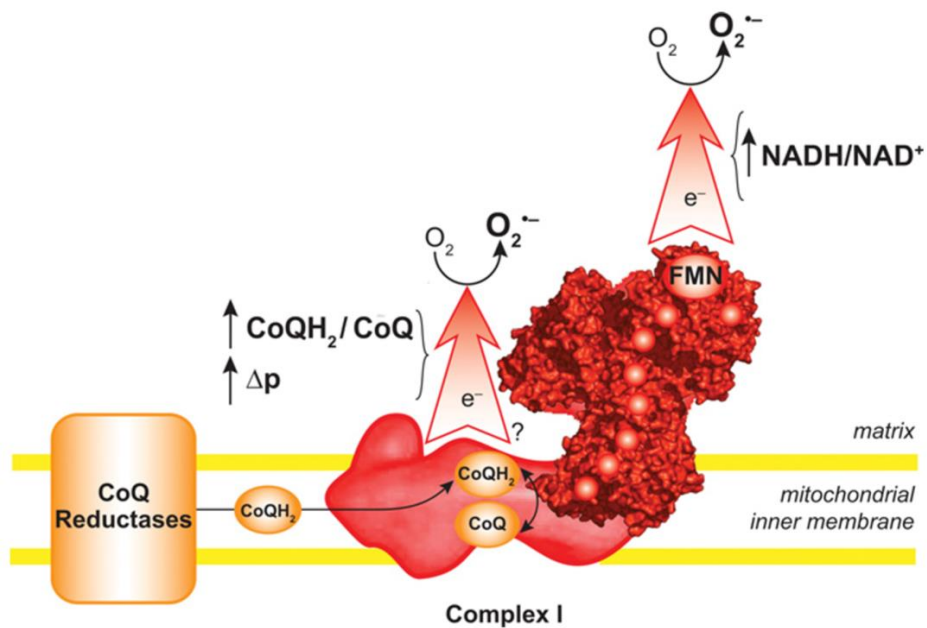
Figure 1.24: Production of $O_2^{\bullet-}$ by Complex I. The location of the FMN and the Fe-S clusters in the hydrophilic arm are indicated, along with the putative CoQ-binding site. In mode1, there is extensive $O_2^{\bullet-}$ production from the FMN in response to a reduced NADH pool. In mode 2, a high Δp and a reduced CoQ pool lead to RET and a high flux of $O_2^{\bullet-}$ from the complex. The site of this $O_2^{\bullet-}$ production is uncertain, hence the question mark, but may be associated with the CoQ-binding site.

A possible explanation is that two sites for oxygen reduction exist in the complex, represented by flavin and an iron-sulphur cluster; the latter site would be predominant in membrane particles whereas the former might be available after Complex I isolation [Lenaz, 2012].

In the present study, we demonstrate a possible different interpretation involving the supramolecular assembly of Complex I

Supercomplexes and ROS production in Complex I

Indirect circumstantial evidence suggests that supercomplex assembly may limit the extent of superoxide generation by the respiratory chain.

Panov et al. (2007) reason that the respirasome helps to maintain the redox components of the complexes in the oxidized state through the facilitation of electron flow by channeling, thus limiting ROS formation.

Similarly, Seelert et al. (2009) also suggest that facilitation of electron transfer by channeling may limit the production of ROS.

As mentioned in the previous section, two potential sites for oxygen reduction exist in Complex I, represented by FMN and iron–sulphur cluster N2.

Controversial results from different laboratories working either on isolated Complex I or on mitochondrial membranes generally indicate that N2 as a source of ROS would be predominant in membrane particles whereas FMN might become available after Complex I isolation.

A reasonable hypothesis is that supercomplexes assembly may modify the conformation of its component complexes confering a more shielded structure to FMN in Complex I, and this prosthetic group becomes exposed to oxygen only when Complex I is dissociated from Complex III (Figure 1.25)

Although the molecular structure of the individual complexes does not allow to envisage a close apposition of the matrix arm of Complex I, where FMN is localized, with either Complex III or IV [Dudkina et al 2005b; Schäfer et al 2007], the actual shape of the $I_1III_2IV_1$ supercomplex from bovine heart [Schäfer et al 2007] suggests a slightly different conformation of Complex I in the supercomplex, showing a smaller angle of the matrix arm with the membrane arm and a higher bending towards the membrane (and presumably Complex III), in line with the notion that Complex I may undergo important conformational changes.

Moreover, the observed destabilization of Complex I in the absence of supercomplex may render the 51 kDa subunit containing the FMN more slightly untied from the protein framework allowing it to interact with oxygen.
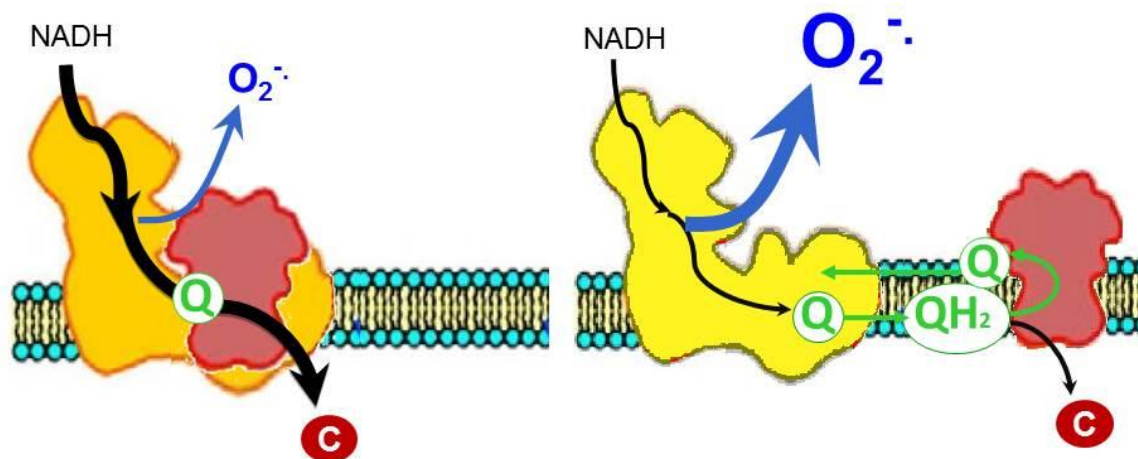
Figure 1.25: Production of $O_2^{\cdot-}$ by Complex I in I_1III_2 supercomplex.

HYPOTHESIS

As discussed in the previous sections, the main redox components responsible for oxygen reduction to superoxide in mitochondria are situated in Complex I and in Complex III. In particular, conditions limiting the electron flow within Complex I induce large excess of superoxide production [Lenaz, 2012].

Since dissociation of the supercomplex I_1III_2 limits electron transfer between Complex I and III and in addition destabilizes Complex I, a reasonable question is whether such condition is also bound to enhance and/or modify the normal ROS production from the Complex I.

In addition, indirect evidence suggests that supercomplex assembly may limit the extent of ROS production by the respiratory chain where respirasomes helps maintaining redox components of the complexes in the oxidized state through channeling of the electron flow [Panov et al, 2007].

A reasonable hypothesis is that reducing prosthetic groups becomes exposed to oxygen only when Complex I is dissociated from Complex III.

Following this line of thought, our study hypothesis is that disruption or prevention of the association between Complex I and Complex III by different means enhace the generation of reactive oxygen species from Complex I.

To demonstrate this hypothesis, we have decided to investigate ROS production by Complex I under conditions in which the complex is arranged as a component of the super-complex I_1III_2 or dissociated as an individual holoenzyme.

Hence, our experimental studies were in two experimental systems in which the supramolecular organization of respiratory assemblies is impaired by:

(i) Treatment either of bovine heart mitochondrial membranes or supercomplex I1III2 reconstituted in liposomes with dodecylmaltoside.

(ii) Reconstitution of Complex I and Complex III at high lipid:protein ratio

MATERIALS AND METHODS

MATERIALS

Reagents and solutions

2',7'-dichlorodihydrofluorescein diacetate (DCFDA) was purchased from Molecular Probes (Invitrogen). All other chemicals were purchased from Sigma-Aldrich, unless specifically indicated and used without further purification.

All solutions were prepared with Milli-Q water (18.2 MΩ cm^{-1}) from a Milli-Q purification system (Branstead, USA). pH is adjusted with either HCl 0.1 N or NaOH 0.1 N.

1. **SUCROSE SOLUTION pH 7.6**

   0.25 M sucrose – 10 mM Tris base

2. **BUFFER SOLUTION B pH 7.2**

   0.22 M *D*-mannitol – 70 mM sucrose – 10 mM Tris base – 1 mM EDTA

3. **TSH SOLUTION pH 8.0**

   0.66 M sucrose – 50 mM Tris base – 1 mM *L*-Histidine

4. **REACTION SOLUTION pH 7.4**

   50 mM KCl – 10 mM Tris base – 1 mM EDTA

5. **BIURET REAGENT**

   0.15% (w:v) $CuSO_4.5H_2O$ - 0.6% (w:v) potassium sodium tartrate - 10% (w:v) NaOH

6. **LOWRY STOCK SOLUTION A**

   2% (w:v) Na_2CO_3 in 0.1 N NaOH

7. **LOWRY STOCK SOLUTION B**

   1% (w:v) $CuSO_4.5H_2O$

8. **LOWRY STOCK SOLUTION C**

   2% (w:v) potassium sodium tartrate

METHODS

Preparation of bovine heart mitochondria (BHM)

B. taurus heart mitochondria (BHM) are prepared by a large scale procedure described by Smith [Smith, 1967] as follows:

One or two beef hearts are obtained from the slaughterhouse within 1 - 2 hours after the animal is slaughtered. The hearts are placed on ice to ensure tissue cooling for transport until use. All subsequent procedures are carried out at 2 - 4°C.

Fat and connective tissue are removed from the heart, and the tissue cut into approximately 5 cm cubes. These meat cubes are washed twice with sucrose solution and passed through a meat grinder which is maintained at 4°C. The plate holes of the meat grinder are 4 - 5 mm in diameter. The resulting ground mince is diluted in sucrose solution (final concentration: 200 grams of meat / 400 ml). Since the pH of this mixture drops between 6 - 5.5 which may affect to mitochondria, it is necessary to adjust the pH to 7.5 ± 0.1 continuously. This is accomplished by the addition of drops of 1M Tris solution (pH 10.8 unneutralized).

The neutralized ground heart mince is placed in a blender. The blender is operated at high speed for 20 seconds and the pH of the homogenate is adjusted to 7.6 with 1 M Tris. The homogenate is centrifuged for 20 minutes at 1,200 *g* at 4°C (Beckman Avanti J25 centrifuge, JA-10 rotor) to remove unruptured muscle tissue and nuclei. The supernatant solution is caully decanted so that the loosely packed layer is not disturbed. The pH of the suspension is readjusted to 7.6, and centrifuged for 30 minutes at 7,800 *g* at 4°C (Beckman Avanti J25 centrifuge, JA-10 rotor).

The resulting pellets consist of a large proportion of light, loosely packed, buff-colored layer of broken mit0ochondria (light beef heart mitochondria, LBHM) and a dark brown layer (heavy beef heart mitochondria, HBHM). Pellets are then dislodged by means of a glass stirring rod, mixed with 10 ml of sucrose solution / tube, and collected.

This suspension is diluted at 200 ml final volume with sucrose solution and centrifuged for 40 minutes as above. Supernatant is caully decanted and discarded. Afterwards, pellet is suspended in approximately 10 ml of sucrose solution/centrifuge tube and collected.

This mitochondrial suspension is hand-homogenized in a Potter-Elvehjem glass tube with Teflon pestle while standing on ice. The volume of the homogenate is adjusted to 100 ml with the sucrose solution, and the pH is adjusted to 7.6 with 1M Tris.
The protein concentration is determined by the biuret method and once the concentration is adjusted by dilution with sucrose solution at 20 - 40 mg protein per milliliter, the samples are stored at -80°C. The average yield should be approximately 1 mg protein per gram of starting mince.

Previous assaying enzymatic activities it is necessary to obtain mitochondria as opened membranes devoid of substrate permeability barriers for NADH and other substrates. To accomplish that, BHM are thawed and frozen 2 - 3 times. Once diluted at 2 mg·ml^{-1} in buffer solution B. The suspension is subjected to ultrasonic irradiation with 10-second periods and 50-second intervals during 5 minutes at 150 W with a probe tip sonicator (Labsonic U2000, B. Braun Biotech International GmbBH) under a nitrogen flux in an ice-water bath.

Preparation of bovine submitochondrial particles (SMP)

Bovine submitochondrial particles (SMP) are prepared from bovine heart mitochondria (BHM) by ultrasound irradiation of the frozen and thawed BHM according to a modified version of Beyer [Beyer, 1967]; resulting in broken membrane fragments [Fato et al, 1993]. More in detail:

Approximately 6 mg of BHM are diluted at approximately 15 mg protein·ml^{-1} in buffer solution B. Thereafter, the mitochondria suspension is subjected to ultrasonic irradiation with 30-second periods and 30-second intervals during 4 minutes, at 220-230 W with a probe tip sonicator (Labsonic U2000, B. Braun Biotech International GmbBH) under a nitrogen flux in an ice-water bath.

The suspension is centrifuged at 11,000 g for 20 minutes at 4°C (Beckman Avanti J25 centrifuge, JA-20 rotor) to remove unruptured mitochondria. The supernatant solution is caully decanted and centrifuged at 145,000 g for 40 minutes at 4°C (Beckman L8M ultracentrifuge, Type 50.2 Ti rotor). The resulting pellet is collected, suspended in about 20 ml of buffer solution B and centrifuged as above at 145,000 g for 40 minutes.

The pellet is washed twice with buffer B solution to remove any traces of mitochondrial superoxide dismutase (SOD), then suspended in 10 ml of this solution, and hand-homogenized in a Potter-Elvehjem glass tube with a Teflon pestle while standing on ice.

Once the protein concentration is determined by the biuret method, samples are aliquoted and stored at -80°C.

Purification of bovine Complex I-III fraction (R4B fraction)

A crude mitochondrial fraction enriched in Complex I and Complex III (R4B) is obtained by a fractioning procedure which involves the use of deoxycholate in conjunction with KCl, for membrane solubilization, and ammonium acetate for precipitation of the desired complexes, as described by Hatefi and Rieske [Hatefi and Rieske, 1967].

In brief, bovine mitochondria (BHM) are treated with deoxycholate / KCl to solubilize complexes I, II, III, and V leaving the Complex IV insoluble. The solubilized material is separated by centrifugation and dialyzed. This procedure results in the precipitation of complexes I, II and III which are separated by centrifugation from Complex V in the supernatant. Then, the binary Complex I-III is separated by precipitation with ammonium acetate (Figure 2.1).
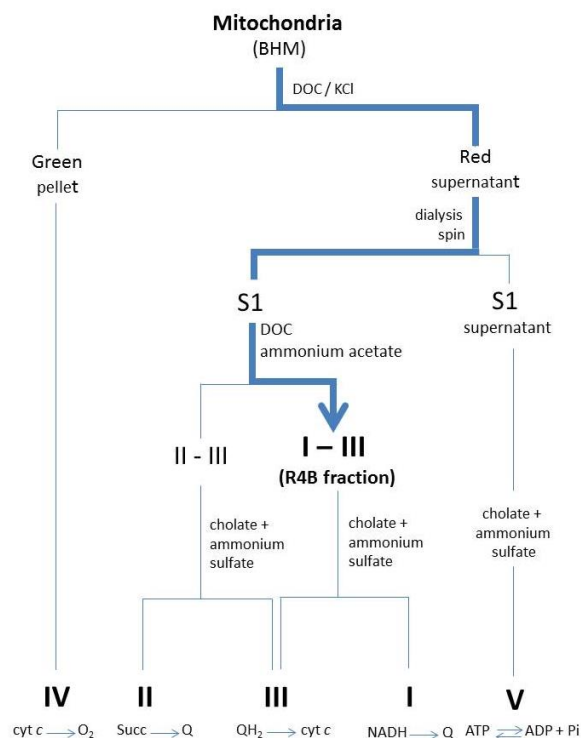
Figure 2.1: Purification of bovine Complex I-III fraction. An outline of the purification scheme devised by Hatefi et al [Hatefi et al, 1967] to obtain all five respiratory complexes from the inner mitochondrial membrane of bovine heart. The complexes are assayed and defined by the reactions shown at the bottom. Bold blue lines point out purification with the procedures performed to obtain Complex I-III (R4B fraction)

More in detail:

The frozen suspension of mitochondria is thawed and diluted to a protein concentration of about 30 mg·ml^{-1} in TSH solution and then centrifuged at 32,000 g for 30 minutes at 4°C (Beckman Avanti J25 centrifuge, JA-20 rotor). After centrifugation, the loosely packed mitochondria pellet is suspended in TSH solution to about 20 mg·ml^{-1}. Sodium deoxycholate (10% w:v, pH 9.0) is added at 0.35 mg per mg of protein followed by the addition of solid KCl to a 72 mg·ml^{-1} ratio.

When the KCl is completely dissolved, the suspension is centrifuged at 75,000 g for 30 minutes at 4°C (Beckman L8M ultracentrifuge, Type 50.2 Ti rotor). The green sediment contains cytochrome c oxidase. The clear red supernatant solution is diluted with 0.25 volumes of cold water and centrifuge as above, at 75,000 g for 30 minutes. The brown-green pellet is discarded and the supernatant, approximately 100 ml, is collected and poured into a dialysis tubing of 12-14 kDa molecular weight cut-off, 14.3 mm diameter, and volume/length of 1.6 ml·cm^{-1} (Visking dialysis tubing, Medicell International Ltd). This sample is dialyzed against 8 volumes of Tris-HCl pH 8.0 for 3 hours.

This dialysis step removes enough KCl and deoxycholate to cause the precipitation of highly insoluble proteins, including complexes I, II, and III. Most of the cytochrome c and other relatively soluble proteins remain in solution. The turbid dialysate is centrifuged again at 75,000 g for 75 minutes. The supernatant is discarded and the red pellet, hereafter erred to as S1 fraction, is suspended in approximately 5 ml of TSH solution and stored overnight at -20°C.

Once the S1 fraction is thawed, protein concentration is determined by biuret method. This suspension is then hand-homogenized in a glass Potter-Elvehjem tube with a Teflon pestle and diluted with the TSH solution to a protein concentration of 10 mg·ml^{-1}. At this point, potassium deoxycholate is added to a concentration of 0.5 mg per milligram of protein followed by the addition of 50% w:v saturated ammonium acetate at 16.5 ml per 100 ml of S1 protein solution. After being allowed to stand for 15 minutes on ice, the turbid sample is centrifuged as above, at 75,000 g for 30 minutes. The residue, a tightly brownish white pellet, will be discarded. The collected supernatant is treated with 6.4 ml of 50% w:v saturated ammonium acetate solution

per 100 ml of supernatant and incubated on ice for 15 minutes. The sample is centrifuged at 75,000 *g* for 30 minutes.

The pellet, consisting of a loosely packed light brown material overlaying a small, more dense, dark brown button, will be be discarded, whereas the supernatant is collected. Afterwards, 50%w:v satured ammonium acetate is added to a ratio of 6 ml per 100 ml solution. The sample is centrifuged as above for 30 minutes at 4°C. The supernatant obtained is then treated with 3.2 ml of 50%w:v satured ammonium acetate solution per milliliter of supernatant solution.

After 15 minutes on ice, the solution is centrifuged as before. The reddish brown pellet designed as R4B fraction is suspended in approximately 2 ml of TSH solution. Protein concentration is determined by the biuret assay. Samples are aliquoted and stored at -80°C.

Preparation of bovine Complex I-III proteoliposomes

Preparation of phospholipid:ubiquinone vesicles

Phospholipid vesicles are prepared according to a modified version of Degli Esposti *et al* [Degli Esposti et al, 1981]:

Dried soybean *L*-α-phosphatidylcholine is dissolved in petroleum ether at 0.3 g·ml^{-1} final concentration. Then, 20 mM Coenzyme Q_{10} (CoQ10) in absolute ethanol is added to a 30 nmole CoQ_{10} per mg phospholipid ratio. Once the mixture is thoroughly mixed, the organic solvent is removed, to yield a lipid film: for small volumes ($\sim$ 1 ml), the solvent is evaporated to dryness under nitrogen stream.

In aqueous solutions phospholipid molecules spontaneously form self-closed spherical or oval structures where several phospholipid bilayers entrap part of the solvent in their interior [Bangham and Horne, 1964. Lasic, 1988]. Thus, multilamellar vesicles (MLVs) are prepared by the swelling of dry phospholipid:ubiquinone films deposited in the walls of the tube. The hydration is accomplished simply by adding an aqueous solution (50 mM KCl, 10 mM Tris, 1 mM EDTA, pH 7.4) at 30 mg phospholipid·ml^{-1} under vigorous mixing and keeping on ice for 10 minutes.

Small unilamellar vesicles are formed when the MLVs dispersion is subjected to ultrasonic irradiation (Figure 2.2)
[Saunders et al, 1962. Papahadjopoulos and Miller, 1967. Papahadjopoulos and Watkins, 1967] at 30-second periods with 30-second intervals for 10 minutes at 150 W with a probe tip sonicator (Labsonic U2000, B. Braun Biotech International GmbBH). In order to prevent overheating and lipid peroxidation, sonication is performed under a nitrogen flux in an ice-water bath. Under these conditions the phospholipid vesicles are monolamellar with a diameter of 350 - 400 Å, as controlled by electron microscopy [Degli Esposti et al, 1981].

The vesicles (PL-vesicles) are stored at 4°C and used within 2 days from preparation.
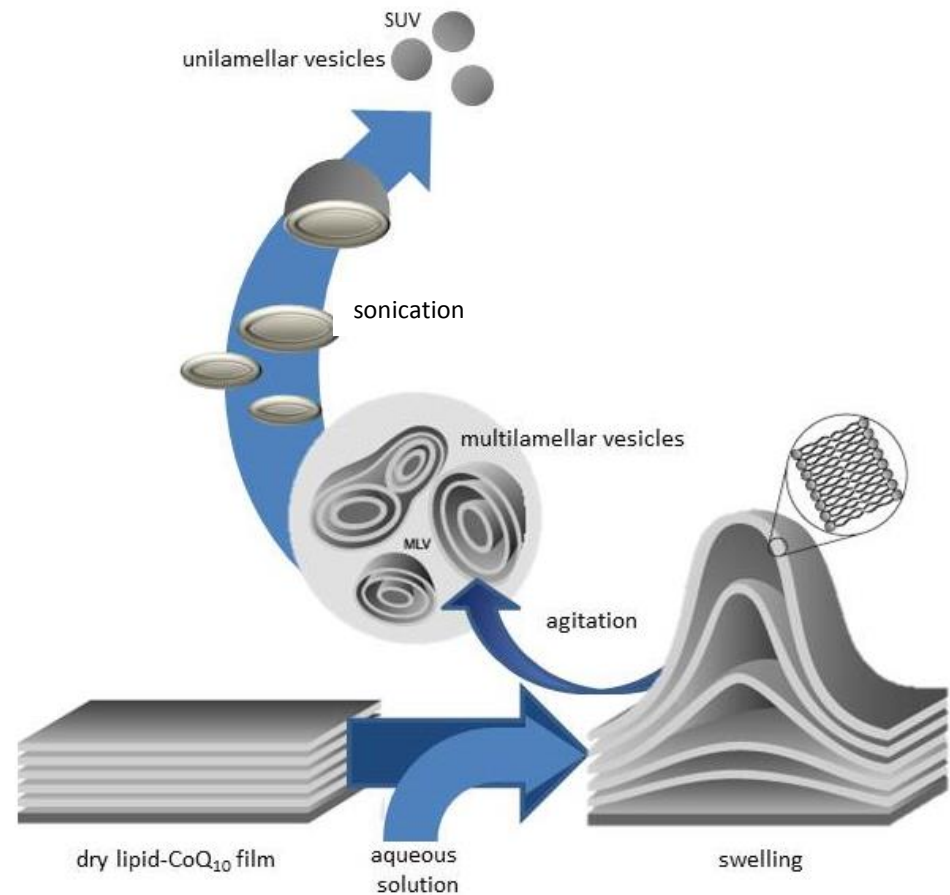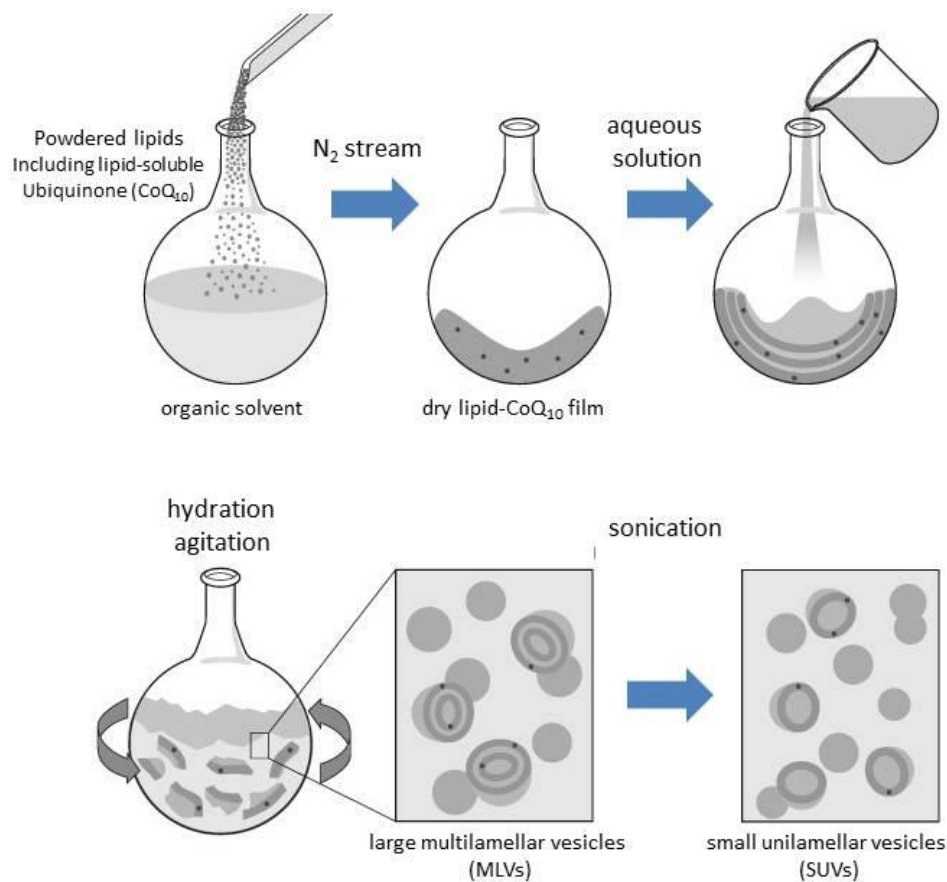
Figure 2.2: Liposomes preparation. Liposomes (lipid vesicles) are formed when thin lipid films are hydrated and stacks of liquid crystalline bilayers become fluid and swell. The hydrated lipid sheets detach during agitation and self-close to form large, multilamellar vesicles (LMV) which prevents interaction of water with the hydrocarbon core of the bilayer at the edges. Once these particles have formed, reducing the size of the particle requires energy input in the form of sonic energy (sonication) or mechanical energy (extrusion).

Proteoliposome reconstitution

The most frequently used strategy for proteoliposome preparation involves the use of detergents. In the standard procedure [Racker et al, 1979], proteins are first co-solubilized with phospholipids in the appropriate detergent in order to form an isotropic solution of lipid-protein-detergent and lipid-detergent micelles. Next, the detergent is removed by diluting the reconstitution mixture resulting in the progressive formation of bilayer vesicles with incorporated protein. Dilution lowers the detergent concentration below its critical micelle concentration (*cmc*) and proteoliposomes form spontaneously [Rigaud et al, 1995. Rigaud and Levy, 2003]. According with a modified procedure of Racker *et al.* [Racker et al, 1979], proteoliposomes are prepared with a crude mitochondrial fraction enriched in Complex I and Complex III (R4B fraction) [Hatefi and Rieske, 1967] and phospholipid:ubiquinone vesicles (PL-vesicles).

Appropriate volumes of R4B sample and PL-vesicles are mixed in the presence of 17 mM n-octyl-D-glucopiranoside to a final concentration of 1.5% w:v at a protein to phospholipid ratio specified in the legends of tables and figures.

After 10 minutes of incubation on ice, the samples are diluted 40-fold with 50 mM KCl, 10 mM Tris, 1 mM EDTA, pH 7.4 to induce proteoliposome formation.

Reconstituted samples are centrifuged at 38,000 *g* for 1 hour at 4°C (centrifuge Beckman Avanti J25, JA-18.1 rotor) to remove detergent traces.

R4B proteoliposomes are diluted to 0.5 mg·ml^{-1} in reaction solution pH 7.4, kept on ice and immediately used.

Determination of protein concentration

Ultraviolet absorbance at 280 nm (range: 0.1 – 1 mg·ml^{-1})

Spectrophotometric measurements of absorption radiation in the near ultraviolet 280 nm to determine the concentration of a protein solution is one of the oldest and most widespread methods for quantitative analysis [Warburg and Christian, 1942 . Layne, 1957. Aitken and Learmonth, 2002].

This method is based on the inherent absorbance by the aromatic amino acid residues tryptophan and tyrosine and provides a fairly sensitive and convenient means for detecting and quantitating pure proteins or mixtures of pure proteins having a concentration in the range of 0.1 to 1 mg·ml^{-1}. This assay is used to calculate the concentration either from its published absorbancy index (absorptivity) at 280 nm or by comparison with a calibration curve prepared from measurements with standard proteins.

The accurate determination of concentration of a standard erence is necessary to know the concentration of an aqueous protein solution.

Bovine serum albumin (BSA) is the most commonly standard erence chosen for any colorimetric method for protein determination in mitochondrial crude lysates and proteins. Numerous values for the absorptivity of BSA have been reported in the literature but assuming a molecular weight of 66,430 Dalton, the molar extinction coefficient is 43,824 M^{-1}·cm^{-1} at 280 nm. Theore, the absorptivity of BSA is ~ 0.67 for a 1 mg·ml^{-1} solution at 280 nm (a$_{280}$) [Gill and von Hippel, 1989].

For this procedure, quartz crystal or fused silica cuvettes are routinely used as plastic and common glasses are not transparent to the ultraviolet radiation. According with this, two cuvettes are first filled with a volume of water (blank) to zero the spectrophotometer (V530 extended model, JASCO). After removing the blank from the sample compartment, a clean cuvette is filled with a 1 mg·ml^{-1} BSA standard solution and after insert it into the sample compartment, absorbance at 280 nm is measured. The resulting media absorbance value at 280 nm is used after subtracting the absorbance value of the blank to calculate the standard erence concentration as

follows: concentration (mg·ml^{-1}) = $\dfrac{\text{Abs}_{280}}{a_{280} \cdot b}$ where a_{280} is the absorbancy index of

the 1 mg·ml^{-1} BSA standard solution and b is the path-length in cm.

Biuret Method (range: 1 – 10 mg·ml^{-1})

The biuret reaction is the basis of this colorimetric method for quantitatively determine total protein concentration of crude lysates [Gornall et al, 1949] whereby in the presence of four or more peptide bonds, cupric ions (Cu^{2+}) form a violet-colored coordination complex in an alkaline environment [Rose, 1853].

The biuret reagent contains hydrated copper (II) sulfate and sodium hydroxide, together with sodium potassium tartrate and reacts with peptide bonds of proteins producing a light blue to deep purple color, with maximum absorbance (λ_{max}) at 540 nm.

The intensity of the color produced is proportional to the number of peptide bonds participating in this reaction. The working range for this assay is from 1 to 10 mg protein·ml^{-1}. Over this concentration range, the measured absorption is linear according to the Lambert-Beer law [Gornall et al, 1949].

The following procedure is a modification of the original protocol of Gornall *et al* [Gornall et al, 1949] which involves protein solubilization by lipid extraction of the mitochondrial membranes with sodium deoxycholate, and rapid development of the blue copper-protein complex on heating [Beyer, 1983] and using bovine serum albumin (BSA) as standard.

Protein and standard samples are prepared as duplicates in test tubes containing c.a 1 mg protein (adjusting with water to 1.5 ml final volume), 0.1 ml of 10% w:v sodium deoxycholate (pH 8.0), and1.5 ml of biuret reagent. Samples blanks are prepared in the same way but containing suspension buffer or water instead of protein.

After vortex mixing, samples are placed in a boiling water bath for 30 seconds until full color development, and once rapidly cooled at room temperature, absorbance is read at 540 nm.

The resulting average absorbance values for any sample is used after subtracting the absorbance value of the blank and the unknown sample concentration is calculated by the following equations:

$$mass_{sample\ protein\ [mg]} = Abs_{540}(protein) \cdot \frac{mass_{BSA\ [mg]}}{Abs_{540}(BSA)}$$

$$concentraton\ [mg \cdot ml^{-1}] = \frac{mass_{sample\ protein\ [mg]}}{volume_{sample\ protein\ [ml]}}$$

Lowry Method (range: 0.01 – 0.1 mg·ml^{-1})

The Lowry method is a colorimetric assay to determine concentration from purified and partially purified proteins, including highly diluted protein solutions.

This method relies on two different steps. Initially, the biuret reaction involves the interaction of cupric ions with the imide form of the polypeptide in alkaline solution followed by the enhancement step, the reduction of the Folin-Ciocalteau reagent [Lowry et al, 1951. Folin and Ciocalteau, 1927] generating a characteristic blue color with maximum absorbance (λ_{max}) at 750 nm.

The mixed acid (phosphomolybdate and phosphotungstate) of the Folin-Ciocalteau reagent is reduced by a rapid reaction with tyrosine and tryptophan amino acids residues. Cupric ions enhances color formation by chelation with the imide form of the peptide.

The reaction results in a strong blue color, which depends on protein sequence variation as color depends not only to the reduced copper-amide bond complex but also to tyrosine, tryptophan, and to a lesser extent cystine, cysteine, and histidine residues [Peterson, 1977 . Peterson, 1979].

This assay uses bovine serum albumin (BSA) as erence standard. The calibration curve consists in serial dilutions from 0 to 40 μg in 1 ml of distilled water of 1 mg·ml^{-1} BSA aqueous solution whose concentration is previously determined at 280 nm.

The Lowry reagent is prepared immediately before use by mixing the three stock solutions *A*, *B,* and *C* in the proportion 100:1:1 (v:v:v) respectively.

Protein samples are prepared at least by duplicate containing about 20 to 30 μg protein, adding 0.1 ml of 10% w:v sodium deoxycholate and completing volume with

water to 1 ml. Blanks are prepared in the same way but using the sample suspension buffer instead of protein. Straight forwards, 2 ml of the Lowry reagent is added to each tube and after mixing, are allowed to stand for 10 minutes at room temperature in the darkness. Subsequently, 0.20 ml of 2-fold diluted Folin-Ciocalteau reagent is added very quickly while vortex mixing considering that this reagent is only reactive for a short time under alkaline conditions.

After 30 minutes at room temperature in the darkness, the absorbance of samples and blanks are read at 750 nm.

For the calibration curve, it is necessary to subtract blank absorbance values to the standard values and the resulting mean absorbance values for each standard samples are plotted with the vertical axis in units of absorbance at 750 nm and horizontal axis in units of protein mass (μg or mg).

The unknown protein sample concentrations are calculated from this calibration curve considering their mean absorbance value at 750 nm after subtracting their respective blank absorbance values.

Enzyme activities

Complex I enzymatic activity (NADH:ubiquinone reductase), integrated Complex I+III activity (NADH:cytochrome c reductase) and aerobic NADH oxidation are assayed at 30°C in a dual-beam, dual-wavelength spectrophotometer (V550 extended model, JASCO) equipped with a mini-magnet cuvette stirrer.

The initial rates are obtained as first derivatives calculated from the resulting absorbance vs. time curve with an appropriate software (Spectra Manager™, JASCO) and expressed in μmoles of NADH·min^{-1}·mg^{-1}.

Samples are diluted to 40 μg·ml^{-1} for BHM or SMP and 14 μg·ml^{-1} for R4B proteoliposomes in reaction solution, pH 7.4.

NADH:ubiquinone oxidoreductase. Complex I activity is measured essentially as described in Lenaz *et al.* and Ventura *et al.* [Lenaz et al, 2004 . Ventura et al, 2002]. Samples are incubated for 5 minutes with 2 μM antimycin A and 1 mM KCN to inhibit electron transfer towards Complex III and IV. In the presence of 60 μM decylubiquinone (DB) as electron acceptor, the rate of electron transfer is measured after the addition of 75 μM NADH. The time-course decrement of NADH absorbance is followed at a wavelength of 340 nm minus 380 nm (absorption coefficient 3.5 mM^{-1}·cm^{-1}).

NADH oxidase. Aerobic NADH oxidation is assayed in a similar way, but both electron acceptor (DB) and inhibitors are omitted from the assay mixture.

NADH:cytochrome c reductase. Integrated Complex I+III activity is measured according to Battino *et al.* [Battino et al, 1991] in the reaction medium with the addition of 1 mM KCN to inhibit Complex IV. The time-course increase absorbance by the reduction of 50 μM cytochrome *c* is monitored at a wavelength of 550 nm minus 540 nm (absorption coefficient 19.1 mM^{-1}·cm^{-1}) after the addition of 75 μM NADH as electron donor.

Measuring Reactive Oxygen Species

ROS is an acronym for *reactive oxygen species*, a variety of intermediates relatively stable produced by the univalent reduction of molecular oxygen.

Superoxide detection. The superoxide anion radical is produced by autooxidation of mitochondrial redox groups such as iron-sulfur clusters and semiquinone radicals [Raha and Robinson, 2000 Turrens, 1997. Turrens, 2003].
The determination of the rate production of $O_2^{\bullet-}$ is based upon the spectrophotometric measurement of oxidation or reduction of a probe in which $O_2^{\bullet-}$ is a reactant. The concentration of the spectrophotometric indicator that reacts with superoxide anion is adjusted to compete effectively with the spontaneous dismutation of $O_2^{\bullet-}$ so that nearly all superoxide anion produced can be detected. According with this approach, native ferricytochrome *c* is an excellent quantitive indicator for $O_2^{\bullet-}$:

$$Fe^{3+}-cyt\ c\ _{(ferricytochrome\ c)} + O_2^{\bullet-} \longrightarrow Fe^{2+}-cyt\ c\ _{(ferrocytochrome\ c)} + O_2$$
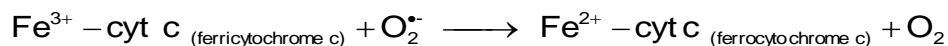
However, when exogenous ferricytochrome *c* is added to mitochondria membrane preparations, it is more effectively reduced by the electron chain cytochrome c reductase than by superoxide. To overcome this limitation and enhance specificity of this assay for $O_2^{\bullet-}$, it is known that the acetylation of some lysine residues of ferricytochrome *c* decreases enzymatic direct electron transfer while preserving the capacity of being chemically reduced [Azzi et al, 1975. Boveris, 1984].
It is theore advisable to use acetylated cytochrome *c* that, although not as rapidly reduced by superoxide as native cytochrome c, is much more slowly reduced by the reductase activity of the mitochondrial membranes and is not efficiently oxidized by cytochrome oxidase [Azzi et al, 1975].

In general, acetylated cytochrome *c* have to be in excess so that the rates of reduction and oxidation can be treated as zero order and depend only on the rate of superoxide production [Dröse et al, 2009]. The superoxide-dependent rate can be deduced as the difference between the reduction rates in the absence and presence of superoxide dismutase (SOD) as the reduction of both native and acetylated cytochrome *c* are highly sensitive to this enzyme.

Nevertheless, when studying the production of superoxide mediated by Complex I is suggested to functionally isolate Complex I from the downstream segments of the respiratory chain by adding mucidin, an inhibitor that blocks Complex III activity and simultaneously prevents the superoxide production from this complex and potassium cyanide that competitively inhibits the cytochrome c oxidase activity [Lenaz et al, 2004].

One should, however, be aware that cyanide inhibits also the Cu,Zn-SOD, theore the Mn-enzyme should be perred when cyanide is present in the reaction medium [Boveris, 1984 . Turrens and Boveris, 1980].

According with these considerations, in the present study, the measurement of superoxide production mediated by Complex I in the R4B proteoliposome is obtained essentially as described by Lenaz *et al* [Lenaz et al, 2004]:

All samples are diluted in reaction medium to a final concentration of 14 μg protein·ml^{-1} in the presence of 1.8 μM mucidin and 4 μM rotenone.

The reduction of 50 μM acetylated cytochrome *c* is followed spectrophometrically with a dual-beam, dual-wavelength spectrophotometer (V550 extended model, JASCO) at 550 - 540 nm (absorption coefficient 19.1 mM^{-1}·cm^{-1}) at 30°C after the addition of 75 μM NADH as electron donor.

The addition of 40 to 50 U/ml Cu,Zn-superoxide dismutase gives the SOD-sensitive rate of acetylated cytochrome c reduction, which gives the stoichiometric rate of $O_2^{\bullet-}$.

According to the method [Azzi et al, 1975. Boveris, 1984], data are shown as the rate of SOD-sensitive and –insensitive reduction of acetylated cytochrome in nmole·min^{-1}·mg^{-1}.

Hydrogen peroxide detection. Due to the rapidly spontaneous and enzyme-catalyzed dismutation of superoxide to hydrogen peroxide its detection is generally more arduous than hydrogen peroxide [Murphy, 2009].

Consequently, the rate of H_2O_2 production can be used as an indirect measurement of $O_2^{\bullet-}$ formation, recognizing that such measurements will also lect direct divalent reduction of molecular oxygen to H_2O_2.

Fluorescent-based methods to detect ROS formation in mitochondria were very early introduced in the literature [Hinkle et al, 1967. Black and Brandt, 1974], particularly the oxidation of the leuco probe 2',7'-dichlorodihydrofluorescein diacetate (DCFDA) to the fluorescent compound dichlorofluorescein (DCF) was initially thought to be a relatively specific indicator of H_2O_2 [Brandt and Keston, 1965 . Keston and Brandt, 1965].

DCFDA is a non-polar, reduced, colorless and non-fluorescent dye that can diffuse through lipid membranes. This probe is rapidly cleaved by cellular esterases, which are also present in mitochondrial preparations, resulting into the polar, non-fluorescent compound 2',7'- dichlorodihydrofluorescein ($DCFH_2$).

It has been demonstrated that mitochondria and submitochondrial preparations are able to deacetylate the probe and oxidize it by ROS [Degli Esposti, 2002].

Nevertheless, when the assay is performed to test the ROS production of purified proteins as R4B fraction, DCFDA requires chemical hydrolysis immediately before use (see below).

In the presence of hydrogen peroxide, $DCFH_2$ is oxidized to 2',7'- dichlorofluorescein (DCF) which emits a strong fluorescence.

In the present study, hydrogen peroxide production by Complex I is measured according with the method of Fato *et al* [Fato et al, 2009]:

All samples are diluted in reaction medium to a final concentration of 0.5 mg protein·ml^{-1} in the presence of 1.8 μM mucidin and 4 μM rotenone when indicated and 5 μM DCFDA.

Each well of a 96-well microtiter plate, optically suitable for fluorescence measurements is filled with the reaction mixture.

The reaction is started with the addition of a large excess of electron donor (150 μM NADH) aimed to guarantee not to consume all the substrate during the 45 min of the assay.

The fluorescence readings are obtained with an excitation / emission wavelength of 485 / 535 nm at 25°C in a fluorescence plate reader (Wallac Victor2 1420 Multilabel counter; PerkinElmer).

The fluorescence intensity change is followed every 5 min, and the results are calculated as the difference of fluorescence units at 45 min minus zero time and given as mean ± S.D. of at least three independent determinations. Interference of NADH, rotenone, mucidin, and other substrates with the background fluorescence of DCF is evaluated in blank samples.

Preliminary laboratory tests include the direct effect of enhancing the fluorescence of the probe by adding 5 and 50 μM H_2O_2 to exclude the possibility that the fluorescence signal produced by the samples are underestimated by a lack of DCF.

As mentioned before, DCFDA is spontaneously deacetylated in mitochondria preparations [Fato et al, 2009] whereas R4B proteoliposomes require alkaline hydrolysis of DCFDA prior to assay.

According to this, 10 μl of DCFDA stock solution are mixed with 40 μl of 0.01 N NaOH for 30 min in the dark at room temperature [Cathcart et al, 1983]. The mixture is neutralized with 200 μl of 10 mM KCl, 1 mM EDTA, 25 mM Tris-HCl pH 7.4 and kept on ice in the dark and immediately used.

Protein electrophoresis analysis

Electrophoresis is a separation technique based on the mobility of charged molecules in an electric field. It is used mainly for the analysis and purification of biological macromolecules such as proteins and nucleic acids.

Polyacrylamide gel electrophoresis (PAGE) is most commonly used for separation of proteins where polyacrylamide gel acts as an anticonvective size-selective sieve with defining pores saturated with an electrically conductive buffered solution of salts.
The size pores of these gels are large enough to admit passage of the migrating macromolecules as they are forced through the gel by an applied voltage, larger molecules are retained in their migration more than smaller molecules.

In an electric field, proteins move toward the electrode of opposite charge. The rate of migration of the macromolecules through the polyacrylamide gel depends upon a complex relationship between the physical characteristics of both the electrophoresis system and the macromolecules. Factors affecting protein electrophoresis include the strength of the electric field, the porosity of the gel, the temperature of the system, the pH, ion type, and concentration of the buffer as well as the size, shape, and charge density of the proteins [Garfin, 1990].

In most PAGE units, the gel has a vertical orientation and is mounted between two buffer chambers that the only electrical connection between the anode (+) and cathode (-) chambers is through the gel. An electric potential is applied across the buffer chambers forcing the sample proteins to migrate into and through the gel toward the bottom [Shi and Jackowski, 1998] (Figure 2.3).
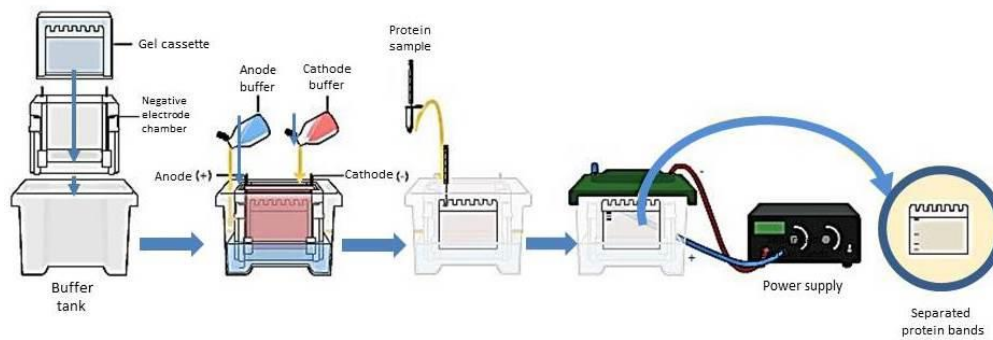
Figure 2.3: Electrophoresis workflow. Electrophoresis involves the selection of the appropriate method, instrumentation, and reagents for the intended experimental goal. Once proteins are separated, they are available for a number of downstream applications, including enzymatic assays, further purification, transfer to a membrane for immunological detection (immunoblotting or western blotting), and elution and digestion for mass spectrometric analysis.

Polyacrylamide gels are chemically inert, electrically neutral, hydrophilic and optically transparent for detection at wavelengths greater than 250 nm. These characteristics make polyacrylamide ideal for protein separations because the matrix does not interarct with the solutes and has a low affinity for common protein stains [Garfin, 2009].

These gels are formed by copolymerization of acrylamide and N,-N'-methylene-bis-acrylamide (bis-acrylamide, cross-linker).

The reaction is a vinyl addition polymerization initiated by a free radical-generating system. Polymerization is initiated by a chemical initiator and a catalyst (e.g. ammonium persulfate (APS) and tetramethylethylenediamine (TEMED)).

The elongating polymer chains are randomly crosslinked by bis-acrylamide, resulting in a gel with a characteristic porosity which depends on the polymerization conditions and monomer concentrations.

Polymerization rates depend on monomer and catalyst concentration, temperature and purity of reagents.

The porosity of the gel is characterized by two parameters: total monomer concentration (%T) and weight percentage of cross-linker (%C). By varying these two parameters, the pore size of the gel can be optimized to yield the best separation and resolution for the proteins of interest. %T indicates the relative pore size of the resulting polyacrylamide gel; a higher %T ers to a larger polymer-to-water ratio and smaller average pore sizes.

Single-percentage gels are used to separate bands that are close in molecular weight. Since optimum separation occurs in the lower half of the gel, it is necessary to choose a percentage in which the protein of interest migrates to the lower half of the gel.

Gradient-gels, by the other side, are used to separate samples containing a broad range of molecular weights. These gels allow resolution of both high- and low-molecular weight bands on the same gel.

The pH and ionic composition of the buffer system determine the power requirements and heavily influence the separation characteristics of a polyacrylamide gel. Buffer systems include the buffers used to cast the gel (gel buffer), prepare the sample (sample buffer), and fill the electrode reservoirs (running buffer).

Two types of buffer systems are commonly used: continuous buffer systems use the same buffer, at constant pH, in the gel, sample, and electrode reservoirs [McLellan, 1982] and discontinuous buffer systems use a gel separated into two sections (a large-pore stacking gel on top of a small-pore, the resolving gel) and different buffers in the gels and electrode solutions [Wheeler et al, 2004].

Most common PAGE applications utilize discontinuous buffer systems, where two ions differing in electrophoretic mobility form a moving boundary when a voltage is applied [Niepmann, 2007].

First dimension: Blue-native polyacrylamide gel electrophoresis

Blue-native polyacrylamide gel electrophoresis (BN-PAGE) has been developed for the isolation of native membrane proteins in the mass range of 10 kDa to 10 MDa at a fixed pH of 7.5 [Schägger and von Jagow, 1991. Schägger et al, 1994]. Even the original protocol and related techniques have been improved and expanded considerably [Schägger, 2001. Wittig et al, 2006b], the basic principles for BN-PAGE however, are unchanged.

Mild neutral detergents are used for solubilization of biological membranes. In principle, any neutral detergent can be used for solubilization of biological membranes for BN-PAGE if the detergent can solubilize the desired protein and keep it in the native form. The choice of a specific nonionic detergent depends on its delipiding properties for a protein of interest.

The very mildest detergent digitonin has been used to isolate supramolecular associations of multiprotein complexes, thus identifying physiological protein-protein interactions without using chemical crosslinking.

Dodecyl-β-D-maltoside (dodecylmaltoside, DDM) by the other side, has stronger delipidating properties compared to digitonin. It is a mild neutral detergent that is suited for isolation of individual complexes [Schägger and von Jagow, 1991. Schägger et al, 1994] (Figure 2.4)

Coomassie blue G 250 is added to the solubilized proteins prior to loading the samples onto the gel. This dye is sufficiently soluble in water, but it can also bind to membrane proteins because of its hydrophobic properties.

Coomassie blue is also added in the cathode buffer to provide a continuous flow of this dye into the gel.

Membrane proteins and proteins with significant surface-exposed hydrophobic area bind Coomassie blue G-250 nonspecifically, acquiring overall negative charges. Consequently these proteins repel each other minimizing considerably the tendency of protein aggregation. Furthermore, these dye-bound proteins are water-soluble, this means that there is no need for the presence of detergent in the polyacrylamide gel, and the risk of denaturation of detergent-sensitive membrane-proteins is also minimized.

Binding of a large number of anionic dye molecules shifts the isoelectric point of proteins that causes even basic proteins to migrate in one direction towards the positive anode at pH 7.5 [Schägger et al, 1994].

In this way, proteins will not be separated according to the charge/mass ratio but according to size in acrylamide-gradient gel, which leads to a mass-dependent reduction of the protein migration velocity and to an almost complete stop at a mass-specific pore size limit during BN-PAGE. Native proteins, stained with Coomassie, are visible as blue bands through the gel and this staining facilitates excision of specific bands.

The potential of this technique to determine native molecular masses and oligomeric states identifying physiological protein-protein interactions led to demonstrate in 2000 that yeast and mammalian respiratory chains exist as a network of supercomplexes, and that detergent-sensitive multiprotein complexes could be isolated without dissociation of detergent-labile subunits [Schägger and Pfeiffer, 2000] (Figure 2.2).

In the present study, separation of supercomplexes and single respiratory complexes is achieved according to a modified version from Beardslee and Updyke [Beardslee and Updyke, 2007], buffers and solutions used for BN-PAGE are listed in Table 2.1. In detail:

Bovine mitochondria or R4B proteoliposomes samples are centrifuged 10 minutes at 20,000 g at 4°C to remove suspension buffer.

Pellets are suspended in Sample Buffer at 4 mg·ml^{-1}. Digitonin or dodecylmaltoside is added at detergent:protein ratios given in Table 2.2 when indicated and mixed by pipetting up and down.

Protein extracts are incubated on ice for 20 minutes before centrifuging 10 minutes at 10,000 g at 4°C (centrifuge Beckman Avanti J25, JA-18.1 rotor).

Pellets are discarded and supernatants are aliquoted and kept on ice until use. Just before loading onto the gel, 5% w:v Coomassie blue G-250 solution is added to the samples so that the final concentration of G-250 is one-tenth that of the detergent concentration.

Prior to loading into the gel, glycerol is added to the samples at a final concentration of 10% (v:v) in order to increase the density and facilitate sample application.

The samples are loaded onto precast 10-wells 3%-12% T gradient gels (NativePAGE™ Novex® Bis-Tris Gel, Invitrogen) which are a 1.0 mm tick, 8 x 8 cm mini gels that resolve proteins in the molecular weight range of 30 - 10,000 kDa. Electrophoresis is performed at 4°C using a vertical apparatus (XCell SureLock ™ Mini-Cell Electrophoresis System, Invitrogen) and Bis-Tris Gel system buffers (NativePAGE™ Novex® Bis-Tris Gel System, Invitrogen).

Samples are loaded up to 25 µl per well. An effort is also made to minimize the amount of time between loading sample onto the gel and beginning electrophoresis.

Five microliters of unstained native protein standards comprising IgM hexamer (1,236 kDa), IgM pentamer (1,048 kDa), Apoferritin band 1 (720 kDa), Apoferritin band 2 (480 kDa), B-phycoerythrin (242 kDa), Lactate Dehydrogenase (146 kDa), Bovine Serum Albumin (66 kDa), and Soybean Trypsin Inhibitor (20 kDa) are used as molecular weight markers on the gels (NativeMark™ unstained protein standard, Invitrogen).

The run is started with the Deep Blue cathode buffer and once the dye front migration is one-third of the way down the gel the run is paused, this cathode buffer is removed with a serological pipette and replaced by the Slightly Blue cathode buffer before resuming the run.

Electrophoresis is performed at 150 V constant for 60 minutes, then the voltage is increased to 250 V constant for the remainder of the run (30 - 90 minutes running at 4°C).

Table 2.1: Gel buffer system formulation for BN-PAGE

	Bis-Tris CHAPS/Tricine-BN PAGE [a]
Sample Buffer	50 mM NaCl, 5 mM 6-aminocaproic acid, 50 mM imidazole/HCl pH 7.0
Gel Buffer	50 mM BisTris/HCl, pH 7.0 0.3 mM CHAPS
Anode Buffer	50 mM Tricine, 50 mM Bis-Tris, pH 6.8
Deep blue cathode buffer	50 mM Tricine, 50 mM Bis-Tris, pH 6.8 0.02% w:v Coomassie blue G-250
Slightly blue cathode buffer	50 mM Tricine, 50 mM Bis-Tris, pH 6.8 0.002% w:v Coomassie blue G-250

(a) [Beardslee and Updyke, 2007]

Table2.2: Quantity of detergent required to solubilize membrane proteins

	BHM (200 μg)	**R4B proteoliposomes** (80 μg)
Dodecylmaltoside (10% w:v)	**5.2 μl** (2.6 g/g)	3.4 μl (4.3 g/g)
Digitonin (10% w:v)	16 μl (8 g/g)	6.4 μl (8 g/g)

The volumes of added detergent and the detergent / protein ratios chosen (w:w), indicated in brackets
are shown for solubilization of bovine heart mitochondria (BHM) and R4B proteoliposomes
(Complex I+III proteoliposomes from BHM)

After BN-PAGE, individual lanes are cut out and processed by an orthogonal second-dimension electrophoresis under denaturing conditions.

The second dimension is performed by sodium dodecyl sulfate polyacrylamide gel electrophoresis (SDS-PAGE). In this way, the mitochondrial membrane protein complexes separated as supramolecular assemblies during the first dimension electrophoresis are resolved in the second dimension into their individual polypeptide subunits (2D BN/SDS-PAGE).

After immunodetection with specific antibodies, 2D BN/SDS-PAGE provides an valuable analytical method for the determination of molecular mass and oligomeric state of complexes, and characterization of stoichiometric associations between protein complexes (Figure 2.5).
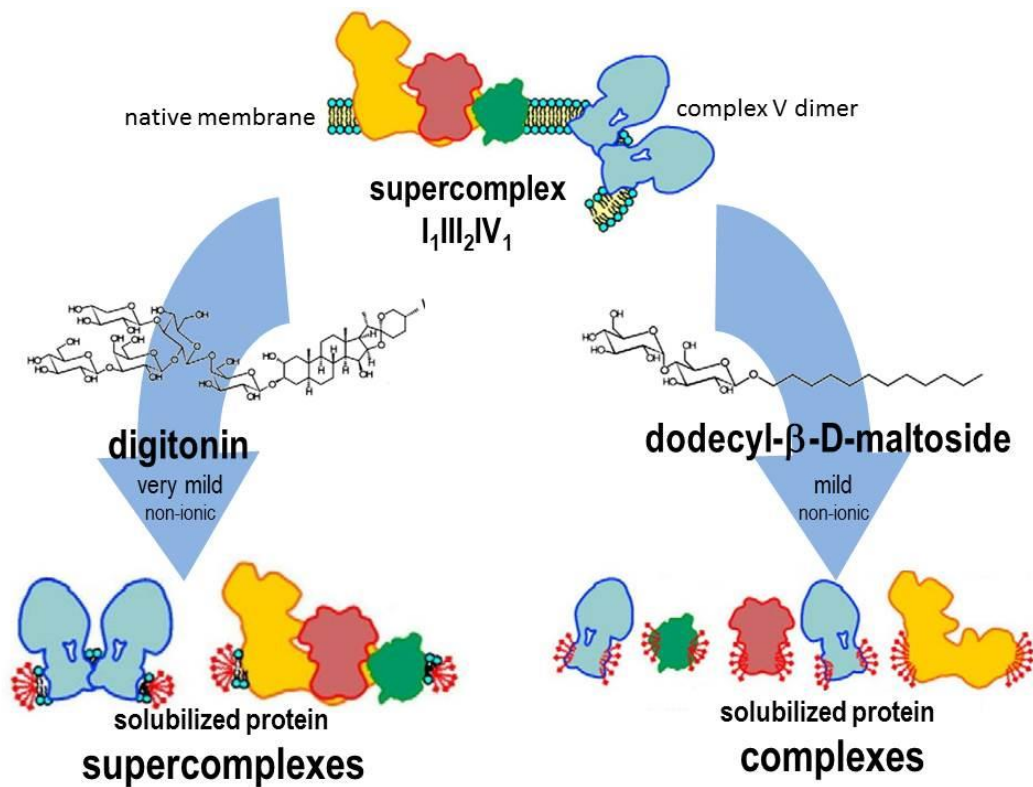
Figure 2.4: Solubilization of native oxidative phosphorylation complexes. Non-ionic detergents disrupt *lipid-lipid* and *lipid-protein* interactions rather than *protein-protein* interactions and are systematically used to investigate the structure and function of the respiratory chain and ATP synthase. Digitonin and dodecyl-β-D-maltoside are routinely used for the isolation of native and functional mitochondrial supercomplexes and complexes. These detergent differ in their solubilization properties as interact with different classes of lipids in biological membranes. Digitonin, a very mild glycoside surfactan obtained from *Digitalis purpurea*, interact mainly with *annular* lipids. By the other side, the alkylglucoside dodecyl-β-D-maltoside, appear to interact also with *non-annular* lipids, showing stronger delipidating
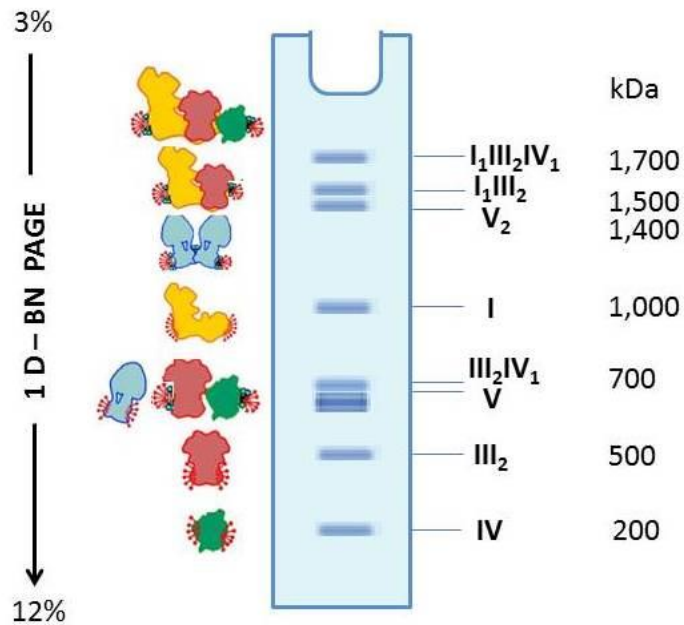
Figure 2.5: Separation of supramolecular assemblies of oxidative phosphorylation complexes by 1D-BN PAGE. Separation of digitonin-solubilized mitochondrial supercomplexes and complexes exemplifying the native mass range (<100 kDa to ~10 MDa) covered by 1D BN-PAGE. I, II. III, IV, V, indicate mitochondrial complexes I-V.
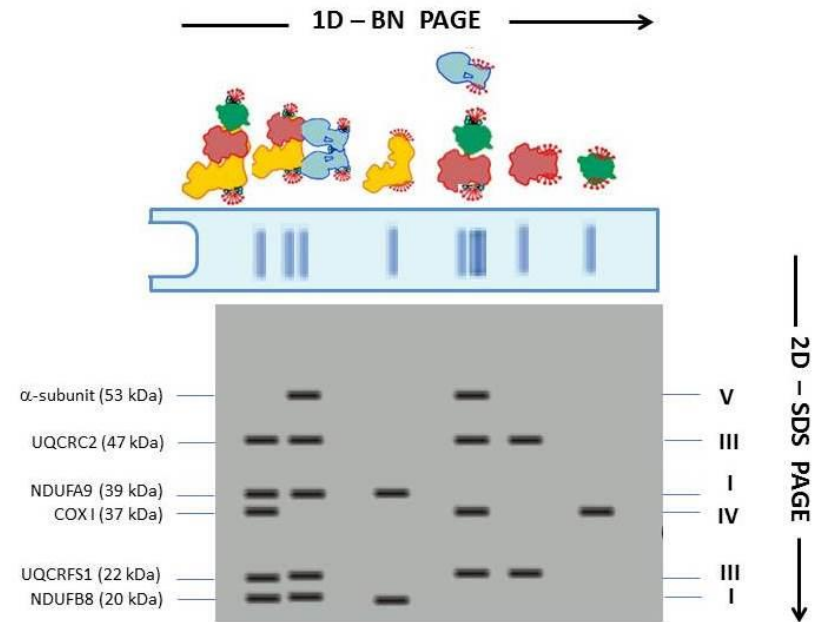
Figure 2.6.: Identification of individual constituents in supramolecular assemblies of oxidative phosphorylation complexes by 2D BN/SDS-PAGE. The gel strip for the 1D BN-PAGE is processed by a second dimension in denaturant conditions. Respiratory supercomplexes are thereby dissociated into their individual constituent complexes and identified after electroblotting and immunodetection with appropriate monoclonal antibodies specific for subunits of OXPHOS complexes. I, II. III, IV, V, indicate mitochondrial complexes I-V.

Second dimension: Sodium dodecyl sulfate polyacrylamide gel electrophoresis

Sodium dodecyl sulfate polyacrylamide gel electrophoresis (SDS-PAGE) is a valuable means for separation of proteins.

The original discontinuous gel system was developed by Ornstein and Davis [Ornstein, 1964. Davis, 1964] for the separation of serum proteins in native conditions [Vavricka et al, 2009]. Laemmli modified this protocol by incorporating the detergent sodium dodecyl sulfate (SDS), creating what has become the most popular form of protein electrophoresis, SDS-PAGE [Laemmli, 1970]. When proteins are separated in the presence of the anionic detergent SDS and reducing agents, they become fully denatured and dissociate into their constituting subunits.

SDS is an anionic detergent that binds non-covalently to proteins in a manner that imparts an overall negative charge on the proteins. Indeed, SDS binds at a consistent rate of 1.4 g of SDS per 1 g protein (a stoichiometry of about one SDS molecule per two amino acids), theore it imparts a similar charge-to-mass ratio for all proteins in a mixture.

The electrostatic repulsion that is created causes proteins to lose their native conformation. The disruption of non-covalent bonds leads proteins to unfold into a rod-like shape thereby eliminating differences in shape which is an important factor for separation of these molecules in the gel.

The addition of a reducing agent in the sample buffer, such as dithiothreitol (DTT) or 2-mercaptoethanol (β-mercaptoEtOH), additionally denatures the proteins by reducing disulfide linkages, thus overcoming some forms of tertiary protein folding, and breaking up quaternary protein structure (oligomeric subunits).

Consequently, the rate at which SDS-bound proteins migrate in a polyacrylamide gel depends primarily on their size, enabling molecular weight estimation.

The 2D SDS-PAGE procedure for mitochondrial complexes in the present study is performed with the Bis-Tris/ MOPS buffer system (NuPAGE™ Novex® Bis-Tris Gel System buffers, Invitrogen).

The BisTris/MOPS-SDS-PAGE was developed by Updyke and Sheldon [Updyke and Engelhorn, 2004]. It is a discontinuous buffer system that involves chloride as the leading ion present in the gel buffer and 3-(N-morpholino) propanesulfonate (MOPS) as the trailing ion in the running buffer. Bis (2-hydroxyethyl) imino-tris (hydroxymethyl) methane (Bis-Tris) cation is the common ion present in the gel and running buffers.

The combination of the lower pH gel buffer (pH 6.4) and the running buffer (pH 7.3 - 7.7) results in a significantly lower operating pH of 7 during electrophoresis (buffers and solutions are listed in Table 2.3). In detail:

Individual strip lanes from BN-PAGE with the protein complexes under study are excised (0.5 cm-broad strips).

Then, these gel strips are successively incubated for 15 minutes at room temperature, first with 50 mM DTT to reduce disulfide bonds between cystines, then with 50 mM N,N-dimethylacrylamide to alkylate the reduced cystines, and afterward with 5 mM DTT to quench the reaction.

The equilibrated strips are loaded onto 2-D well precast 4%-12% T gradient gels (NuPAGE™ Novex® Bis-Tris Gel, Invitrogen) which are a 1.0 mm tick, 8 x 8 cm mini gels that resolves proteins in the molecular weight range of 10 - 200 kDa. Electrophoresis is performed at 4°C using a vertical apparatus (XCell SureLock ™ Mini-Cell Electrophoresis System, Invitrogen).

Five microliters of an unstained protein standards in the range of 20 - 220 kDa comprising recombinant proteins containing repetitive units of a fusion protein which contain an IgG binding site (MagicMark™ XP Western Protein Standard, Invitrogen). This standard marker allows visualization of the protein standard bands using the same reagents and protocols for the target proteins by immunodetection. Electrophoresis is performed at 200 V constant for 50 minutes at 4°C.

Table 2.3: Gel buffer system formulation for SDS-PAGE

	Bis-Tris/MOPS-SDS PAGE [a]
Sample Buffer	25 mM Tris-HCl, 35 mM Tris base, 0.5 % w:v LDS, 2.5% v:v glycerol, 0.127 mM EDTA, 0.004% w:v SERVA Blue G250, 0.0015% w:v phenol red
Reducing Solution	50 mM DTT in Sample Buffer
Alkylating Solution	50 mM N,N-dimethylacrylamide in Sample Buffer
Quenching Solution	5 mM DTT in Sample Buffer
Gel Buffer	0.375 M Bis-Tris/HCl, pH 6.5
Running Buffer	2.5 mM MOPS, 2.5 mM Bis-Tris (or Tris), pH 7.7, 0.005% w:v SDS and 0.05 mM EDTA

(a) [Updyke and Engelhorn, 2004]

Protein Immunoblotting

On completion of the separation of proteins by 2D BN/SDS-PAGE, the next step is detecting and identifying protein subunits with the aim to establish specific protein-protein associations between mitochondrial complexes.

Immunoblotting (western blotting), was developed as a result of the need to probe proteins that were inaccessible to antibodies while embedded in the polyacrylamide matrix. This method is based on building an antibody:protein complex via specific binding of antibodies to proteins immobilized in a membrane of nitrocellulose and detecting the bound antibodies. Several detection methods are available [Towin et al, 1979. Brunette, 1981].

Immunoblotting involves a first step, the transfer phase which means moving the proteins from the polyacrylamide gel onto a solid support membrane and immobilizing them at their respective relative migration positions at the time point when the electric current of gel was stopped (blotting).

The most commonly support membranes used are nitrocellulose or polyvinylidene difluoride (PVDF).

The second phase, detection, entails probing the membrane with either a primary antibody specific to the protein/s of interest and subsequent visualization of the labeled proteins.

Blotting

Wet electrotransfer relies on the same electromobility principles that drive the migration of proteins during separation in PAGE: an electric field is used to eluate proteins from gels and transfer them to membranes where they are captured in a pattern that perfectly mirrors their migration positions of the separated protein in the gel.

The membrane and protein-containing gel, together with filter paper, are assembled in a sandwich. A non-conducting cassette holds the membrane in close contact with the gel and the cassette assembly is placed between two electrodes, transverse to the electrical field and fully immersed in a conducting transfer buffer [Towin et al, 1979. Brunette, 1981] (Figure 2.7).

A current is applied by a voltage across the electrodes in the direction of the gel to the membrane following Ohm's law. The electric field strength that is generated between the electrodes is the driving force for transfer.

There are practical limits on field strength, however due to the production of heat during transfer. The heat generated during transfer increases temperature and decreases resistance of the transfer buffer.

Such changes in resistance may lead to inconsistent field strength and may cause the transfer buffer to lose its buffering capacity. In addition, excessive heat may cause the gel to deteriorate and stick to the membrane.

Additionally, most buffers become heated, increasing in temperature to a point where proteins may be irreversibly damaged. It is theore important to start the transfer process using cooled buffer and to maintain a low temperature.

Although the large volumes of buffer in the tank dissipate the heat generated and provide the conducting capacity for extended transfer conditions, wet transfer requires cooling of the tank blotter system and internal recirculation of the transfer buffer by the presence of a stirring magnet.

Another common procedure is to perform the entire wet transfer in a 4°C environment, such as a cold room keeping the blotting tank on ice.

Transfer buffer should act as an electrically conducting medium in which proteins are soluble and that does not interfere with binding of the proteins to the membrane. Most transfer buffers contain methanol.

The addition of methanol is necessary to achieve efficient binding to the membrane, particularly nitrocellulose membranes [Gershoni and Palade, 1982].

Buffers containing methanol may deteriorate if stored for long periods, theore methanol is added just prior to transfer.

In addition to buffer characteristics such as pH, salt type, salt concentration, and the presence of detergents, the degree to which molecules bind to a membrane is influenced by the physical and chemical characteristics of the membrane itself.

Membranes are porous materials with pore sizes from 0.2 to 0.45 μm in diameter. The binding capacity of a membrane depends primarily on the pore size.

Nitrocellulose and PVDF membranes are the most common types of membranes used for Western blotting. Nitrocellulose membranes are the most frequently used and their main advantage is a tendency to have low background.

The exact mechanism by which biomolecules interact with the membrane is not known, but it is assumed to be a combination of non-covalent and hydrophobic forces.
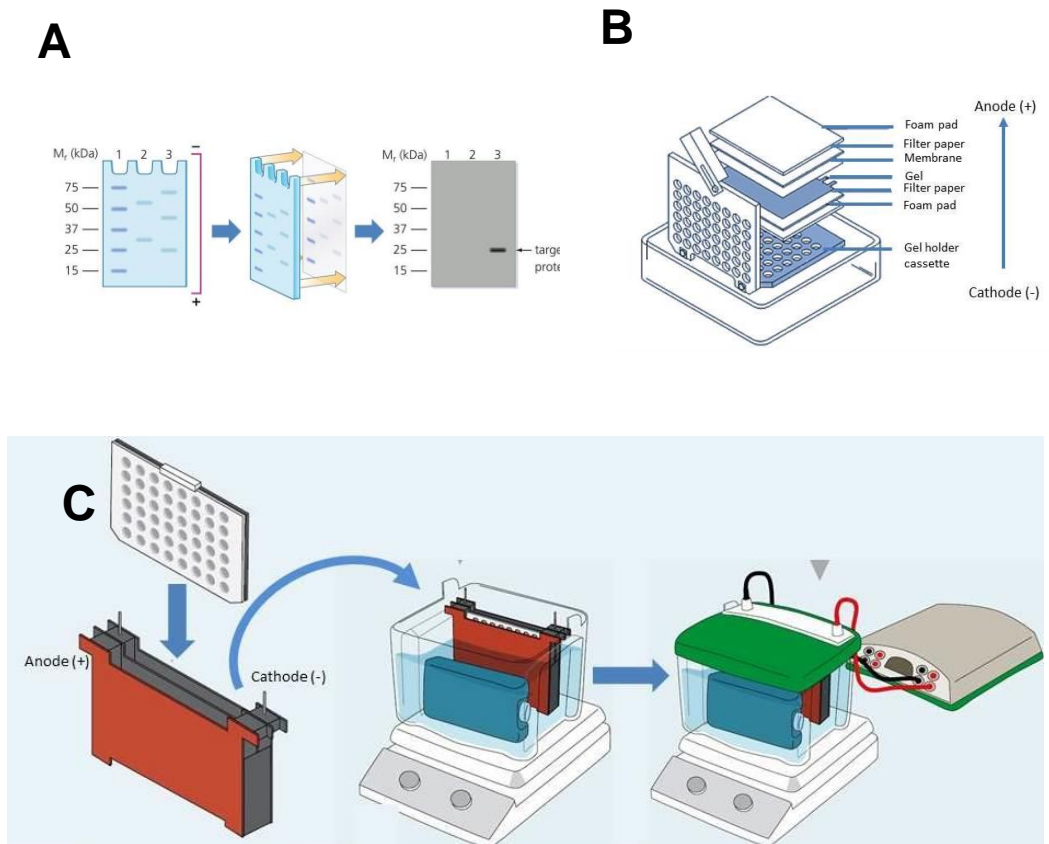
Figure 2.7: Protein blotting workflow. **A)** Once proteins are separated by electrophoresis, they are available to electrophoretic transfer onto a nitrocellulose membrane (blotting) for further immunological detection. **B)** Gel and membrane setup for blotting. The cassette holds the gel and membrane while fiber pads and filter paper on both sides provide complete contact within the gel sandwich. **C)** Transfer sandwich assembly. The cassete is inserted vertically in the buffer tank.

In the present study, 2D BN/SDS-PAGE gels with separated mitochondrial complexes are blotted as follows:

For each gel, one piece of nitrocellulose membrane (Amersham Hybond ECL™, GE Healthcare) and two pieces of filter paper (Whatman® 3MM Chr, GE Healthcare) are cut to the dimensions of the gel (7.5 x 10 cm).

Membranes, cotton filter paper and fiber blotting pads are thoroughly wetted (pre-equilibration) in Transfer Buffer (25 mM Bicine, 25 mM Bis-Tris, 1 mM EDTA pH 7.2 buffer, NuPAGE® Transfer Buffer, Invitrogen) with 20% v:v methanol prior to assembly of the gel-membrane sandwich.

A soaked fiber blotting pad is placed on top of the black side of the cassette (Mini Trans-Blot®, Bio-Rad), submerged in buffer, then a piece of filter paper on top of the blotting pad and then the pre-equilibrated gel on top of the filter paper.

Caully a small roller is run across the gel to remove any air bubbles that may be trapped underneath the gel. Removing air bubbles is essential as they can block the transfer of proteins.

Thereafter, the pre-equilibrated membrane is placed on top of the gel and air bubbles are removed with the roller to ensure proper contact between the gel and membrane.

The second piece of filter paper is placed on top of the membrane and afterwards, a soaked fiber blotting pad is placed on top of the filter paper.

Once the cassette is closed and locked, it is inserted into the tank blotting cell (Mini Trans-Blot®, Bio-Rad) with the black cassette plate facing the black electrode plate.

After transfer buffer is added to the tank and closed, the electrodes are connected to the power supply (PowerPac™ Universal Power Supply, Bio-Rad).

The electrotransfer is performed at 100 V constant during 90 minutes with stirring magnet in cold room keeping the blotting tank on ice.

Protein immunodetection

Once mitochondrial complex subunits are separated and transferred onto a membrane, the protein of interest is detected and localized using a specific antibody (immunological detection).

Western blotting protocols, usually utilize a non-labeled primary antibody directed against the target protein and a species-specific, labeled secondary antibody directed against the constant region of the primary antibody [Kurien and Scofield, 2006].

The secondary antibody can be labeled or conjugated to an enzyme such as horseradish peroxidase (HRP) for subsequent detection.

Western blotting involves the immobilization of proteins on a membrane via hydrophobic interactions. As non-specific binding of antibodies to the membrane is detrimental to the specificity and sensitivity of the assay, it is essential to block spaces not already occupied by proteins.

Failure to completely block these sites can lead to high background.

Two main classes of blocking agents, proteins and non-ionic detergents, are commonly used for Western blotting:

Antibodies are also proteins, and they can also bind non-specifically to the membranes. To counteract this problem, membranes have to be "blocked" to prevent non-specific antibody interactions. The most common permanent blocking agents include bovine serum albumin (BSA) and non-fat milk.

Non-ionic detergents inhibit non-specific hydrophobic binding of proteins. They are considered non-permanent blocking agents since they do not attach to the membrane and can be removed in a simple washing step.

A solution of Tween-20 is commonly used in immunodetection procedures.

Antibody incubations are generally carried out in antibody buffer containing phosphate buffered salt (PBS) with Tween-20 and a blocking protein reagent. The entire blot must be covered with antibody-containing solution.

The optimum antibody concentration is the greatest dilution of antibody that still yields a strong positive signal without background or nonspecific reactions.

In detail, following transfer of mitochondrial complex proteins, immunodetection is performed as follows: nitrocellulose membrane is washed three times with 0.05% v:v Tween-20 in PBS (Tween/PBS) for 5 minutes and incubated with Blocking Solution (2% w:v BSA, 2% w:v non-fat milk, 0.05% v:v Tween-20 in PBS) overnight at 4°C.

Alternatively, the membrane is incubated with blocking solution for 1 hour at room temperature with orbital shaking and after washing with Tween/PBS, incubated with primary antibody over night at 4°C.

Monoclonal antibodies specific for single subunits of each respiratory complexes (MitoSciences®, abcam) are diluted according with the manufacturer's indications

A first exposure is made with the MS111 antibody directed against the NDUFA9 subunit (39 kDa) of Complex I and is followed by double overlaid exposure either with the MS604 cocktail of antibodies against subunits of complexes I, II, III, IV, and V or with the MS305 antibody against the Rieske protein (22 kDa) of Complex III, respectively as indicated in the legend of the figures in the Results section.

After washing with Tween/PBS, 5 ml of primary antibody diluted in blocking solution is added and the membrane is incubated for 1 hour at room temperature with orbital shaking.

Afterwards, the membrane is washed three times with Tween/PBS for 5 minutes and incubated with goat anti-mouse IgG $_{H+L}$ secondary antibody conjugated with horseradish peroxidase (Molecular Probes, Invitrogen) for 1 hour at room temperature with constant agitation.

Chemiluminescent detection is carried out using ECL reagents (Amersham[TM] ECL[TM] Western Blotting Detection Reagent, GE Healthcare) according with the manufacturer's indications.

This enzymatic detection system is based on antibodies conjugated to horseradish peroxidase (HRP) that catalyze the oxidation of luminol in presence of peroxide, and results in light emission. The HRP-conjugated secondary antibody binds to the primary antibody, specifically bound to the target protein on the membrane. After the addition of a luminol peroxide detection reagent, the HRP enzyme catalyzes the oxidation of luminol in a multi-step reaction [Della Ciana, 2010a. Della Ciana, 2010b]. The reaction is accompanied by the emission of light at 428 nm in a process known as enhanced chemiluminescence (ECL). The intensity of signal is a result of the number of reacting HRP molecules and is thus proportional to the amount of antibody, which is related in turn to the amount of protein on the blot.

The light signal is captured in a charge-couple device (CCD) camera-based Imager (ChemiDoc[TM] XRS+ system, Bio-Rad).

Imaging - Analysis and documentation

The light signal from ECL-immunodetection (see section 8.3.2) can be detected by digital imaging with a charge-coupled device (CCD) camera-based imager which can collect and convert the emitted light to an electrical signal. The electrical signal is then digitized for image display and analysis.

Detection of signals results in one or more visible protein bands on the membrane image. The molecular weight of the protein can be estimated by comparison with marker proteins and the amount of protein can be determined as this is related to band intensity (within the limits of the detection system).

Qualitative protein analysis is performed in order to verify the presence or absence of a specific protein of interest.

In addition, a good software package can magnify, rotate, resize, overlay, and annotate the corresponding gel and blot images, allowing export of the images to common documentation software.

In the present study, after blot development, the chemiluminescence detection of the mitochondrial proteins of interest is done with ChemiDoc^{TM} XRS+ system (Bio-Rad), an imager controlled by Image Lab^{TM} software (Bio-Rad).

This software can be also used to determine accurate quantification and purity of samples.

For data analysis, the 3-D view option is used to transform the gel image into a solid three-dimensional model spinning in space with x, y, and z dimensions for better localization of spot volumes.

Then, with the volume tools of the software, an area of interest is defined by manually surrounding it with a shape. After remove the background pixels, the result of the volume subtraction for a specific dot appears in the Adjusted Volume column of the analysis table report.

This procedure is performed to compare the relative ratio of dot intensity signal between free Complex I vs total Complex I:

The chemiluminiscence signals of NDUFB9 subunit (39 kDa) from Complex I in western blots were quantified by densitometry.

If Complex I is a component of supercomplexes, chemiluminescent spots of NDUFB9 are found in the same vertical line together with the spots of specific subunits of complex III and IV.

By the other side, if Complex I is separated from respirasomes, a single spot is found in the orthogonal vertical line relative to the ~1,000 kDa position in the horizontal direction (1D-BN PAGE) (Figure 2.6).

RESULTS

Effects of DDM-treatment over respiratory mitochondrial membranes

Isolated bovine heart mitochondria (BHM) were solubilized with dodecylmaltoside and separated by 2D BN/SDS-PAGE. The identity of respiratory supercomplexes and complexes was verified by immunodetection with monoclonal antibodies specific for single units of each OXPHOS complex (Figure 3.1)

The chemiluminiscence signal of NDUFB8 subunit (22 kDa) from Complex I was obtained from three independent western blots and quantified by densitometry.

In Figure 3.1.A, two spots are shown for this subunit: one spot is found in the same vertical line together with the spots of Complex III and IV, indicating that Complex I is a component of the respirasomes $I_1III_2IV_{0-4}$, whereas a second spot is found in the orthogonal vertical line relative to $\sim$1,000 kDa position in the horizontal direction (1D-BN PAGE), which can be recognized as "free" Complex I not assembled into supercomplex.

The two individual spot signals are clearly different in chemiluminescent intensity.

When expressed as percentage of total Complex I content (*i.e.* free+bound), the "free" form is $\sim$13% in Figure 3.1.A, whereas it increases to $\sim$98% in Figure 3.1.B These results are in agreement with previous findings [Schägger and Pfeiffer, 2000].

The functional significance of stable interaction between Complex I and Complex III within the supercomplex has been analyzed by comparing the detergent dependence of the integrated enzymatic activity of complex I + complex III (NADH:cytochrome *c* reductase), the catalytic activity of Complex I itself (NADH: ubiquinone reductase), and the production of reactive oxygen species from Complex I.

As shown in Figure 3.2.A, when mitochondria are solubilized with dodecylmaltoside, Complex I activity was decreased by 30%, indicating only marginal effect on the activity of the enzyme whereas a 70% decrease was observed in the activity of NADH:cytochrome *c* reductase (Figure 3.2.B), indicating less efficient electron transfer between the two enzymes after DDM-treatment.

The antimycin A-insensitive residual rates of NADH:cytochrome *c* actvity were <10% of the total rates shown in the figure.

On the other hand, oxidase activity (Figure 3.3.) was almost completely lost after addition of dodecylmaltoside, probably due to the dissociation and dilution of endogenous cytochrome *c*.

The functional significance of stable interaction between Complex I and Complex III within the supercomplex has been analyzed by comparing the detergent dependence of the integrated enzymatic activity of complex I + complex III (NADH:cytochrome *c* reductase), the catalytic activity of Complex I itself (NADH: ubiquinone reductase), and the production of reactive oxygen species from Complex I.

As shown in Figure 3.2.A, when mitochondria are solubilized with dodecylmaltoside, Complex I activity was decreased by 30%, indicating only marginal effect on the activity of the enzyme whereas a 70% decrease was observed in the activity of NADH:cytochrome *c* reductase (Figure 3.2.B), indicating less efficient electron transfer between the two enzymes after DDM-treatment.

The antimycin A-insensitive residual rates of NADH:cytochrome *c* actvity were <10% of the total rates shown in the figure.

On the other hand, oxidase activity (Figure 3.3) was almost completely lost after addition of dodecylmaltoside, probably due to the dissociation and dilution of endogenous cytochrome *c*.

The production of reactive oxygen species (ROS) from complex I was measured with the probe 2',7'- dichlorodihydrofluorescein diacetate (DCFDA) as described in *Materials and Methods*.

The assays were performed both in the presence of 1.8 µM mucidin and mucidin plus 4 µM rotenone. Samples pretreated only with 1.8 µM mucidin were used as control for all assays [Fato *et al*, 2009. Genova *et al*,2001].

Previous studies from our laboratory had shown that under these conditions ROS production from Complex III is prevented and the addition of rotenone enhances the generation of superoxide radicals from Complex I that represents the only source of ROS [Fato et al, 2009]. Consequently, we can consider that mucidin functionally isolates Complex I from downstream segments on the respiratory chain.

Fluorescence intensity data were expressed against Complex I activity to normalize the NADH-dependent leakage of electrons by the fraction of catalytically active molecules of the enzyme in the control and in the detergent-treated mitochondria control samples.

As shown in Figure 3.4, after solubilization of mitochondrial membranes with dodecylmaltoside, the production of ROS is significantly enhanced.

However, it is worth mentioning that in the DDM-treated samples rotenone had no further effect over the conspicuous increase of ROS production above the non-treated sample.
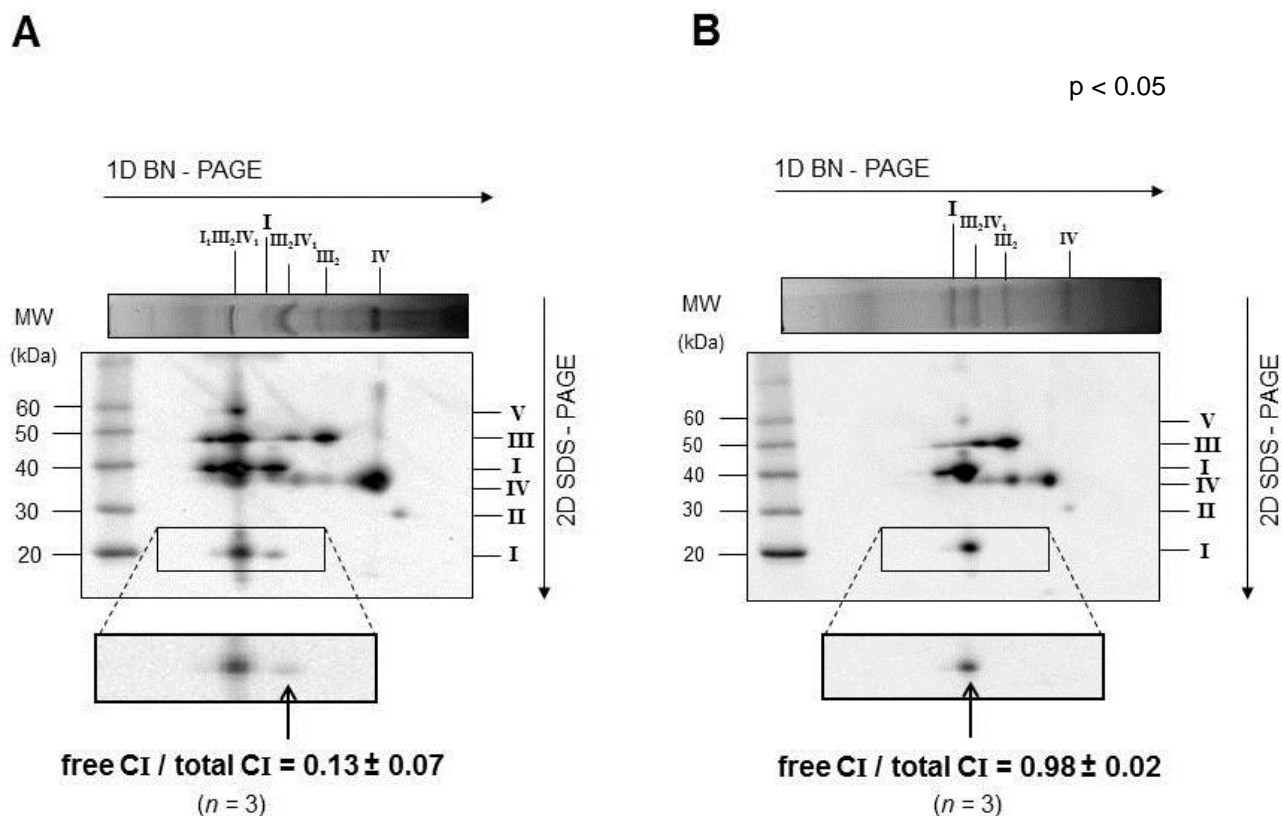
Figure 3.1: Supercomplex disassembling in bovine heart mitochondria (BHM). Respiratory supercomplexes and complexes from **(A)** digitonin-solubilized BHM with a detergent to protein ratio (w:w) of 8 and from **(B)** DDM-solubilized BHM with a detergent to protein ratio (w:w) of 2.6 were resolved by western blotting after 2D-BN/SDS-PAGE. *Arrows* point to monomeric Complex I. Monoclonal antibodies specific for single subunits of each OXPHOS complex are as follows: NDUFB8 (20 kDa) and NDUFA9 (39 kDa) of Complex I, SDHB (30 kDa) of Complex II, Core protein 2 (47 kDa) of Complex III and COX-I (57 kDa, apparent 35 kDa) of Complex IV and alfa subunit (53 kDa) of ATP synthase. The images shown in the picture were obtained *in camera* by double *overlaying* exposures (not post-production computer-graphic overlay) to the antibody against the NDUFA9-subunit and, in sequence, to a mixture of the remaining antibodies listed above. The ratio of free Complex I *versus* total Complex I (free CI / total CI) were determined by densitometric analysis of the immunoblots as described in the section "*Materials and Methods*". Data are given as mean ± S.D. *n* shows the number of independent samples. *p*-value was calculated according to the Student's *t* - test.
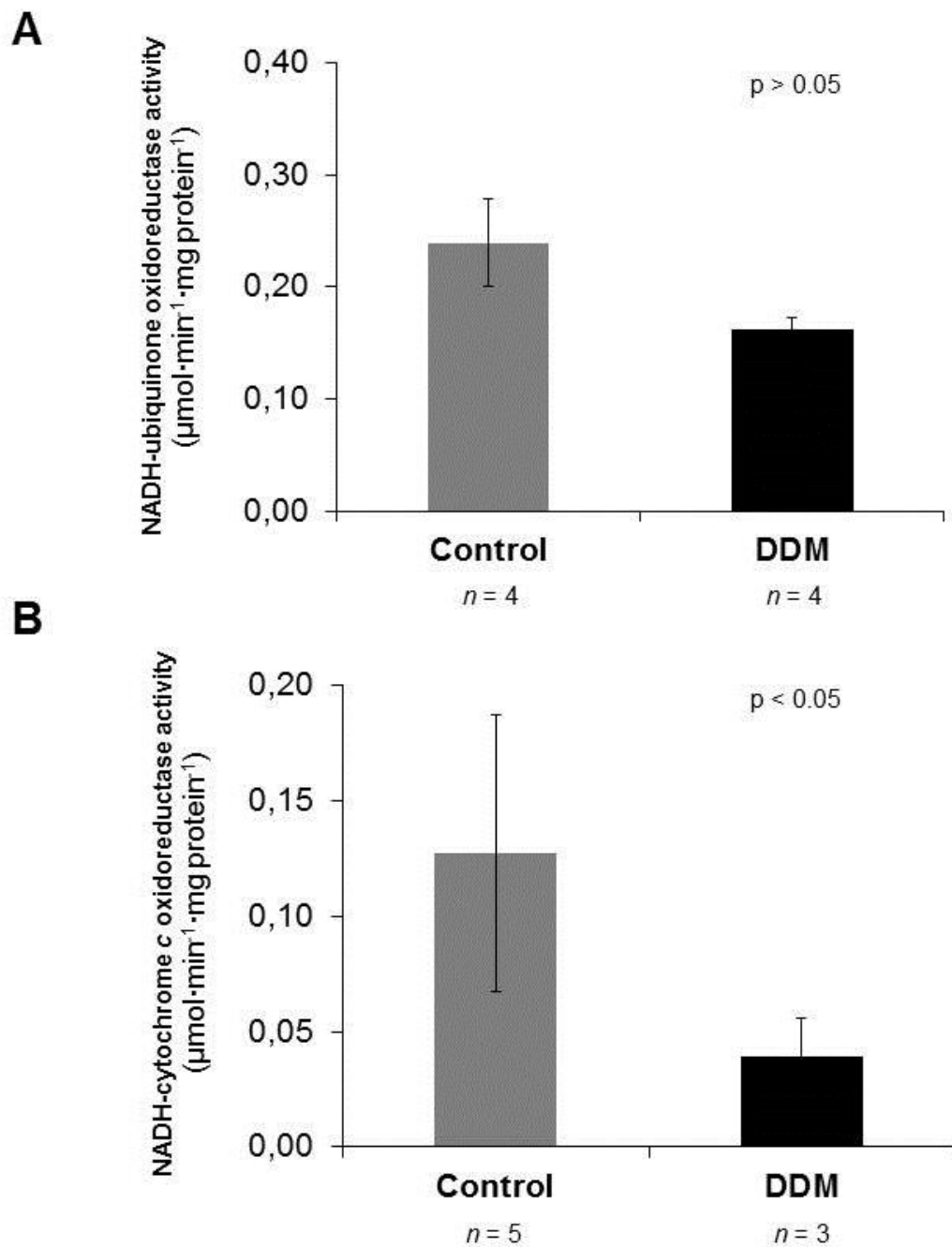
Figure 3.2: Functional analysis of supercomplex I_1III_2 and complex I in detergent-solubilized bovine heart mitochondria (BHM). Detergent dependence of **(A)** NADH-ubiquinone oxidoreductase activity **(B)** NADH-cytochrome c oxidoreductase activity. Activity rates are expressed in µmoles of NADH·min^{-1}·mg protein^{-1}. DDM: sample treated with 2.6 g dodecylmaltoside / g of protein. Data are given as mean ± S.D. n shows the number of independent samples. p-values were calculated using the Student's t-test.
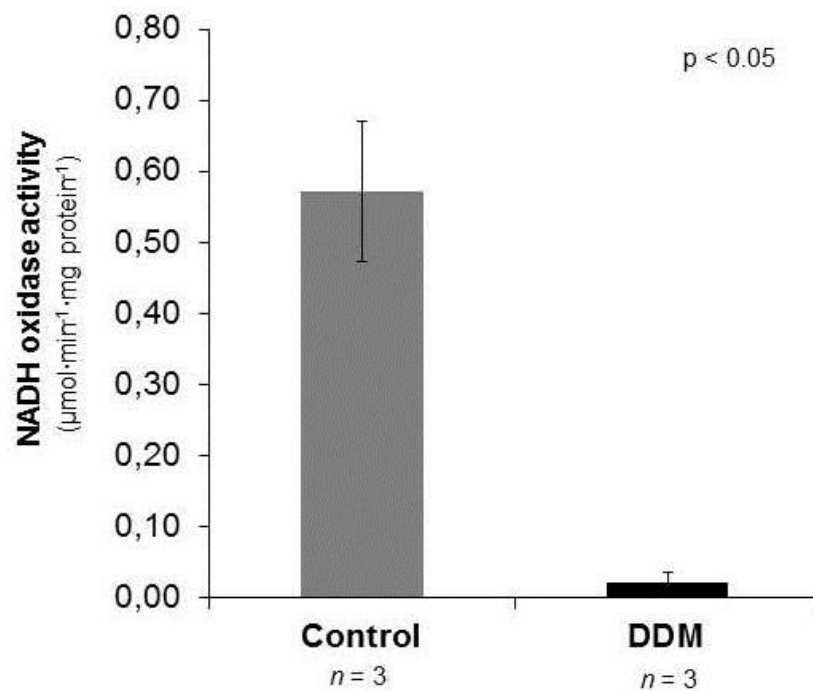
Figure 3.3: Functional analysis of supercomplex I_1III_2 and complex I in detergent-solubilized bovine heart mitochondria (BHM). Detergent dependence of NADH-oxidase activity. Activity rates are expressed in µmoles of NADH$\cdot$min$^{-1}\cdot$mg protein^{-1}. DDM: sample treated with 2.6 g dodecylmaltoside / g of protein. Data are given as mean ± S.D. n shows the number of independent samples. p-values were calculated using the Student's t – test
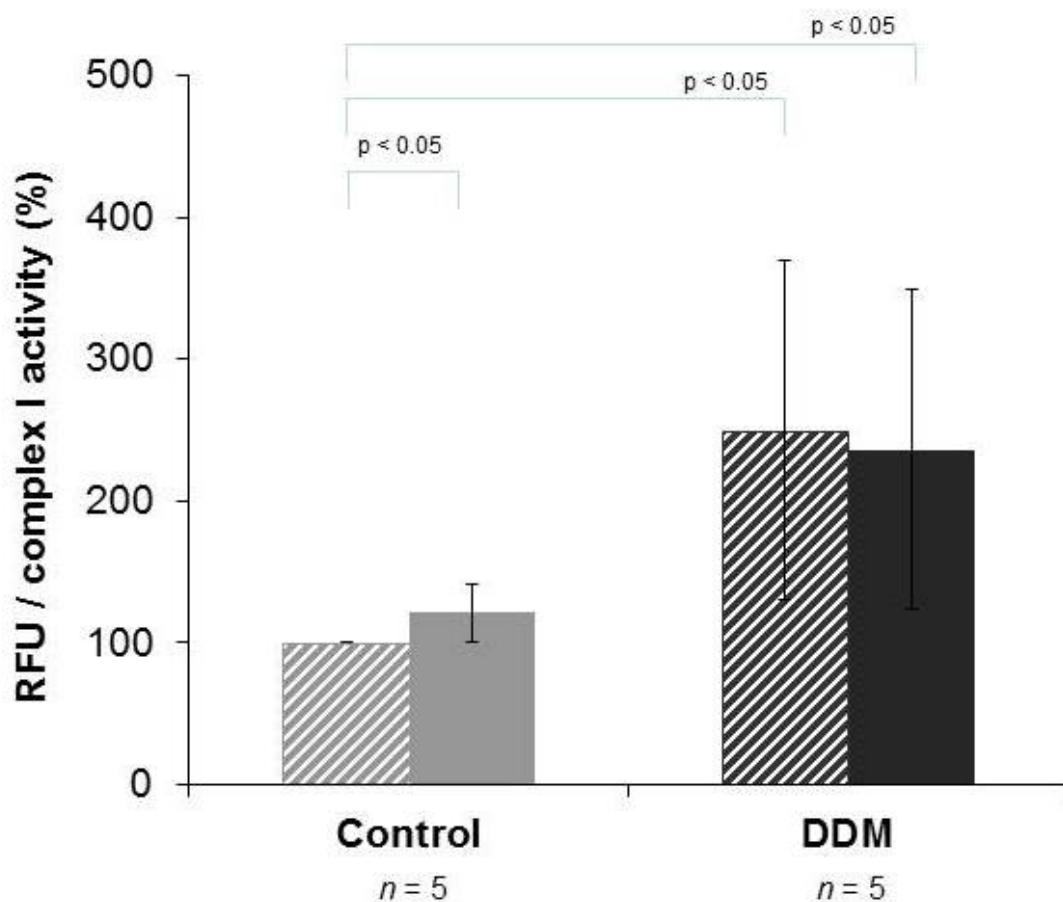
Figure 3.4: Functional analysis of supercomplex I_1III_2 and complex I in detergent-solubilized bovine heart mitochondria (BHM). The production of hydrogen peroxide was measured in the presence of 1.8 µM mucidin (*dashed bars*) and 1.8 µM mucidin plus 4 µM rotenone (*solid bars*). Values are expressed as relative fluorescence intensity (RFU) by DCF normalized against Complex I activity and shown as percentage values of the erence sample (*i.e.* control BHM in the presence of mucidin only). DDM: sample treated with 2.6 g dodecylmaltoside/g of protein. Data are given as mean ± S.D. *n* shows the number of independent samples. *p*-values were calculated using the Student's *t* - test.

Effects of lipid dilution and DDM-treatment in reconstituted supercomplex I$_1$III$_2$

R4B proteoliposomes were reconstituted with different amounts of phospholipids.

Preliminary results from our laboratory [Lenaz and Genova, 2009b. Lenaz et al, 2010] demonstrated that the NADH: cytochrome *c* oxidoreductase activity, experimentally determined, in a system at 1:30 (w:w) phospholipid dilution, overlaps with the values expected by theoretical calculation applying the pool equation of Kröger and Klingenberg [Kröger and Klingenberg, 1973a], whereas at 1:1 protein:lipid (w:w) ratio pool behavior is not effective anymore.

Kinetic testing according to the metabolic flux control analysis validated the hypothesis of a random organization in the 1:30-model and of a functional association between Complex I and Complex III in the 1:1-model [Genova et al, 2008].

Our analysis by bidimensional Blue-Native/SDS polyacrylamide gel electrophoresis (2D BN/SDS-PAGE) confirms that the proteoliposomes at high protein to lipid ratio are strongly enriched in the supercomplex I$_1$III$_2$ (Figure 3.5.A), whereas the relative amount of bound Complex I compared to its free form appears drastically diminished in the fraction having high phospholipid content (*i.e.* Complex I free/total = 0.08 *vs.* 0.76, respectively in the 1:1 and 1:30 samples) (Figure 3.5.B).

As shown in Figure 3.6, Complex I activity is the same at both phospholipid dilutions, whereas the integrated activity of NADH:cytochrome *c* reductase is about half in the 1:30 sample with respect to the 1:1 sample.

Then, the production of ROS was evaluated both by the superoxide dismutase (SOD)-sensitive reduction of acetylated cytochrome *c* for the detection of superoxide and by the DCF assay.

Both assays showed a dramatic increase of ROS production in the R4B 1:30 with respect to the R4B 1:1 sample (Figure 3.7).

The fraction of SOD-insensitive NADH-acetylated cytochrome *c* reductase activity that may possibly due to direct, not superoxide-mediated reduction of acetylated cytochrome *c* in the R4B 1:30 sample is low (<12%), showing unchanged absolute values compared to the SOD-insensitive activity in the 1:1 proteoliposomes (1.9 ± 0.7 and 2.8 ± 0.7 nmol·min^{-1}·mg $_{protein}^{-1}$, respectively in the 1:30 *vs.* 1:1 samples).

A further proof of our interpretation of the higher values of ROS production is due to disruption of association between Complex I and Complex III in the supercomplex I_1III_2 is given by the effect of the dodecylmaltoside treatment in the R4B 1:1 sample (Figure 3.8): The ratio of free to total Complex I increases to 0.79 after solubilization with dodecylmaltoside, compared to a erence value of 0.08 in the control.

Conversely, the integrated NADH:cytochrome *c* reductase activity dramatically decreases to less than 10% of the control, while Complex I activity is not altered (Figure 3.9).

ROS production from Complex I is increased more than threefold when the 1:1 proteoliposomes are treated with dodecylmaltoside (Figure 3.10).
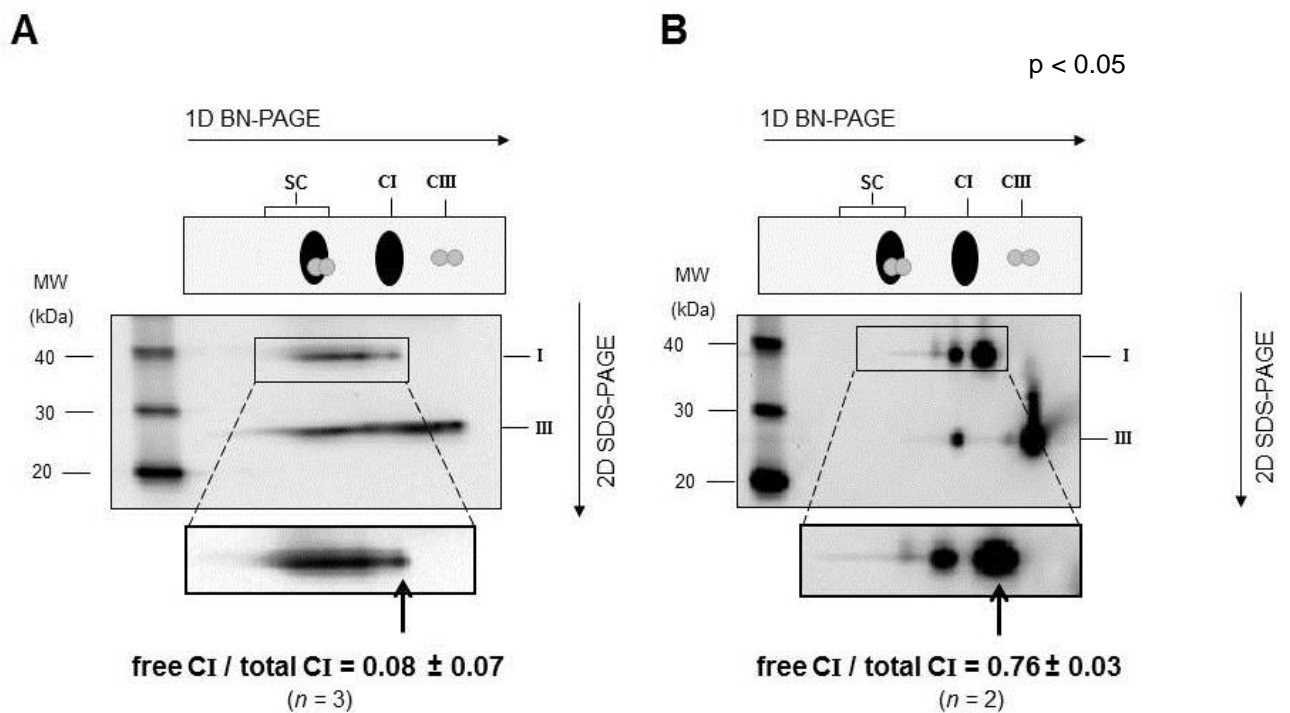
Figure 3.5: Supramolecular organization of respiratory Complex I and Complex III in R4B 1:1 and R4B 1:30 proteoliposomes. (A) R4B 1:1 and **(B)** R4B 1:30 samples were separated by 2D BN / SDS-PAGE after solubilization with digitonin at a detergent to protein ratio of 8 (w:w) and resolved by western blotting followed by immunodetection using monoclonal antibodies specific for single respiratory subunits. The images shown in the picture were obtained *in camera* by double overlaying exposures (not postproduction computer-graphic overlay) to the antibody against the NDUFA9 (39 kDa) subunit of Complex I and, in sequence, to the antibody against the Rieske protein (22 kDa) of Complex III. *Arrows* point to monomeric Complex I. The *upper panel* of the figures schematically shows the position of supercomplex I_1III_2 (SC), Complex I (CI) and dimeric Complex III (CIII) in the 1D BN-gel prior to second dimension electrophoresis (2D SDS-PAGE). The ratio of free Complex I *versus* total Complex I (free CI / total CI) were determined by densitometric analysis of the immunoblots as described in the section "*Materials and Methods*". Data are given as mean ± S.D. *n* shows the number of independent samples. *p*-value was calculated according to the Student's *t* - test.

Figure 3.6: Functional analysis in R4B 1:1 and R4B 1:30 proteoliposomes. (A) NADH-ubiquinone oxidoreductase activity **(B)** NADH-cytochrome c oxidoreductase activity. Activity rates are expressed in µmoles of NADH·min^{-1}·mg protein^{-1}. Data are given as mean ± S.D. n shows the number of independent samples. p-values were calculated using the Student's t-test.
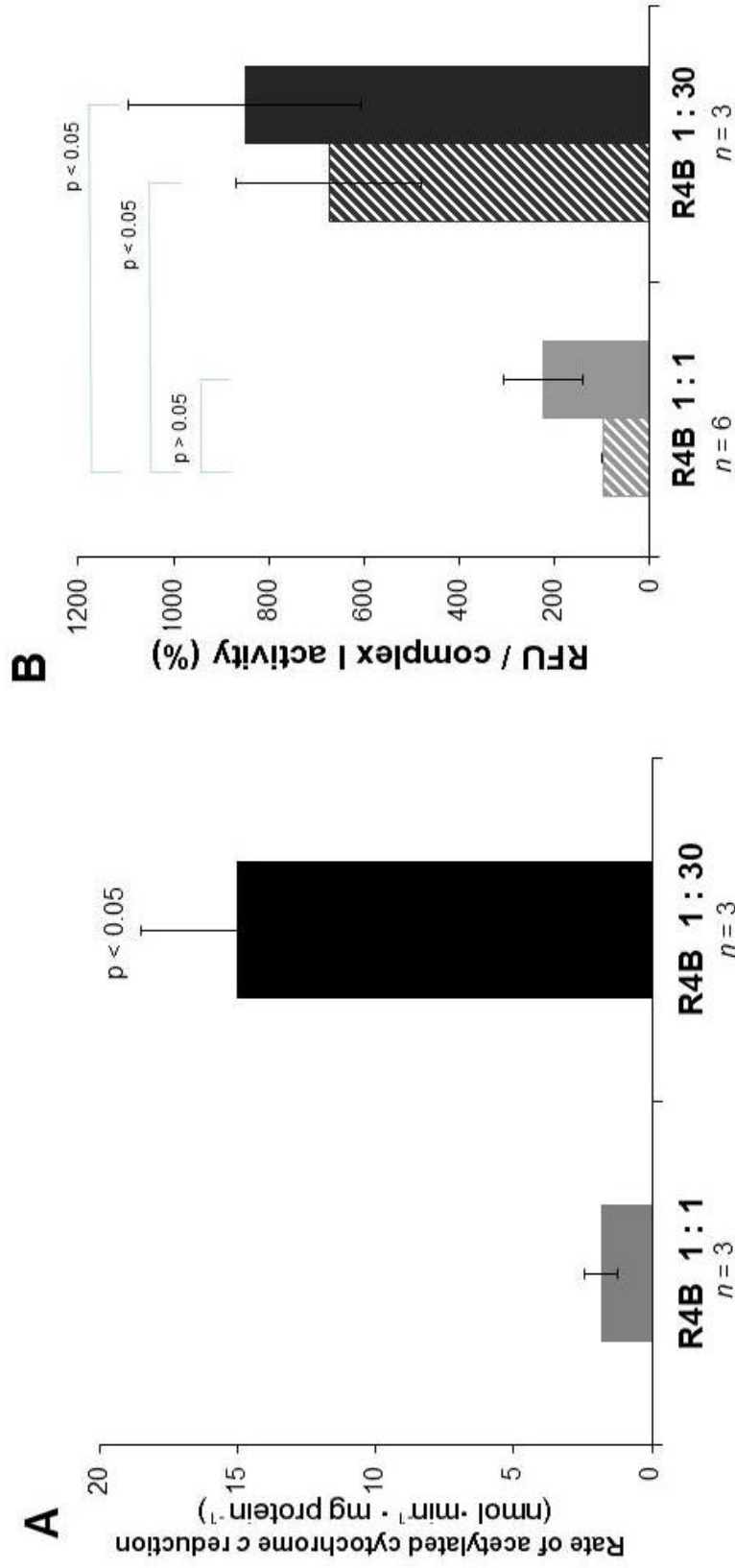
Figure 3.7: ROS production mediated by Complex I in R4B 1:1 and R4B 1:30 proteoliposomes. (A) The rate of superoxide formation is determined as the superoxide dismutase (SOD)-sensitive rate of acetylated cytochrome c reduction in the presence of 1.8 μM mucidin and 4 μM rotenone. The corresponding rates of SOD-insensitive activity are: 2.8 ± 0.7 and 1.9 ± 0.7 $nmol \cdot min^{-1} \cdot mg$ protein^{-1}, respectively in the 1:1 *versus* 1:30 samples. (B) The production of hydrogen peroxide was measured in the presence of 1.8 μM mucidin (*dashed bars*) and 1.8 μM mucidin plus 4 μM rotenone (*solid bars*). Values are expressed as relative fluorescence units (RFU) by DCF normalized against Complex I activity and shown as percentage values of the erence sample (*i.e.* R4B 1:1 in the presence of mucidin only). Data are given as mean ± S.D. n shows the number of independent samples. p-values were calculated using the Student's t-test.
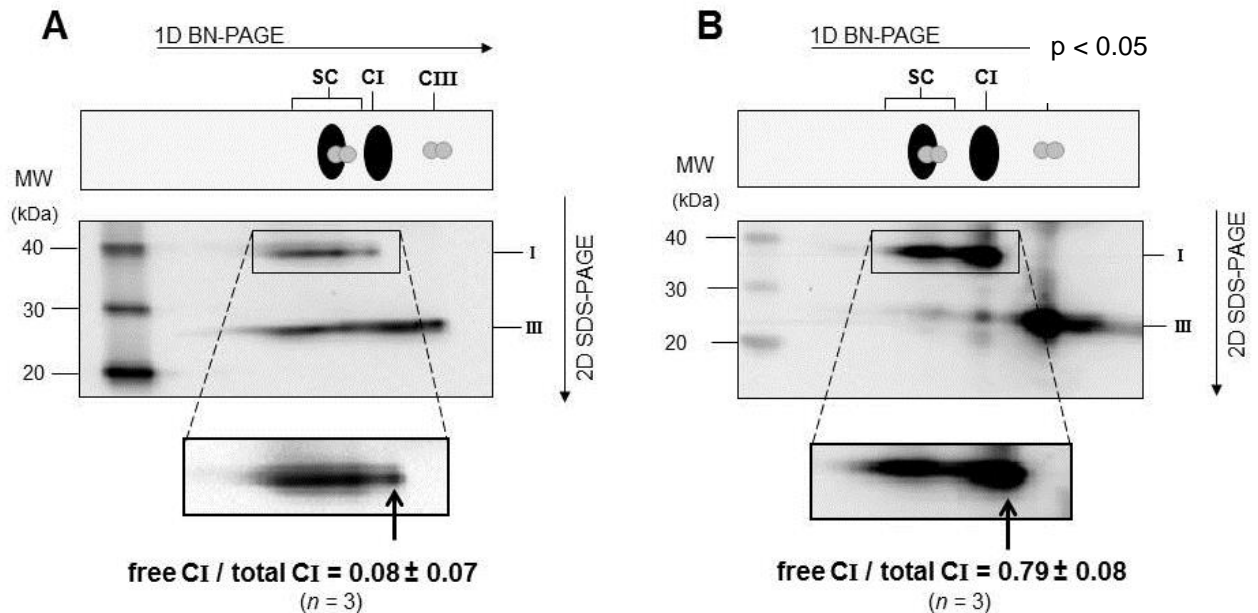
Figure 3.8: Disassembling of supercomplex I₁III₂ in R4B 1:1 proteoliposomes after detergent solubilization. Respiratory complexes were separated by 2D BN/SDS-PAGE after solubilization with **(A)** digitonin with a detergent to protein ratio (w:w) of 8 and with **(B)** DDM with a detergent to protein ratio (w:w) of 4.3 and were resolved by western blotting using monoclonal antibodies for single respiratory subunits. The images shown in the picture were obtained *in camera* by double overlaying exposures (not postproduction computer-graphic overlay) to the antibody against the NDUFA9 (39 kDa) subunit of Complex I and, in sequence, to the antibody against the Rieske protein (22 kDa) of Complex III. *Arrows* point to monomeric Complex I. The *upper panel* of the figures schematically shows the position of supercomplex I₁III₂ (SC), Complex I (CI) and dimeric Complex III (CIII) in the 1D BN-gel prior to second dimension electrophoresis (2D SDS-PAGE). The ratio of free Complex I *versus* total Complex I (free CI / total CI) were determined by densitometric analysis of the immunoblots as described in the section "*Materials and Methods*". Data are given as mean ± S.D. *n* shows the number of independent samples. *p*-value was calculated according to the Student's *t* - test.

Figure 3.9: Functional analysis of supercomplex I$_1$III$_2$ and complex I in detergent-solubilized R4B 1:1 proteoliposomes. Detergent dependence of **(A)** NADH-ubiquinone oxidoreductase activity and **(B)** NADH-cytochrome c oxidoreductase activity. Activity rates are expressed in µmoles of NADH·min^{-1}·mg·protein^{-1}. DDM: sample treated with 4.3 g dodecylmaltoside / g of protein. Data are given as mean ± S.D. n shows the number of independent samples. p-values were calculated using the Student's t-test.
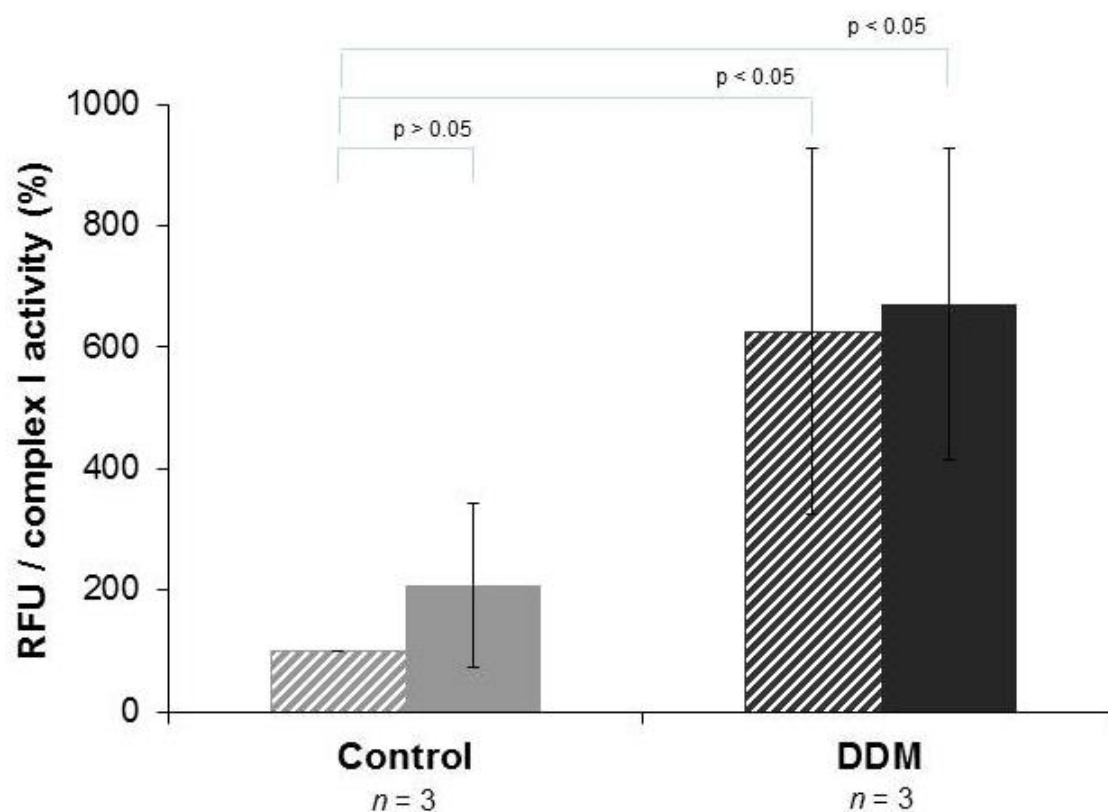
Figure 3.10: Functional analysis of supercomplex I$_1$III$_2$ and complex I in detergent-solubilized R4B 1:1 proteoliposomes. The production of hydrogen peroxide was measured in the presence of 1.8 μM mucidin (*dashed bars*) and 1.8 μM mucidin plus 4 μM rotenone (*solid bars*). Values are expressed as relative fluorescence intensity (RFU) by DCF normalized against Complex I activity and shown as percentage values of the erence sample (*i.e.* control R4B 1:1 in the presence of mucidin only). DDM: sample treated with 4.3 g dodecylmaltoside/g of protein. Data are given as mean ± S.D. *n* shows the number of independent samples. *p*-values were calculated using the Student's *t*-test.

## Effects of chaotrope-treatment in SMP and reconstituted supercomplex I₁III₂

Another experimental approach to disrupt supercomplex association is addition of chaotropic agents [Boumans *et al*, 1998].

Following this line of thought, 0.2 M KSCN was tested to weaken hydrophobic interactions between Complex I and Complex III inside supercomplexes in submitochondrial particles from bovine heart mitochondria (SMP) and R4B (1:1) proteoliposomes.

As shown in Figure 3.11, 2D BN/SDS-PAGE analysis reveals only partial disassembling of the supercomplex when submitochondrial particles were previously treated with 0.2 M KSCN (less than 40% of free Complex I) with a partial loss of Complex I activity. Nevetherless, under these experimental conditions we can observe enhanced ROS generation.

The same treatment with KSCN in 1:1 proteoliposomes did not produce clear evidence of supercomplex disassembling and only 9% of Complex I was found as free monomer compared to a rerence value of 8% in the control (Figure 3.12)

However, NADH:ubiquinone reductase activity was decreased by 45% showing a significant increase of reactive oxygen species production from Complex I.

These last results allows to infer that chaotropic solutes seem unlikely solubilize in and disassemble supramolecular assemblies in bovine mitochondria and 1:1 proteoliposomes.

When increasing SCN⁻ concentration to 0.4 M is possible to partially increase supercomplex disassembly in SMP, as 45% of free Complex I were detected in 2D BN/SDS-PAGE (Figure 3.13A).

Although a significant increase of ROS production was observed, Complex I activity decreased by about 50% respect control (Figure 3.13C and 3.13B). Similar results were observed in 1:1 proteoliposomes (Figure 3.13).

Thus, rising SCN⁻ concentration leads to a considerable increase on ROS production from Complex I but NADH:ubiquinone activities decay in a concentration-dependent manner in both SMP and 1:1 proteoliposomes samples.
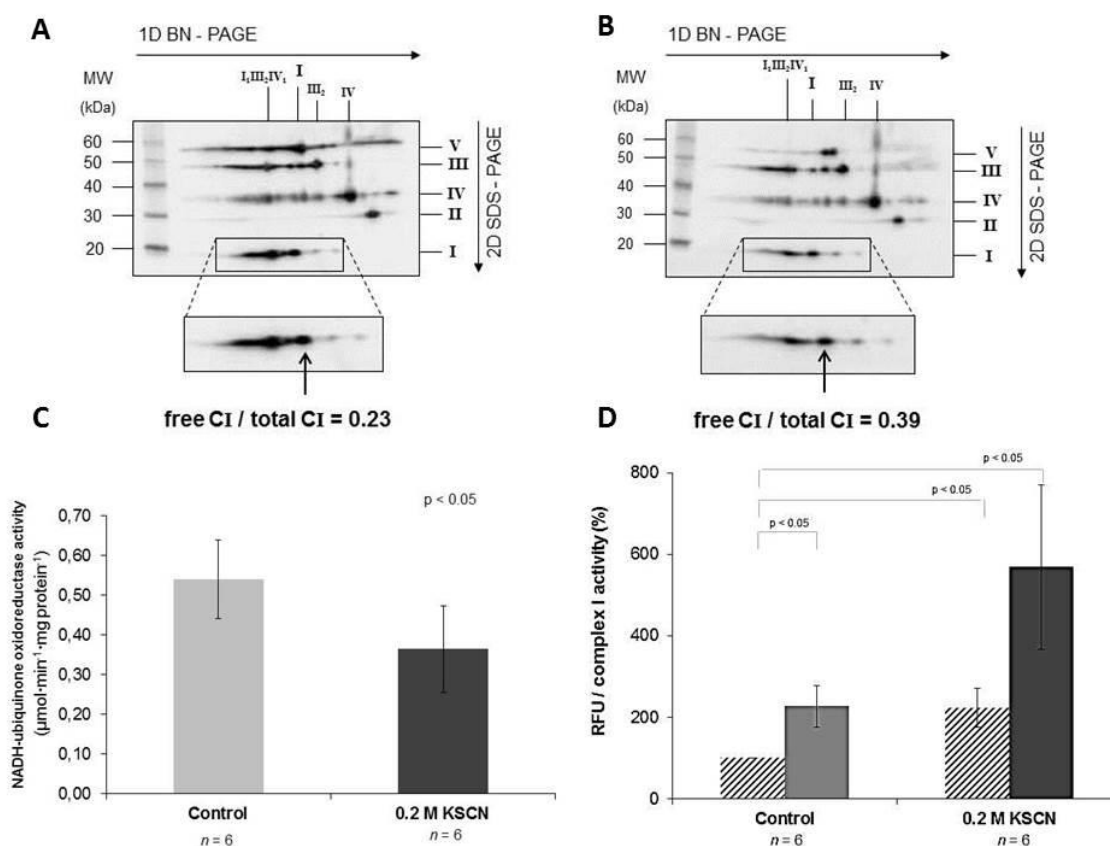
Figure 3.11: Disassembling of supercomplex I₁III₂ in bovine heart submitochondrial particles (SMP) after treatment with 0.2 M KSCN. Respiratory supercomplexes and complexes from (**A**) control SMP and from (**B**) KSCN-treated SMP were solubilized with digitonin with a detergent to protein ratio (w:w) of 8 and resolved by western blotting after 2D BN/SDS-PAGE. The ratio of free complex I vs total complex I was determined by densitometric analysis. *Arrows* point to monomeric complex I. Monoclonal antibodies specific for single subunits of each OXPHOS complex are as follows: NDUFB8 (20 kDa) of Complex I, SDHB (30 kDa) of Complex II, Core protein 2 (47 kDa) of Complex III and COX-I (57 kDa, apparent 35 kDa) of Complex IV and alfa subunit (53 kDa) of ATP synthase. The images shown in the picture were obtained *in camera* (not post-production computer-graphic overlay). The ratio of free Complex I *versus* total Complex I (free CI / total CI) were determined by densitometric analysis of the immunoblots as described in the section "*Materials and Methods*". (**C**) Potassium thiocyanate dependence of NADH-ubiquinone oxidoreductase activity. Activity rates (measured after removal of KSCN by ultracentrifugation) are expressed in µmoles of NADH·min⁻¹·mg protein⁻¹ .(**D**) The production of hydrogen peroxide was measured, after removal of KSCN by ultracentrifugation, in the presence of 1.8 µM mucidin (dashed bars) and 1.8 µM mucidin plus 4 µM rotenone (solid bars). Values are expressed as relative fluorescence intensity (RFU) by DCF normalized against Complex I activity and shown as percentage values of the erence sample (*i.e.* control SMP in the presence of mucidin only). Data are given as mean ± S.D. *n* shows the number of independent samples. *p*-values were calculated using the Student's *t* - test.
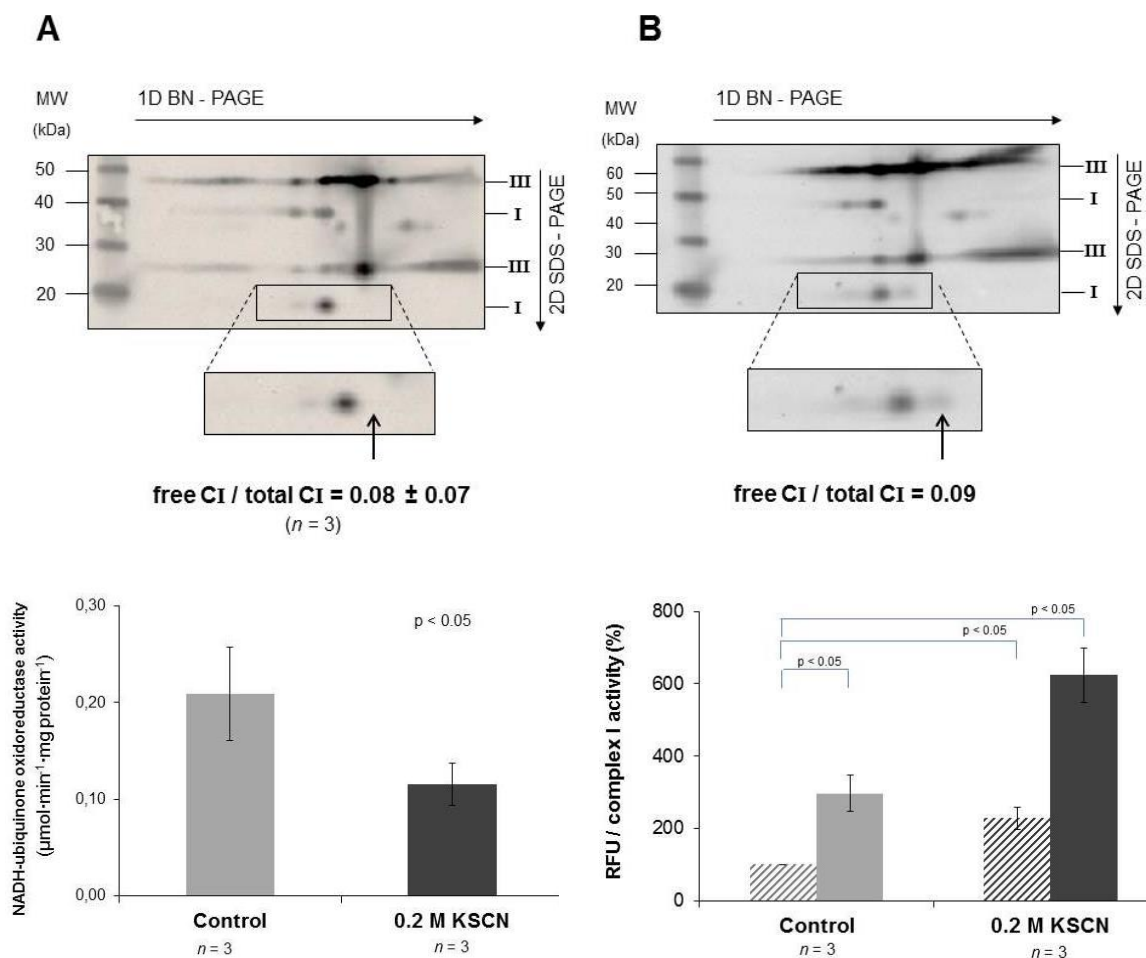
**Figure 3.12: Disassembling of supercomplex I₁III₂ in R4B 1:1 proteoliposomes after treatment with 0.2 M KSCN. (A)** Respiratory supercomplexes and complexes from KSCN-treated R4B 1:1 were solubilized with digitonin with a detergent to protein ratio (w:w) of 8 and resolved by western blotting after 2D BN/SDS-PAGE followed by immunodetection using monoclonal antibodies specific for single respiratory subunits. The image shown in the picture was obtained *in camera* by double overlaying exposures (not postproduction computer-graphic overlay) to the antibody against the NDUFA9 (39 kDa) and NDUFB8 (20 kDa) subunits of Complex I and, in sequence, to the antibodies against the Rieske protein (22 kDa) and Core protein 2 (47 kDa) of Complex III. *Arrows* point to monomeric Complex I. The ratio of free Complex I *versus* total Complex I (free CI / total CI) were determined by densitometric analysis of the immunoblots as described in the section "*Materials and Methods*". **(B)** Potassium thiocyanate dependence of NADH-ubiquinone oxidoreductase activity, measured after removal of KSCN by ultracentrifugation. Activity rates are expressed in µmoles of NADH·min^{-1}·mg protein^{-1} **(D)** The production of hydrogen peroxide was measured, after removal of KSCN by ultracentrifugation, in the presence of 1.8 µM mucidin (dashed bars) and 1.8 µM mucidin plus 4 µM rotenone (solid bars). Values are expressed as relative fluorescence intensity (RFU) by DCF normalized against Complex I activity and shown as percentage values of the erence sample (*i.e.* control R4B 1:1 in the presence of mucidin only). Data are given as mean ± S.D. *n* shows the number of independent samples. *p*-values were calculated using the Student's *t* - test.

Figure 3.13: Complex I activity and ROS production in bovine heart submitochondrial particles (SMP) after treatment with KSCN. (**A**) Respiratory supercomplexes and complexes from control SMP and from KSCN-treated SMP were solubilized with digitonin with a detergent to protein ratio (w:w) of 8 and resolved by western blotting after 2D BN/SDS-PAGE. The ratio of free complex I vs total complex I was determined by densitometric analysis. *Arrows* point to monomeric complex I. Monoclonal antibodies specific for single subunits of each OXPHOS complex are as follows: NDUFB8 (20 kDa) of Complex I, SDHB (30 kDa) of Complex II, Core protein 2 (47 kDa) of Complex III and COX-I (57 kDa, apparent 35 kDa) of Complex IV and alfa subunit (53 kDa) of ATP synthase. **(B)** and **(C)**. Potassium thiocyanate dependence of NADH-ubiquinone oxidoreductase activity and ROS production (measured after removal of KSCN by ultracentrifugation), respectively. Activity rates are expressed in μmoles of NADH·min^{-1}·mg protein^{-1}. The production of hydrogen peroxide was measured in the presence of 1.8 μM mucidin (dashed bars) and 1.8 μM mucidin plus 4 μM rotenone (solid bars). Values are expressed as relative fluorescence intensity (RFU) by DCF normalized against Complex I activity and shown as percentage values of the erence sample (*i.e.* control SMP in the presence of mucidin only). Data are given as mean ± S.D. *n* shows the number of independent samples. *p*-values were calculated using the Student's *t* - test.
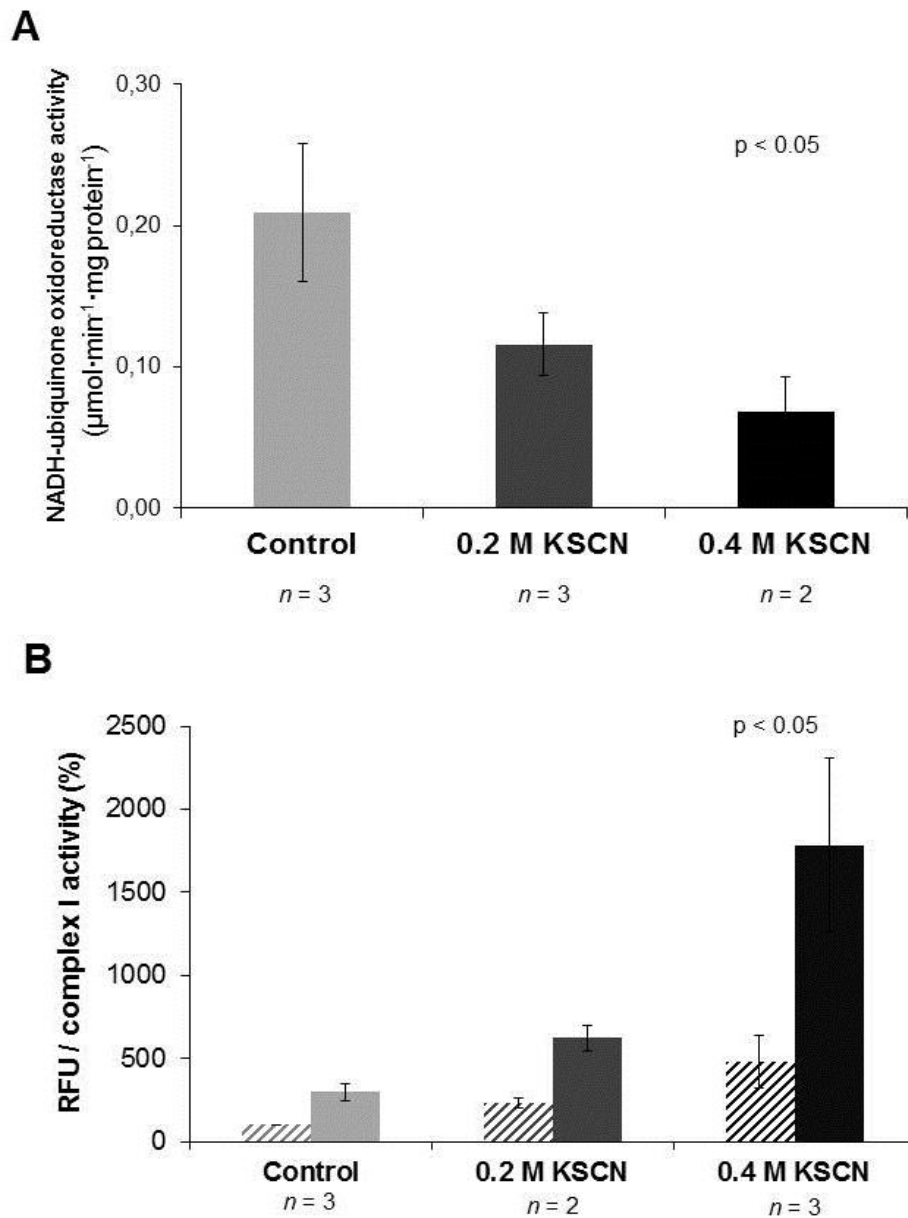
Figure 3.14: Complex I activity and ROS production in R4B 1:1 proteoliposomes after treatment with KSCN. Potassium thiocyanate dependence (measured after removal of KSCN by ultracentrifugation) of **(A)** NADH-ubiquinone oxidoreductase activity and **(B)** ROS production, respectively. Activity rates are expressed in µmoles of NADH$\cdot$min$^{-1}\cdot$mg protein^{-1} The production of hydrogen peroxide was measured in the presence of 1.8 µM mucidin (dashed bars) and 1.8 µM mucidin plus 4 µM rotenone (solid bars). Values are expressed as relative fluorescence intensity (RFU) by DCF normalized against Complex I activity and shown as percentage values of the erence sample (*i.e.* control R4B 1:1 in the presence of mucidin only). Data are given as mean ± S.D. *n* shows the number of independent samples. *p*-values were calculated using the Student's *t* - test.

The following figure and table summarize the results of this study:
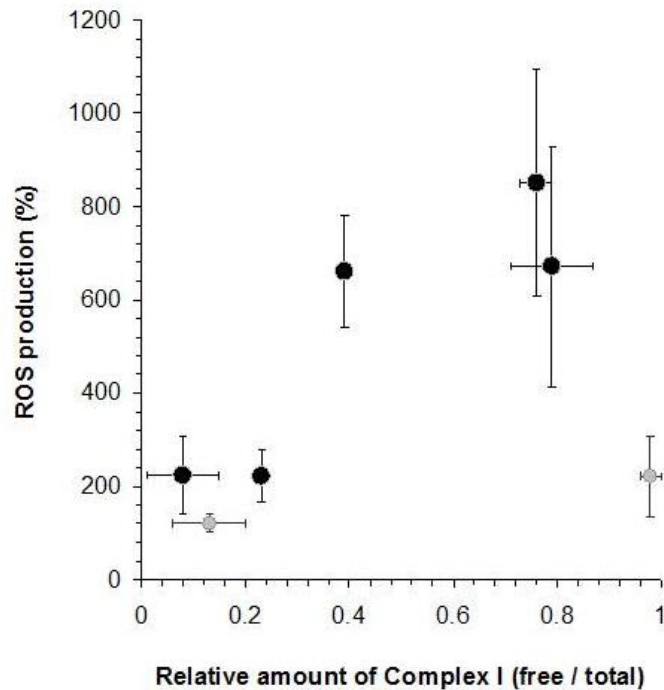
Figure 3.15: Production of ROS by mitochondrial Complex I in different situations where supercomplexes are maintained or dissassembled. The percent value of ROS production measured in all the samples listed in Table…is plotted in the graph against the corresponding ratio of free Complex I versus total Complex I. The statistical analysis of the data using the Pearson's parametric test indicates a positive correlation (r = 0.884, p<0.05) between ROS generation and relative amount of free Complex I in the R4B and in the SMP samples (black symbols). The BHM samples (grey symbols) were not included in the correlation analysis because the existence of endogenous antioxidants systems operating to reduce ROS levels in the mitochondria might have counteracted the dramatic effects of the complete dissociation of Complex I, thus leading to a two-fold only increase of the measured ROS production. SMP, submitochondrial particles.

Table 3.1: Production of Reactive Oxygen Species by mitochondrial Complex I in different situations where supercomplexes are maintained or disassembled

	ROS production (%)	Relative amount of Complex I (free/total)
R4B 1:1	224 ± 83 (6)	0.08 ± 0.07 (3)
R4B 1:1 + DDM 4.3 g / g	672 ± 257 (3) p<0.05	0.79 ± 0.08 (3) p<0.001
R4B 1:30	851 ± 243 (3) p<0.05	0.76 ± 0.03 (2) p<0.001
SMP	223 ± 56 (5)	0.23 (1)
SMP + 0.2 M KSCN	662 ± 120 (5) p<0.05	0.39 (1)
BHM	121 ± 20 (5)	0.13 ± 0.07 (3)
BHM + DDM 2.6 g / g	223 ± 86 (5) p<0.05	0.98 ± 0.02 (3) p<0.001

The samples were assayed in the presence of 1.8 μM mucidin and 4 μM rotenone as described in the section "Materials and Methods". The production of ROS is expressed as the relative fluorescence intensity of diclorofluorescein normalized against Complex I activity. Data are shown as percentage values of the corresponding erence sample (i.e. R4B 1:1, SMP, and BHM, respectively assayed in the presence of 1.8 μM mucidin only). The ratio of free Complex I versus total Complex I was determined by densitometric analysis of immunoblots after 2D BN/SDS-PAGE as described in the section "Materials and Methods". Values in round brackets indicate the number of independent samples. Results are significantly different from their respective control according to the Student's *t*-test.

DISCUSSION

Disassembling of respiratory supercomplexes has several functional consequences on mitochondrial respiration:

Loss of enzymatic channeling between Complex I and Complex III

Previous work in our laboratory have shown this effect in the CoQ region by demonstrating that the integral NADH:cytochrome *c* reductase activity decreased when Complex I and Complex III are present as individual enzymatic entities in proteoliposomes reconstituted at high lipid to protein ratios (30:1) [Bianchi et al, 2003].

In that case, the observed rate of electron transfer between Complex I and Complex III was found to approximate the theoretical values predicted from the CoQ-pool equation [Kröger and Klingenberg, 1973a], indicating a random organization of these components [Hackenbrock et al, 1986].

The diminution of the integral Complex I - Complex III activity is not a result of enzyme inactivation or inhibition, since the individual activities of these complexes (NADH:ubiquinone reductase and ubiquinol:cytochrome *c* reductase, respectively) were not affected when comparing with proteoliposomes with lower lipid content (*i.e.* lipid:protein ratio of 1) [Bianchi *et al,* 2003].

In the present study, we confirmed that the overall NADH:cytochrome *c* reductase activity, which is ascribable to functional association between Complex I and Complex III into supercomplexes, was dramatically decreased in proteoliposomes 30:1 (lipid:protein ratio) respect to proteoliposomes enriched on I_1III_2 supercomplexes (*i.e.,* 1:1 lipid:protein ratio), while the activity of Complex I was unaffected when increasing the lipid content (Figure 4.6).

Moreover, we show that Complex I and Complex III are not assembled into supercomplexes in the 30:1 (lipid to protein)-samples, as most Complex I was detected as free holoenzyme in 2D BN/SDS-PAGE analyses (Figure 4.5).

The functional significance of Complex I - Complex III interactions in supercomplexes has been also demonstrated by the drastic decrease of NADH:cytochrome *c* reductase, but not of NADH:ubiquinone reductase and of ubiquinol:cytochrome *c* reductase in mitochondria-solubilized with dodecylmaltoside, a very mild detergent suitable to disassemble supercomplexes [Schägger and Pfeiffer, 2000].

Similar results were obtained in the present work with both mitochondria and 1:1 proteoliposomes (Figures 3.1, 3.2 and 3.8, 3.9).

These evidences clearly demonstrate that, depending on the experimental conditions, electron transfer between Complex I and Complex III can take place both by CoQ channeling within the core I_1III_2 supercomplex and by the less efficient collision-based pool behavior when Complex I - Complex III interactions are disrupted by lipid-dilution or solubilized with a non-ionic detergent.

Production of reactive oxygen species from Complex I

The possibility that supercomplex assembly prevents excessive ROS generation from Complex I has been advanced on theoretical grounds [Panov et al, 2007. Seelert et al, 2009. Lenaz and Genova, 2012] but no direct experimental study was previously addressed to this issue.

Indeed, in complex biological systems is difficult to ascertain a clear relationship of cause - effect between supercomplex alteration and ROS production, since the two phenomena may influence each other.

In this study we induce a primary condition in isolated mitochondria and Complex I- Complex III proteoliposomes by means able to disrupt supercomplex interactions (*i.e.* DDM-treatment or lipid dilution) increasing the ratios of Complex I present as free and functionally active holoenzyme and we obtain the first direct demonstration that loss of supercomplex organization causes an enhancement of ROS generation by Complex I itself.

This demonstration is clearly evident (Table 4.1 and Figure 4.15) both in reconstituted proteoliposomes, where the dissociation of Complex I from the respirasome is accompanied by a three/four-fold increase of ROS generation (Figure 4.7 and 4.10), and in DDM-solubilized mitochondrial membranes (Figure 4.4).

In the latter case, the existence of endogenous systems operating to reduce ROS levels in the mitochondrial sample (*i.e.* mitochondrial glutathione peroxidase, Mn-superoxide dismutase and non-enzymatic endogenous antioxidants) might have counteracted the effects of the complete dissociation of Complex I, thus leading to a two-fold increase of the measured ROS production.

The enhancement of ROS production from Complex I does not appear to be a result of Complex I denaturation after the solubilization of the bovine mitochondria and 1:1 proteoliposomes with dodecylmaltoside.

As discussed above, the NADH:ubiquinone reductase activities are not affected (Figure 4.9) are or marginally decreased (Figure 4.2), though Complex I is functionally intact as free holoenzyme under these conditions (Figures 4.1 and 4.8).

A further demonstration that the disruption of Complex I-Complex III interactions within supercomplex increases ROS levels from Complex I was obtained in reconstituted Complex I/ Complex III proteoliposomes at high lipid to protein ratio (30:1) whereas formation of the supercomplex I_1III_2 is prevented:

Likewise, the generation of superoxide is several fold higher than in proteoliposomes with lower lipid content (1:1) which are rich in supercomplexes I_1III_2 (Figure 4.7).

In agreement with this finding, dissociation with dodecylmaltoside of the I_1III_2 supercomplexes in R4B 1:1 induces a strong enhancement of ROS generation (Figure 4.9)

Moreover, the hypothetical reasoning that facilitation of electron flow by substrate channeling within the respirasome helps maintaining the redox components of the complexes in the oxidized state, thus limiting ROS formation, cannot be the only explanation. In fact, in the experiments reported in this study, ROS production is investigated in presence of inhibitors (mucidin and rotenone) that prevent electron transfer to any possible acceptor, so that we can guess that the redox centers in

Complex I are maximally reduced both in the situations where supercomplexes are maintained and in the situations where Complex I is free.

On the other hand, such as chaotropic solutes that were previously found to dissociate the supercomplex in yeast mitochondria [Boumans et al, 1998], were partially effective in our mitochondrial membranes and proteoliposomes.
However, under these experimental conditions we observed an increase in ROS production (Figures 4.11 and 4.12).

Unlike non-ionic detergent-treatment or lipid dilution, we observed a partial loss of NADH:ubiquinone reductase activities after treatment of R4B 1:1 proteoliposomes and SMP with SCN$^-$ (Figure 4.11C and 4.12B).

In addition, increasing SCN$^-$ concentration led to a considerable decay in Complex I activities, showing at the same time higher levels of ROS production without any significant disassembling of Complex I from supercomplexes (Figure 4.13 and 4.14).

A possible reason to explain this effect is that SCN$^-$ destabilize membrane proteins by electrostatic interactions facilitating protein unfolding [Möglich et al, 2005. Makhatadze and Privalov, 1992], rather than solubilizing annular and non-annular lipids as dodecylmaltoside does [Rabilloud, 2009].
Thus SCN$^-$ treatment in mitochondrial membrane proteins would increase the number of hydrophobic regions exposed to the solvent which could be involved in the reduction of oxygen.

Stability of Complex I

Another functional consequence previously described from disruption of the supercomplex I_1III_2 core structure is loss of stability of Complex I.

In spite that loss of NADH:ubiquinone activity was reported in mutant cell models lacking respiratory supercomplexes [Acín-Pérez et al, 2008. D'Aurelio et al, 2006. Diaz et al, 2006. Schägger et al, 2004. Stroh et al, 2004], this was not observed in the present study, since the activity of Complex I decreases only marginally upon supercomplex disassembling in mitochondrial membranes but not in proteoliposomes enriched of I_1III_2 supercomplexes (Figures 4.2, 4.6, and 4.9).

In addition, free Complex I holoenzyme stably appears in the native gels (Figures 4.1, 4.5 and 4.8).

These evidences show that monomeric Complex I persist functionally intact under our experimental conditions.

Indeed, Complex I upon isolation and purification was shown to be sufficiently stable to allow high turnover number [Hatefi et al, 1962c . Schägger and Pfeiffer, 2000].

The marginal decrese in NADH:ubiquinone activity observed in mitochondrial membranes solubilized with dodecylmaltoside would be adscribable to the fact that when Complex I is a free holoenzyme it becomes more susceptible to free radical damage.

In regard to this, it is noteworthy that these results are compatible with very recent observations by Diaz *et al.* [Diaz et al, 2012] showing that diminished stability of supercomplexes and Complex I is correlated with increased levels of ROS in mouse lung fibroblasts–lacking the Rieske iron-sulphur protein of Complex III and hence devoid of the supercomplexes containing Complex I.

Although the higher ROS formation in free Complex I with respect to the supercomplex could be a result of slower electron transport along the respiratory chain, as this could increase the lifetime of some reactive species, we belive that in our samples the increased production of ROS by Complex I as free holoenzyme is due to different structural features.

In fact, when the supercomplex is dissociated, we also observe increased ROS production after rotenone treatment, which abolishes electron flow from NADH to ubiquinone in either experimental condition (i.e. free complex I and supercomplex I-III).

CONCLUSIONS

In conclusion, as summarized in Table 4.1 and in Figure 4.15 the results of the present study provide experimental evidence that the production of reactive oxygen species is strongly increased in either model, supporting the hypothesis that disruption or prevention of the association between Complex I and Complex III by different means enhances the generation of superoxide from Complex I.

Indeed, this work is the first demonstration that dissociation of the supercomplex I_1III_2 in the mitochondrial membrane is cause of oxidative stress from Complex I [Maranzana et al, 2013]

Even though the results in the present work are an *in vitro* study, but it is supported by several observations in cellular and animal models linking together supercomplex dissociation and enhanced ROS production:

Enhanced ROS generation and oxidative stress were found in yeast mutants lacking the supercomplex assembly factor Rcf1 and thus devoid of supercomplexes III-IV [Chen et al, 2012. Strogolova et al, 2012. Vukotic et al, 2012].

Since the yeast *S. cerevisiae* lacks Complex I, in this case we may consider the origin of the extra ROS being presumably free Complex III, while supposing that other potential sources of ROS (*i.e.* external alternative NADH dehydrogenase) are not affected in the Rcf1 mutants.

Numerous pathological states are accompanied by enhanced generation of ROS [Chen and Keaney, 2012] and both mitochondria and other systems, such as plasma membrane NADPH oxidase, have been implicated as the sources of ROS.

In an experimental model of heart failure, the decrease of oxidative phosphorylation has been associated with a decrease of respiratory supercomplexes [Rosca and Hoppel, 2009. Rosca and Hoppel, 2010. Rosca et al, 2008].

Lymphoblasts from patients affected by Barth Syndrome, due to genetic loss of tafazzin, an enzyme involved in cardiolipin remodelling, have altered mitochondrial supercomplexes [McKenzie et al 2006]; likewise, in a yeast experimental model of

tafazzin mutation, Chen *et al.* [Chen et al, 2008] observed an increased oxidative stress in response to ethanol.

Also, Baracca *et al.* [Baracca et al, 2010. Lenaz et al, 2010] demonstrated a strong decrease of supercomplex assemblies in mouse fibroblasts expressing the activated form of the *k*-ras oncogene associated with higher ROS generation in comparison with wild type fibroblasts.

Aging is also accompanied by a decline of supercomplex association [Gómez et al, 2009. Frenzel et al, 2010]; despite some uncertainties and challenges, aging is generally associated with increased ROS and oxidative damage [for a recent review *cf.* [Cui et al, 2012].

Gomez and Hagen [Gómez and Hagen, 2012] reason that age-associated destabilization of respiratory supercomplexes may be important for the development of the mitochondrial aging phenotype by means of impaired bioenergetics and enhanced ROS production.

In addition, Frenzel *et al.* [Frenzel et al, 2010] on the basis of the 3D-structures of supercomplexes and the close spatial arrangement of the respective electron carrier binding sites [Schäfer et al, 2007] conclude that less superoxide radical formation is expected to occur in supercomplexes than in randomly distributed individual complexes.

These latter studies, however, fail to show which is the causing event (*i.e.* supercomplex dissociation causing ROS increase or, alternatively, ROS increase causing supercomplex dissociation) or even if they are independent phenomena.

In this perspective we can conclude that the present study contribute to a better understanding of the observations made in cellular and animal systems and represent a starting point to further elucidate the intricate relationship between the supramolecular organization of the respiratory chain and the production of ROS, which can modulate some signalling pathways from mitochondria to the cell and also act as damaging agents, depending on the amounts produced [Anilkumar et al, 2009. Ide et al, 2000. Ray et al, 2012].

In addition, this study confirms the hypothesis that primary causes of oxidative stress may perpertuate reactive oxygen species production by a vicious circle involving supercomplex dissociation as a major determinant. Thus, it is easy to foresee the implications of these findings in human diseases and in aging, where oxidative stress plays a major etiologic and pathogenic role.

Moreover, we can comment that the postulated dynamic structure of supercomplexes [Acin Perez *et al* 2008. Acin Perez and Enriquez, 2014] and the modulation of their association may represent a physiological means to control the production of ROS as redox signals from the mitochondria to the cell.

REFERENCES

[Abdrakhmanova et al, 2006] Abdrakhmanova, A.; Zwicker, K.; Kerscher, S.; Zickermann, V.; Brandt, U. (2006). Tight binding of NADPH to the 39-kDa subunit of complex I is not required for catalytic activity but stabilizes the multiprotein complex. *Biochim Biophys Acta* 1757:1676 – 1682

[Acin-Perez and Enriquez, 2014] Acin-Perez R, Enriquez JA. (2014). The function of the respiratory supercomplexes: The plasticity model. Biochim Biophys Acta. 2014 Apr;1837(4):444-450.

[Acín-Pérez et al, 2004] Acín-Pérez, R.; Bayona-Bafaluy, M.P.; Fernández-Silva, P.; Moreno-Loshuertos, R.; Pérez-Martos, A.; Bruno, C.; Moraes, C.T.; Enríquez, J.A. (2004). Respiratory complex III is requiered to maintain complex I in mammalian mitochondria. *Mol Cell* 13: 805-815

[Acín-Pérez et al, 2008] Acín-Pérez R, Fernández-Silva P, Peleato, ML, Pérez-Martos A, Enríquez JA (2008). Respiratory active mitochondrial supercomplexes. *Mol Cell* 32: 529-539

[Acín-Pérez et al, 2009] Acín-Pérez, R.; Salazar, E.; Brosel, S.; Yang, H.; Schon, E.A.; Manfredi, G. (2009). Modulation of mitochondrial protein phosphorylation by soluble adenyl cyclase ameliorates cytochrome oxidase defects. *EMBO Mol Med* 1: 392 – 406

[Ahlers et al, 2000] Ahlers, P.M.; Zwicker,K.; Kerscher,S.; Brandt,U. (2000). Function of conserved acidic residues in the PSST homologue of complex I (NADH:ubiquinone oxidoreductase) from *Yarrowia lipolytica. J Biol Chem* 275: 23577 – 23582

[Aitken and Learmonth, 2002] Aitken, A.; Learmonth, M.P. (2002). Protein determination by UV absorption. From: *The protein protocols handbook* 2nd edition. pp 3 - 6. Edited by Walker, J.M. Humana Press, Inc. Totowa, NJ (USA)

[Albracht, 1993] Albracht, S.P. (1993). Intimate relationships of the large and the small subunits of all nickel hydrogenases with two nuclear-encoded subunits of mitochondrial NADH: ubiquinone oxidoreductase. *Biochim Biophys Acta* 1144: 221 - 224

[Althoff *et al,* 2011] Althoff, T.; Mills, D.J.; Popot, J.L.; Kühlbrandt, W. (2011). Arragement of electron transport chain components in bovine mitochondrial supercomplex $I_1III_2IV_1$. *EMBO J* 30: 4652-4664

[Angerer et al, 2011] Angerer,H.; Zwicker, K.; Wumaier, Z.; Sokolova, L.; Heide, H.; Steger, M.; Kaiser, S.; Nübel, E.; Brutschy, B.; Radermacher, M. Brandt, U.; Zickermann, V. (2011). A scaffold of accessory subunits links the peripheral arm and the distal proton-pumping module of mitochondrial complex I. *Biochem J* 437: 279 – 288

[Anilkumar et al, 2009] Anilkumar, N.; Sirker, A.; Shah, A.M. (2009). Redox sensitive signaling pathways in cardiac remodeling, hypertrophy and failure. *Front Biosci* 14: 3168–3187

[Antonicka et al, 2003] Antonicka, H.; Ogilvie, I.; Taivassalo, T.; Anitori, R. P.; Haller, R. G.; Vissing, J.; Kennaway, N. G.; Shoubridge, E. A. (2003). Identification and characterization of a common set of complex I assembly intermediates in mitochondria from patients with complex I deficiency. *J Biol Chem* 278: 43081 – 43088

[Arnold et al, 1998] Arnold, I.; Pfeiffer, K.; Neupert, W.; Stuart, R.A.; Schägger, H. (1998). Yeast mitochondrial F_1F_0-ATP synthase exists as a dimer: identification of three dimer-specific subunits. *EMBO J* 17: 7170-7178

[Atteia et al, 2003] Atteia, A.; van Lis, R.; Mendoza-Hernandez, G.; Henze, K.; Martin, W.; Riveros-Rosas, H.; Gonzalez-Halpen, D. (2003). Bifunctional aldehyde/alcohol dehydrogenase (ADHE) in chlorophyte algal mitochondria. *Plant Mol Biol* 53: 175-188

[Azzi et al, 1975] Azzi, A.; Montecucco, C.; Richter, C. (1975). The use of acetylated ferricytochrome c for the detection of superoxide radicals produced in biological membranes. *Biochem Biophys Res Commun* 65: 597 - 603

[Balaban et al, 2005] Balaban, R.S.; Nemoto, S.; Finkel, T. (2005) Mitochondria, oxidants, and aging. *Cell* 120: 483 – 495

[Balaskaran et al, 2010] Balaskaran Nina, R.; Dudkina, N.V.; Kane, L.A., van Eyk, J.E.; Boekema, E.J. Mather, M.W.; Vaidya, A.B. (2010). Highly divergent mitochondrial ATP synthase complexes in *Tetrahymena thermophila*. *PloS Biol* 8, e1000418

[Balaskaran et al, 2011] Balaskaran Nina, P.; Morrisey, J.M.; Ganesan, S.M.; Ke, H.; Pershing, A.M.; Mather, M.W.; Vaidya, A.B. (2011). ATP synthase complex of *Plasmodium falciparum*: dimeric assembly in mitochondrial membranes and resistance to genetic disruption. *J Biol Chem* 286: 41312-41322

[Balsa et al, 2012] Balsa, E.; Marco, R.; Perales-Clemente, E.; Szklarczyk, R.; Calvo, E.; Landázuri, M.O.; Enríquez, J.A. (2012). NDUFA4 is a subunit of complex IV of the mammalian electron transport chain. *Cell Metab* 16: 378 – 386

[Bangham and Horne, 1964] Bangham, A.D.; Horne, R.W. (1964). Negative staining of phospholipids and their structural modification by surface-active agents as observed in the electron microscope. *J Mol Biol* 8: 660 – 668

[Baracca et al, 2010] Baracca, A.; Chiaradonna, F.; Sgarbi, G.; Solaini, G.; Alberghina, L.; Lenaz, G. (2010). Mitochondrial Complex I decrease is responsible for bionergetic dysfunction in K-ras transformed cells. *Biochem Biophys Acta* 1797: 314-323

[Baradaran et al, 2013] Baradaran, R.; Berrisford, J.M.; Minhas, G.S.; Sazanov, L.A. (2013). Crystal structure of the entire respiratory complex I. *Nature* 494: 443 - 448

[Barth et al 1983] Barth, P.G.; Scholte, H.R.; Berden, J.A.; van der Klei-van Moorsel, J.M.; Luyt-Houwen, I.E.; van't veer-Korthof, E.T.; van der Harten, J.J.; Sobotka-Plojhar, M.A. (1983). A X-linked mitochondrial disease affecting cardiac muscle, skeletal muscle and neutrophil leucocytes. *J Neurol Sci* 62: 327-355

[Battino et al, 1991] Battino, M.; Bertoli, E.; Formiggini, G.; Sassi, S.; Villa, R.F.; Lenaz, G. (1991). Structural and functional aspects of the respiratory chain in synaptic and nonsynaptic mitochondria derived from selected brain regions. *J Bioenerg Biomembr* 23: 345 – 363

[Beardslee and Updyke, 2007] Beardslee, T.A.; Updyke, T.V. (2007). Compositions and methods for improving resolution of biomolecules separated on polyacrylamide gels. U.S. patent application publication 2007/0151853. July 5, 2007

[Bednarz-Prashad and Mize, 1978] Bednarz-Prashad, A.J.; Mize, C.E. (1978). Phospholipid, enzymatic, and polypeptide analyses of the mitochondrial membranes from *Saccharomyces carlsbergensis*. *Biochemistry* 17: 4178-4186

[Benard *et al*, 2008] Benard G, Faustin B, Galinier A, Rocher C, Bellance N, Smolkova K, Casteilla L, Rossignol R, Letellier T (2008). Functional dynamic compartmentalization of respiratory chain intermediate substrates: implications for the control of energy production and mitochondrial diseases, *Int. J. Biochem. Cell Biol.* 40 1543–1554.

[Berrisford and Sazanov, 2009] Berrisford, J.M.; Sazanov, L. A. (2009). Structural basis for the mechanism of respiratory complex I. *J Biol Chem* 284: 29773 – 29783

[Berrisford et al, 2008] Berrisford, J. M., Thompson, C. J.; Sazanov, L. A. (2008). Chemical and NADH-induced, ROS-dependent, cross-linking between subunits of complex I from *Escherichia coli* and *Thermus thermophilus*. *Biochemistry* 47: 10262 - 10270

[Berry and Trumpower, 1985] Berry EA, Trumpower BL (1985). Isolation of ubiquinol oxidase from *Paracoccus denitrificans* and resolution into cytochrome bc_1 –aa_3 complexes. *J Biol Chem* 260: 2458-2467

[Beyer, 1967] Beyer, R.E. (1967). Preparation, properties, and conditions for assay of phosphorylating electron transport particles (ETPH) and its variations. *Methods Enzymol* 10: 186 – 194

[Beyer, 1983] Beyer, R.E. (1983). A rapid biuret assay for protein of whole fatty tissues. *Anal Biochem* 129: 483 - 485

[Bianchi *et al*, 2003] Bianchi C, Fato R, Genova ML, Parenti Castelli G, Lenaz G (2003). Structural and functional organization of Complex I in the mitochondrial respiratory chain. *Biofactors* 18: 3 – 9

[Bianchi *et al*, 2004] Bianchi C, Genova ML, Parenti Castelli G, Lenaz G (2004). The mitochondrial respiratory chain is partially organized in a supercomplex assembly: kinetic evidence using flux control analysis, *J. Biol. Chem.* 279 36562–36569.

[Birner et al 2001] Birner, R.; Bürgermeister, M.; Schneiter, R.; Daum, G. (2001). Roles of phosphatidylethanolamine and its several biosynthetic pathways in *Saccharomyces cerevisiae. Mol Biol Cell* 12: 997-1007

[Black and Brandt, 1974] Black, M. J.; Brandt, R.B. (1974). Spectrofluorometric analysis of hydrogen peroxide. *Anal Biochem* 58: 246 - 254

[Blair, 1967] Blair PV (1967) Preparation and properties of repeating units of mitochondrial electron transfer. *Methods Enzymo*l 10:208–212

[Böhm et al, 1990] Böhm, R.; Sauter, M.; Böck, A. (1990). Nucleotide sequence and expression of an operon in *Escherichia coli* coding for formate hydrogenlyase components. *Mol Microbiol* 4: 231 - 242

[Böttinger et al 2012] Böttinger, L.; Horvath, S.E.; Kleinschroth, T.; Hunte, C.; Daum, G.; Pfanner, N.; Becker, T. (2012). Phosphatidylethanolamine and cardiolipin differentially affect the stability of mitochondrial respiratory chain supercomplexes. *J Mol Biol* 423: 677-686

[Boumans *et al*, 1998] Boumans, H.; Grivell, L.A.; Berden, J.A. (1998). The respiratory chain in yeast behaves as a single unit. *J Biol Chem* 273: 4872-4877

[Bourges et al, 2004] Bourges, I.; Ramus, C.; Mousson, C.B.;Beugnot, R.; Remacle, C.; Cardol, P.; Hofhaus, G.; Issartel, J. P.(2004). Structural organization of mitochondrial human complex I: role of the ND4 and ND5 mitochondria-encoded subunits and interaction with prohibitin. *Biochem J* 383: 491 – 499

[Boveris, 1984] Boveris, A. (1984). Determination of production of superoxide radicals and hydrogen peroxide in mitochondria. *Methods Enzymol* 105: 429 - 435

[Boyer *et al*, 1977] Boyer, P.D.; Chance, B.; Ernster, L.; Mitchell, P.; Racker, E.; Slater, E.C. (1977). Oxidative phosphorylation and photophosphorylation. *Annu Rev Biochem* 46: 955-966

[Brandner et al, 2005] Brandner, K.; Mick, D.U.; Frazier, A.E.; Taylor, R.D.; Meisinger, C.; Rehling, P. (2005). Taz1, an outer mitochondrial membrane protein, affects stability and assembly of inner membrane protein complexes: implications for Barth syndrome. *Mol Biol Cell* 16: 5202-5214

[Brandt, 2006] Brandt, U. (2006). Energy converting NADH:quinone oxidoreductase (complex I). *Annu Rev Biochem* 75: 69 – 92

[Brandt and Keston, 1965] Brandt, R.; Keston, A.S. (1965). Synthesis of diacetyldichlorofluorescin: A stable reagent for fluorometric analysis. *Anal Biochem* 11: 6 - 9

[Bruel *et al*, 1996] Bruel C, Brasseur R, Trumpower BL (1996). Subunit 8 of the *Saccharomyces cerevisiae* cytochrome bc_1 complex interacts with succinate-ubiquinone reductase complex. *J Bioenerg Biomembr* 28: 59-68

[Brunette, 1981] Brunette, W.N. (1981). "Western blotting": electrophoretic transfer of proteins from sodium dodecylsulfate-polyacrylamide gels to unmodified nitrocellulose and radiographic detection with antibody and radioiodinated protein. *Anal Biochem* 112: 195 - 203

[Bultema et al 2009] Bultema, J.B.; Braun, H.P.; Boekema, E.J.; Kouril, R. (2009). Megacomplex organization of the oxidative phosphorylation system by structural analysis of respiratory supercomplexes from potato. *Biochim Biophys Acta* 1787: 84-93

[Bungert et al, 1999] Bungert, S.; Krafft, B.; Schlesinger, R.; Friedrich, T. (1999) One-step purification of the NADH dehydrogenase fragment of the *Escherichia coli* by means of Strep-tag affinity chromatography. *FEBS Lett* 460: 207 - 211

[Calvo et al, 2010] Calvo, S. E.; Tucker, E. J.; Compton, A. G.; Kirby, D. M.; Crawford, G.; Burtt, N. P.; Rivas, R.; Guiducci, C.; Bruno, D. L.; Goldberger, O.A.; Redman, M. C.; Wiltshire, E.; Wilson, C. J.; Altshuler, D.; Gabriel, S. J.; Daly, M. J.; Thorburn, D. R.; Mootha, V. K. (2010) High-throughput, pooled sequencing identifies mutations in NUBPL and FOXRED1 in human complex I deficiency. *Nat Genet* 42: 851 - 858

[Carilla-Latorre et al, 2010] Carilla-Latorre, S.; Gallardo, M.E.; Annesley, S.J.; Calvo-Garrido, J.; Grana, O.; Accari, S.L.; Smith, P.K.; Valencia, A.; Garesse, R.; Fisher, P.R.; Escalante, R. (2010). MidA is a putative methyltransferase that is required for mitochondrial complex I function, *J Cell Sci* 123: 1674 - 1683

[Carroll et al, 2003] Carroll, J.; Fearnley, I. M.; Shannon, R. J.; Hirst, J.; Walker, J. E. (2003). Analysis of the subunit composition of complex I from bovine heart mitochondria. *Mol Cell Proteomics* 2: 117 - 126

[Carroll et al, 2006a] Carroll, J.; Fearnley, I.M.; Skehel, J.M.; Shannon, R.J.; Hirst, J.; Walker, J.E. (2006). Bovine complex I is a complex of 45 different subunits. *J Biol Chem* 281: 32724 – 32727

[Carroll et al, 2006b] Carroll, J.; Fearnley, I.M.; Walker, J.E.(2006). Definition of the mitochondrial proteome by measurement of molecular masses of membrane proteins. *Proc Natl Acad Sci U.S.A.* 103: 16170 -16175

[Castelle et al, 2008] Castelle, C.; Guiral, M.; Malarte, G.; Ledgham, F.; Leroy, G.; Brugna, M.; Guidici-Orticoni, M.T. (2008). A new iron-oxidizing/O2 –reducing supercomplex spanning both inner and outer membranes, isolated from the extreme acidophile *Acidithiobacillus ferroxidans*. *J Biol Chem* 283: 25803-2581

[Cathcart et al, 1983] Cathcart, R.; Schwiers, E.; Ames, B. N. (1983). Detection of picomole levels of hydroperoxide using fluorescent dichlorofluorescein assay. *Anal Biochem* 134: 111 - 116

[Chaban *et al*, 2013] Chaban Y, Boekema EJ, Dudkina NV (2013). Structures of mitochondrial oxidative phosphorylation supercomplexes and mechanisms for their stabilisation. *Biochim Biophys Acta* 2013.http://dx.doi.org/10.1016/j.bbabio.2013.10.004

[Chance, 1977] Chance B (1977). Electron transfer: pathways, mechanisms, and controls. *Ann Rev Biochem* 46: 967-980

[Chance and Hollunger, 1960] Chance, B.; Hollunger, G. (1960). Energy-linked reduction of mitochondrial pyridine nucleotide. *Nature* 185: 666 - 672

[Chance and Williams, 1955] Chance B, Williams GR (1955). Respiratory enzymes in oxidative phosphorylation. I. Kinetics of oxygen utilization. *J Biol Chem* 217: 383-395

[Chance and Williams, 1956] Chance B, Williams GR (1956). The respiratory chain and oxidative phosphorylation. *Adv Enzymol Relat Subj Biochem* 17: 65 – 134

[Chen and Keaney, 2012] Chen, K.; Keaney, J.F. Jr. (2012). Evolving concepts of oxidative stress and reactive oxygen species in cardiovascular disease. *Curr Atheroscler Rep* 14: 476-483

[Chen et al, 2004] Chen, R.; Fearnley, I.M.; Peak-Chew, S.Y.; Walker, J. E. (2004) The phosphorylation of subunits of complex I from bovine heart mitochondria. *J Biol Chem* 279: 26036 – 26045

[Chen et al, 2008] Chen, S.; He, Q.; Greenberg, M.L. (2008). Loss of tafazzin in yeast leads to increased oxidative stress during respiratory growth. *Mol Microbiol* 68: 1061-1072

[Chen et al, 2012] Chen, Y.C.; Taylor, E.B.; Dephoure, N.; Heo, J.M.; Tonhato, A.; Papandreou, I.; Nath, N.; Denko, N.C.; Gygi, S.P.; Rutter, J. (2012). Identification of a protein mediating respiratory supercomplex stability. *Cell Metab* 15: 348-360

[Chomyn et al, 1986] Chomyn, A.; Cleeter, M.W.; Ragan, C.I.; Riley, M.; Doolittle, R.F. Attardi, G. (1986). URF6, last unidentified reading frame of human mtDNA, codes for an NADH dehydrogenase subunit. *Science* 234: 614 - 618

[Claypool et al 2008] Claypool, S.M.; Oktay, Y.; Boontheung, P.; Loo, J.A.; Koehler, C.M. (2008). Cardiolipin defines the interactome of the major ADP/ATP carrier protein of the mitochondrial inner membrane. *J Cell Biol* 182: 937-950

[Crane *et al*, 1956] Crane FL, Glenn JL, Green DE (1956). Studies on the electron transfer system. IV. The electron transfer particle. *Biochim Biophys Acta* 22: 475-487

[Crane *et al*, 1957] Crane FL, Hatefi Y, Lester RL, Widmer C. (1957). Isolation of a quinone from beef heart mitochondria. *Biochim Biophys Acta* 25: 220-221

[Crane *et al*, 1959] Crane FL, Widmer C, Lester RL, Hatefi Y (1959). Studies on the electron transport system. XV. Coenzyme Q (Q275) and the succinoxidase activity of the electron transport particle. *Biochim Biophys Acta* 31: 476-489

[Cronan et al, 2005] Cronan, J. E.; Fearnley, I. M.; Walker, J. E. (2005) Mammalian mitochondria contain a soluble acyl carrier protein. *FEBS Lett* 579: 4892 - 4896

[Cruciat *et al*, 2000] Cruciat, C.M.; Brunner, S.; Baumann, F.; Neupert, W.; Stuart, R.A. (2000). The cytochrome bc_1 and cytochrome c oxidase complexes associate to form a single supracomplex in yeast mitochondria. *J Biol Chem* 275: 18093-18098

[Cui et al, 2012] Cui, H.; Kong, Y.; Zhang, H. (2012). Oxidative stress, mitochondrial dysfunction, and aging. J Signal Transduct 2012: doi:10.1155/2012/646354

[D'Aurelio et al, 2006] D'Aurelio, M.; Gajewski, C.D.; Lenaz, G.; Manfredi, G. (2006). Respiratory chain supercomplexes set the threshold for respiration defects in human mtDNA mutant cybrids. *Human Mol Genet* 15: 2157 - 2169

[Davies et al, 2011] Davies, K.M.; Strauss, M.; Daum, B.; Kief, J.H.; Osiewacz, H.D.; Rycovska, A.; Zickermann, V.; Kühlbrandt, W. (2011). Macromolecular organization of ATP synthase and complex I in whole mitochondria. *Proc Natl Acad Sci USA* 108: 14121-14126

[Davis, 1964] Davis, B.J. (1964). Disc electrophoresis. II. Method and application to human serum proteins. *Ann NY Acad Sci* 121: 404–427

[Degli Esposti, 1998] Degli Esposti, M. (1998). Inhibitors of NADH-ubiquinone reductase: an overview. *Biochim Biophys Acta* 1364: 222 – 235

[Degli Esposti, 2002] Degli Esposti, M. (2002). Measuring mitochondrial reactive oxygen species. *Methods* 26: 335 - 340

[Degli Esposti et al, 1981] Degli Esposti, M.; Bertoli, E.; Parenti Castelli, G.; Fato, R.; Mascarello, S.; Lenaz, G. (1981). Incorporation of ubiquinone homologs into lipid vesicles and mitochondria membranes. *Arch Biochem Biophys* 210: 21 – 32

[Della Ciana, 2010a] Della Ciana, L. (2010). Preparation of high purity phenothiazine N-alkylsulfonates and their use in chemiluminescent assays for the measurement of peroxidase activity. U.S. patent 7,855,287. December 21, 2010.

[Della Ciana, 2010b] Della Ciana, L. (2010). Method for increasing light emission from a chemiluminescent reaction. U.S. patent 7,803,573. September 28, 2010.

[De los Rios Castillo et al, 2011] De los Rios Castillo, D. Zarco-Zavala, M.; Olvera-Sanchez, S.; Pardo, J.P.; Juarez, O.; Martinez, F.; Mendoza-Hernandez, G.; Garcia-Trejo, J.J.; Flores-Herrera, O. (2011). Atypical cristae morphology of human syncytiotrophoblast mitochondria: role for complex V. *J Biol Chem* 286:23911-23919

[Dencher et al, 2007] Dencher, N.A.; Frenzel, M.; Reifschneider, N.H.; Sugawa, M.; Krause, F. (2007). Proteome alterations in rat mitochondria caused by aging. *Ann N Y Acad Sci* 1100: 291-298

[Diaz et al, 2006] Diaz, F.; Fukui, H.; Garcia, S.; Moraes, C.T. (2006). Cytochrome c oxidase is required for the assembly / stability of respiratory complex I in mouse fibroblasts. *Mol Cell Biol* 26: 4872-4881

[Diaz et al, 2012] Diaz, F.; Enriquez, J.A.; Moraes, C.T. (2012). Cells lacking Rieske iron-sulfur protein have a reactive oxygen species –associated decrease in respiratory complexes I and IV. *Mol Cell Biol* 32: 415 - 429

[Djafarzadeh et al, 2000] Djafarzadeh, R.; Kersher, S.; Zwicker, K.; Radermacher, M.; Lindahl, M.; Schägger, H.; Brandt, U. (2000). Biophysical and structural characterization of proton-translocating NADH-dehydrogenase (complex I) from the strictly aerobic yeast *Yarrowia lipolytica. Biochim Biophys Acta* 1459: 230 – 238

[Dröse et al, 2009] Dröse, S.; Galkin, A.; Brandt, U. (2009). Measurement of superoxide formation by mitochondrial complex I of Yarrowia lipolytica. *Methods Enzymol* 456: 475 – 490

[Duarte et al, 2002] Duarte, M.; Populo, H.; Videira, A.; Friedrich, T.; Schulte, U. (2002). Disruption of iron-sulphur cluster N2 from NADH: ubiquinone oxidoreductase by site-directed mutagenesis. *Biochem J* 364: 833 - 839

[Dudkina *et al*, 2005a] Dudkina, N.V.; Heinemeyer, J.; Keegstra, W.; Boekema, E.J.; Braun, H.P. (2005). Structure of dimeric ATP sythase from mitochondria: an angular association of monomers induces the strong curvature of the inner membrane. FEBS *Lett* 579: 5769-5772

[Dudkina *et al*, 2005b] Dudkina, N.K.; Eubel, H.; Keegstra, W.; Boekema, E.J.; Braun, H.P. (2005). Structure of mitochondrial supercomplex formed by respiratory-chain complexes I and III. *Proc Natl Acad Sci USA* 102: 3225-3229

[Dudkina *et al*, 2006] Dudkina, N.V.; Heinemeyer, J.; Sunderhaus, S.; Boekema, E.J.; Braun, H.P. (2006). Respiratory chain supercomplexes in the plant mitochondrial membrane. *Trends Plant Sci* 11:232-240

[Dudkina *et al*, 2008] Dudkina NV, Sunderhaus S, Boekema E, Braun HP (2008). The higher level of organization of the oxidative phosphorylation system: mitochondrial supercomplexes. *J Bioenerg Biomembr* 40:419-424

[Dudkina *et al*, 2011] Dudkina, N.V.; Kudryashev, M.; Stahlberg, H.; Boekema, E.J. (2011). Interaction of complexes I, III, and IV within the bovine respirasome by single particle cryoelectron tomography. *Proc Natl Acad Sci USA* 108: 15196-15200

[Efremov and Sazanov, 2010] Efremov, R.G.; Sazanov, L.A. (2010) Structure of the membrane domain of respiratory complex I. *Nature* 476: 414 – 420

[Efremov and Sazanov, 2011] Efremov RG, Sazanov LA (2011). Structure of the membrane domain of respiratory complex I. Nature 476, 414-420.

[Efremov and Sazanov, 2012] Efremov, R.G.; Sazanov, L.A. (2012). The coupling mechanism of respiratory complex I – A structural and evolutionary perspective. *Biochim Biophys Acta* 1817: 1785 - 1795

[Efremov et al, 2010] Efremov, R.G.; Baradaran, R.; Sazanov, L.A. (2010). The architecture of respiratory complex I. *Nature* 465: 441 - 445

[Ernster and Schatz, 1981] Ernster L, Schatz G (1981). Mitochondria: A historical review. *J Cell Biol 91*: 227s-255s

[Eubel et al, 2003] Eubel, H.; Jansch, L.; Braun, H.P. (2003). New insights into the respiratory chain in plant mitochondria. Supercomplexes and a unique composition of complex II. *Plant Physiol* 133: 274-286

[Eubel et al, 2004] Eubel, H.; Heinemeyer, J.; Braun, H.P. (2004). Identification and characterization of respirasomes in potato mitochondria. *Plant Physiol* 134: 1450-1459

[Fato et al, 1993] Fato, R.; Cavazzoni, M.; Casteluccio, C.; Parenti Castelli, G.; Palmer, G.; Degli Esposti, M.; Lenaz, G. (1993). Steady-state kinetics of ubiquinol-cytochrome c reductase in bovine submitochondrial particles: diffusional effects. *Biochem J* 290: 225 – 236

[Fato et al, 2009] Fato, R.; Bergamini, C.; Bortolus, M.; Maniero, A. L.; Leoni, S.; Ohnishi, T.; Lenaz, G. (2009). Differential effects of mitochondrial Complex I inhibitors on production of reactive oxygen species. *Biochim Biophys Acta* 1787: 384 - 392

[Fearnley and Walker, 1992] Fearnley, I.M.; Walker, J.E. (1992). Conservation of sequences of subunits of mitochondrial complex I and their relationships with other proteins. *Biochim Biophys Acta* 1140: 105 – 134

[Fearnley et al, 2001] Fearnley, I. M.; Carroll, J.; Shannon, R. J.; Runswick, M. J.; Walker, J. E.; Hirst, J. (2001). GRIM-19, a cell death regulatory gene product, is a subunit of bovine mitochondrial NADH: ubiquinone oxidoreductase (complex I). *J Biol Chem* 276: 38345 – 38348

[Fecke et al, 1994] Fecke, W.; Sled, V.D.; Ohnishi, T.; Weiss, H. (1994). Disruption of the gene encoding the NADH-binding subunit of NADH: ubiquinone oxidoreductase in *Neurospora crassa*. Formation of a partially assembled enzyme without FMN and the iron-sulphur cluster N-3. *Eur J Biochem* 220: 551 - 558

[Fendel et al, 2008] Fendel, U.; Tocilescu, M.A.; Kerscher, S.; Brandt, U. (2008). Exploring the inhibitor binding pocket of respiratory complex I. *Biochim Biophys Acta* 1777: 660 - 665

[Fernandez-Vizarra et al, 2007] Fernandez-Vizarra, E. Bugiani, M.; Goffrini, P.; Carrara, F.; Farina, L.; Precopio, E.; Donati, A.; Uziel, G.; Ferrero, I.; Zeviani, M. (2007). Impaired

complex III assembly associated with BCS1L gene mutations in isolated mitochondrial encephalopathy. *Hum Mol Genet* 16: 1241 – 1252

[Finel, 1998] Finel, M. (1998). Organization and evolution of structural elements within complex I. *Biochim Biophys Acta* 1364: 112 - 121

[Flemming et al, 2003] Flemming, D.; Schlitt, A.; Spehr, V.; Bischof, T.; Friedrich, T. (2003). Iron-sulfur cluster N2 of the *Escherichia coli* NADH:ubiquinone oxidoreductase (complex I) is located on subunit NuoB. *J Biol Chem* 278: 47602 – 47609

[Folin and Ciocalteau, 1927] Folin, O.; Ciocalteau, V. (1927). On tyrosine and triptophane determinations in proteins. *J Biol Chem* 73: 627 - 650

[Fowler *et al*, 1962] Fowler LR, Richardson SH, Hatefi Y (1962). A rapid method for the preparation of highly purified cytochrome oxidase. *Biochim Biophys Acta* 64: 170-173

[Fraaije and Mattevi, 2000] Fraaije, M. W.; Mattevi, A. (2000). Flavoenzymes: diverse catalysts with recurrent features. *Trends Biochem Sci* 25: 126 – 32

[Frenzel et al, 2010] Frenzel, M.; Rommelspacher, H.; Sugawa, M.D.; Dencher, N.A. (2010). Ageing alters the supramolecular architecture of OxPhos complexes in rat brain cortex. *Exp Gerontol* 45: 563-572

[Friedrich, 2001] Friedrich, T. (2001). Complex I: a chimera of a redox and conformation-driven proton pump? *J Bioenerg Biomembr* 33: 169 – 177

[Friedrich and Scheide, 2000] Friedrich, T.; Scheide, D. (2000). The respiratory complex I of bacteria, archea and eukarya and its module common with membrane-bound multisubunit hydrogenases. *FEBS Lett* 479: 1 – 5

[Friedrich and Weiss, 1997] Friedrich, T.; Weiss, H. (1997). Modular evolution of the respiratory NADH:ubiquinone oxidoreductase and the origin of its modules. *J Theor Biol* 187: 529 – 540

[Friedrich et al, 1994] Friedrich, T.; Van Heek, P.; Leif, H.; Ohnishi, T.; Forche, E.; Kunze, B.; Jansen, R.; Trowitzsch-Kienast, W.; Höfle, G.; Reichenbach, H.; Weiss, H. (1994). Two binding sites of inhibitors in NADH:ubiquinone oxidoreductase (complex I). *Eur J Biochem* 219: 691 - 698

[Fry and Green, 1981] Fry, M.; Green, D.E. (1981). Cardiolipin requirement for electron transfer in complex I and III of the mitochondrial respiratory chain. *J Biol Chem* 256: 1874-1880

[Gabaldon et al, 2005] Gabaldon, T.; Rainey, D.; Huynen, M. A. (2005) Tracing the evolution of a large protein complex in the eukaryotes, NADH: ubiquinone oxidoreductase (complex I). *J Mol Biol* 348: 857 – 870

[Galante and Hatefi, 1978] Galante, Y. M.; Hatefi, Y. (1978) Resolution of complex I and isolation of NADH dehydrogenase and an iron–sulfur protein. *Methods Enzymol* 53: 15 – 21

[Gao et al, 2012] Gao, Y.; Meyer, B.; Sokolova, L.; Zwicker, K.; Karas, M.; Brutschy, B.; Peng, G.; Michel, H. (2012). Heme-copper terminal oxidase using both cytochrome c and ubiquinol as electron donors. *Proc Natl Acad Sci USA* 109:3275-3280

[Garcia Montes de Oca et al, 2012] Garcia Montes de Oca, L.Y.; Chagolla-López, A.; González de la Vara, L.; Cabellos-Avelar, T.; Gómez-Lojotero, C.; Gutierrez Cirlos, E.B. (2012). The composition of the *Bacillus subtilis* aerobic respiratory chain supercomplexes. *J Bionenerg Biomembr* 44: 473-486

[Garfin, 1990] Garfin, D.E. (1990). One-dimensional gel electrophoresis. *Methods Enzymol* 182: 425 – 441

[Garfin, 2009] Garfin, D.E. (2009). One-dimensional gel electrophoresis. *Methods Enzymol* 463: 497 - 513

[Garofano et al, 2003] Garofano, A.; Zwicker, K.; Kerscher,S.; Okun, P.; Brandt, U. (2003). Two aspartic acid residues in the PSST-homologous NUKM subunit of complex I from *Yarrowia lipolytica* are essential for catalytic activity. *J Biol Chem* 278: 42435 - 42440

[Gasparre et al, 2013] Gasparre, G.; Porcelli, A.M.; Lenaz, G.; Romeo, G. (2013). Relevance of mitochondrial genetics and metabolism in cancer development. *Cold Spring Harb Perspect Biol* 5, a011411

[Genova and Lenaz, 2013] Genova ML, Lenaz G (2013). Functional role of mitochondrial respiratory supercomplexes. *Biochim Biophys Acta* 2013. http://dx.doi.org/10.1016/j.bbabio.2013.11.002

[Genova *et al*, 2001] Genova, M. L.; Ventura, B.; Giuliano, G.; Bovina, C.; Formiggini, G.; Parenti Castelli, G.; Lenaz, G. (2001). The site of production of superoxide radical in mitochondrial complex I is not a bound ubisemiquinone but presumably iron-sulfur cluster N2. *FEBS Lett* 505: 364 - 368

[Genova *et al*, 2008] Genova ML, Baraca A, Biondi G, Casalena M, Faccioli M, Falasca AI, Formiggini G, Sgarbi G Solaini G, Lenaz G (2008). Is supercomplex organization of the respiratory chain required for optimal electron transfer activity?. *Biochim Biophys Acta* 1777: 740-746

[Gershoni and Palade, 1982] Gershoni, J.M.; Palade, G.E. (1982). Electrophoretic transfer of proteins from sodium dodecyl sulfate-polyacrilamide gels to a positively charged membrane filter. *Anal Biochem* 124: 396 - 405

[Gershoni et al, 2010] Gershoni, M.; Fuchs, A.; Shani, N.; Fridman, Y.; Corral-Debrinski, M.; Aharoni, A.; Frishman, D.; Mishmar, D. (2010). Coevolution predicts direct interactions

between mtDNA-encoded and nDNA-encoded subunits of oxidative phosphorylation complex I. *J Mol Biol* 404: 158 – 171

[Gill and von Hippel, 1989] Gill, S. C.; von Hippel, P. H. (1989). Calculation of protein extinction coefficients from amino acid sequence data. *Anal Biochem* 182: 319 - 326

[Gómez and Hagen, 2012] Gomez, L.A.; Hagen, T.M. (2012). Age-related decline in mitochondrial bioenergetics: does supercomplex destabilization determine lower oxidative capacity and higher superoxide production? *Semin Cell Dev Biol* 23: 758-767

[Gómez et al, 2009] Gómez, L.A.; Monette, J.S.; Chavez, J.D.; Maier, C.S.; Hagen, T.M. (2009). Supercomplexes of the mitochondrial electron transport chain decline in the aging rat heart. *Arch Biochem Biophys* 490: 30-35

[Gonzalvez et al 2013] Gonzalvez, F.; D'Aurelio, M.; Boutant, M.; Moustapha, A.; Puech, J.P.; Landes, T.; Arnaune-Pelloquin, L.; Vial, G.; Taleux, N.; Slomianny, C.; Wanders, R.J.; Houtkooper, R.H.; Bellenguer, P.; Moller, I.M.; Gottlieb, E.; Vaz, F.M.; Manfredi, G.; Petit, P.X. (2013). Barth syndrome: cellular compensation of mitochondrial dysfunction and apoptosis inhibition due to changes in cardiolipin remodeling linked to tafazzin (TAZ) gene mutation. *Biochim Biophys Arcta* 1832: 1194-1206

[Gornall et al, 1949] Gornall, A. G.; Bardawill, C.J.; David, M.M. (1949). Determination of serum proteins by means of the biuret reaction. *J Biol Chem* 177: 751 - 766

[Grad and Lemire, 2004] Grad, L.I.; Lemire, D. (2004). Mitochondrial complex I mutations in *Caenorhabditis elegans* produce cytochrome c oxidase deficiency, oxidative stress and vitamin-response lactic acidosis. *Hum Mol Genet* 13: 303 – 314

[Grad and Lemire, 2006] Grad, L.I.; Lemire, D. (2006). Riboflavin enhances the assembly of mitochondrial cytochrome c oxidase in *C. elegans* NADH ubiquinone reductase mutants. *Biochim Biophys Acta* 1757: 115 - 122

[Green and Tzagoloff, 1966] Green DE, Tzagoloff A (1966). The mitochondrial electron transfer chain. *Arch Biochem Biophys* 116: 293-304

[Grigorieff, 1998] Grigorieff, N. (1998). Three-dimensional structure of bovine NADH:ubiquinone oxidoreductase (complex I) at 22 Å in ice. *J Mol Biol* 277: 1033 - 1046

[Guenebaut et al, 1998] Guenebaut, V.; Schlitt, A.; Weiss, H.; Leonard, K.; Friedrich, T. (1998). Consistent structure between bacterial and mitochondrial NADH:ubiquinone oxidoreductase (complex I). *J Mol Biol* 276: 105 - 112

[Guiral et al, 2009] Guiral, M.; Prunetti, L.; Lignon, S.; Lebrun, R.; Moinier, D.; Giudici-Orticonit, M.T. (2009). New insights into the respiratory chains of the chemolithoautotrophic and hyperthermophilic bacterium *Aquifex aeolicus*. *J Proteome Res* 8: 1717-1730

[Gupte and Hackenbrock, 1988a] Gupte SS, Hackenbrock CR (1988). Multidimensional diffusion modes and collision frequencies of cytochrome c with its redox partners. *J Biol Chem* 263: 5441 - 5247

[Gupte and Hackenbrock, 1988b] Gupte SS, Hackenbrock CR (1988). The role of cytochrome c diffusion in mitochondrial electron transport. *J Biol Chem* 263: 5248 – 5253

[Gupte *et al*, 1984] Gupte SS, Wu ES, Hoechli L, Hoechli M, Jacobson K, Sower AW, Hackenbrock CR (1984). Relationship between lateral diffusion, collision frequency, and electron transfer of mitochondrial inner membrane oxidation-reduction components. *Proc Natl Acad Sci USA* 81: 2606 - 2616

[Hackenbrock *et al*, 1986] Hackenbrock CR, Chazzote B, Gupte SS (1986). The random collision model and a critical assessment of diffusion and collision in mitochondrial electron transport. *J Bioenerg Biomembr* 18: 331-368

[Hatefi and Rieske, 1967] Hatefi Y, Rieske JS (1967). Preparation and properties of DPNH-cytochrome (Complex I-III of the Respiratory Chain). *Methods Enzymol* 10: 225-231

[Hatefi *et al*, 1959] Hatefi, Y.; Lester, R.L.; Crane, F.L.; Widmer, C. (1959). Studies on the electron transport system XVI. Enzymic oxidoreduction reactions of coenzyme Q. *Biochim Biophys Acta* 31: 490-501

[Hatefi et al, 1961] Hatefi Y, Haavik AG, Jurtshuk P (1961). Studies on the electron transport system. XXX. DPNH-cytochrome c reductase I. *Biochim Biophys Acta* 52: 106-118

[Hatefi et al, 1962a] Hatefi Y, Haavik AG, Griffiths DE (1962). Studies on the electron transfer system. XLI. Reduced coenzyme Q (QH2)-cytochrome c reductase. *J Biol Chem* 237: 1681-1685

[Hatefi et al, 1962b] Hatefi Y, Haavik AG, Fowler LR, Griffiths DE (1962). Studies on the electron transfer system. XLII. Reconstitution of the electron transfer system. *J Biol Chem* 237: 2661-2669

[Hatefi et al, 1962c] Hatefi, Y.; Haavik, A.G.; Griffiths, D.E. (1962). Sutides on the electron transfer system. Preparation and properties of mitochondrial DPNH-coenzyme Q reductase. J Biol Chem 237: 1676-1680

[Hedderich, 2004] Hedderich R. (2004). Energy-converting [NiFe] hydrogenases from archaea and extremophiles: ancestors of complex I. *J Bioenerg Biomembr* 36(1):65-75

[Heron *et al*, 1978] Heron C, Ragan CI, Trumpower BL (1978). The interaction between mitochondrial NADH-ubiquinone oxidoreductase and ubiquinol-cytochrome c oxidoreductase restoration of ubiquinone-pool behaviour, *Biochem. J.* 174 (1978) 791–800.

[Herrero and Barja, 2000] Herrero, A.; Barja, G. (2000). Localization of the site of oxygen radical generation inside the complex I of heart and nonsynaptic brain mammalian mitochondria. *J Bioenerg Biomembr* 32: 609 - 615

[Heinemeyer et al, 2007] Heinemeyer J, Braun HP, Boekema EJ, Kouril R. A structural model of the cytochrome C reductase/oxidase supercomplex from yeast mitochondria. J. Biol. Chem. 2007;282:12240–12248.

[Hinkle et al, 1967] Hinkle, P.C.; Butow, R.A.; Racker, E.; Chance, B. (1967). Partial resolution of the enzymes catalyzing oxidative phosphorylation. XV. Reverse electron transfer in the flavin-cytochrome c region of the respiratory chain of beef heart sumbitochondrial particles. *J Biol Chem* 242: 5169 - 5173

[Hirst et al, 2008] Hirst, J.; King, M.S.; Pryde, K.R. (2008). The production of reactive oxygen species by complex I. *Biochem Soc Trans* 36: 976 - 980

[Hofhaus et al, 1991] Hofhaus, G.; Weiss, H.; Leonard, K. (1991). Electron microscopic analysis of the peripheral and membrane parts of mitochondrial NADH dehydrogenase (complex I). *J Mol Biol* 221: 1027 – 1043

[Huang et al, 2005] Huang, L.S.; Cobessi, D.; Tung, E.Y.; Berry, E.A. (2005) Binding of the respiratory chain inhibitor antimycin to the mitochondrial bc1 complex: a new crystal structure reveals an altered intramolecular hydrogen-bonding pattern. *J Mol Biol* 351: 573-597

[Hunte et al, 2010] Hunte, C.; Zickermann, V.; Brandt, U. (2010) Functional modules and structural basis of conformational coupling in mitochondrial complex I. *Science* 329:448–451.

[Ide et al, 2000] Ide, T.; Tsutsui, H.; Kinugawa, S.; Suematsu, N.; Hayashidani, S.; Ichikawa, K.; Utsumi, H.; Machida, Y.; Egashira, K.; Takeshita, A. (2000). Direct evidence for increased hydroxyl radicals originating from superoxide in the failing myocardium. *Circ Res* 86: 152–157

[Ingledew and Ohnishi, 1980] Ingledew, W.J.; Ohnishi, T. (1980). An analysis of some thermodynamic properties of iron-sulphur centres in site I of mitochondria. *Biochem J* 186:111 – 117

[Iwasaki et al, 1995] Iwasaki T, Matsuura K, Oshima T (1995). Resolution of the aerobic respiratory system of the thermoacidophilic archeon, *Sulfolobus sp.* Strain 7. The archaeal terminal oxidase supercomplex is a functional fusion of respiratory complexes III and IV with no c-type cytochromes. *J Biol Chem* 270: 30881-30892

[Janssen et al, 2006] Janssen, R. J.; Nijtmans, L. G.; van den Heuvel, L. P.; Smeitink, J. A. (2006) Mitochondrial complex I structure, function and pathology. *J Inherit Metab Dis* 29: 499 - 515

[Jiang et al, 2000] Jiang, F.; Ryan, M.T.; Schlame, M.; Zhao, M.; Gu, Z.: Klingenberg, M.; Pfanner, N.; Greenberg, M.L. (2000). Absence of cardiolipin in the *crd1* null mutant results in decreased mitochondrial membrane potential and reduced mitochondrial function. *J Biol Chem* 275: 22387-22394

[Joshi et al 2012] Joshi, A.S.; Thompson, M.N.; Fei, N.; Hüttemann, M.; Greenberg, M.L. (2012). Cardiolipin and mitochondrial phosphatidylethanolamine have overlapping functions in mitochondrial fusion in *Saccharomyces cerevisiae*. *J Biol Chem* 287: 17589-17597

[Jezek and Hlavatà, 2005] Jezek, P.; Hlavatà, L. (2005). Mitochondria in homeostasis of reactive oxygen species in cell, tissues, and organism. *Int J Biochem Cell Biol* 37: 2478 - 2503

[Kean et al, 1971] Kean, E. A.; Gutman, M. Singer, T.P. (1971). Studies on the respiratory chain-linked nicotinamide adenine dinucleotide dehydrogenase. XXII. Rhein, a competitive inhibitor of the dehydrogenase. *J Biol Chem* 246: 2346 - 2353

[Keefe and Maier, 1993] Keefe RG, Maier RJ (1993). Purification and characterization of an O_2-utilizing cytochrome c oxidase complex from *Bradyrhizobium japonicum* bacteroid membranes. *Biochim Biophys Acta* 1183: 91-104

[Keston and Brandt, 1965] Keston, A. S.; Brandt, R. (1965). The fluorometric analysis of ultramicro quantities of hydrogen peroxide. *Anal Biochem* 11: 1 - 5

[Klingenberg and Slenczka, 1959] Klingenberg, M.; Slenczka, W. (1959). [Pyridine nucleotide in liver mitochondria. An analysis of their redox relationships]. [Article in German]. *Biochem Z* 331:486 – 517

[Kohlstädt et al, 2008] Kohlstädt, M.; Dörner, K.; Labatzke, R.; Koç, C.; Hielscher, R.; Schiltz, E.; Einsle, O.; Hellwig, P.; Friedrich,T. (2008). Heterologous production, isolation, characterization and crystallization of a soluble fragment of the NADH:ubiquinone oxidoreductase (complex I) from *Aquifex aeolicus*. *Biochemistry* 47: 13036 – 13045

[Koopman et al, 2010] Koopman, W. J.; Nijtmans, L. G.; Dieteren, C.E.; Roestenberg, P.; Valsecchi, F.; Smeitink, J.A.; Willems, P. H. (2010). Mammalian mitochondrial complex I: biogenesis, regulation, and reactive oxygen species generation. *Antioxid Redox Signal* 12:1431 – 1470

[Kowaltowski et al, 2009] Kowaltowski, A. J.; De Souza-Pinto, N. C.; Castilho, R. F.; Vercesi, A. E. (2009) Mitochondria and reactive oxygen species. *Free Radic Biol Med* 47: 333 - 343

[Krause et al, 2004a] Krause, F.; Scheckhuber, C.Q.; Werner, A.; Rexroth, S.; Reifschneider, N.H.; Dencher, N.A.; Osiewacz, H.D. (2004) Supramolecular organization of

cytochrome c oxidase- and alternative oxidase-dependent respiratory chains in the filamentous fungus *Podospora anserina*. *J Biol Chem* 279: 26453-26461

[Krause et al, 2004b] Krause, F.; Reifschneider, N.H.; Vocke, D.; Seelert, H.; Rexroth, S.; Dencher, N.A. (2004). "Respirasome"-like supercomplexes in green leaf mitochondria of spinach. *J Biol Chem* 279: 48369-48375

[Kröger and Klingenberg, 1973a] Kröger A, Klingenberg M (1973).The kinetics of the redox reactions of ubiquinone related to the electron-transport activity in the respiratory chain. *Eur J Biochem* 34: 358-368

[Kröger and Klingenberg, 1973b] Kröger A, Klingenberg M (1973). Further evidence of the pool function of ubiquinone as derived from the inhibition of the electron transport by antimycin. *Eur J Biochem* 39: 313-323

[Kuboyama *et al*, 1962] Kuboyama M, Takemori S, King TE (1962). Reconstitution of respiratory chain enzyme systems. X. Reconstitution of succinate oxidase with cytochrome c-cytochrome oxidase of heart muscle. *Biochem Biophys Res Commun* 19: 540-544

[Kurien and Scofield, 2006] Kurien, B.T.; Scofield, R.H. (2006). Western blotting. *Methods* 38: 283 - 293

[Kuroda et al 2011] Kuroda, T.; Tani, M.; Moriguchi, A.; Tokunaga, S.; Higuchi, T.; Kitada, S.; Kuge, O. (2011). FMP30 is required for the maintenance of a normal cardiolipin level and mitochondrial morphology in the absence of mitochondrial phosphatidylethanolamine synthesis. *Mol Microbiol* 80: 248-265

[Laemmli, 1970] Laemmli, U.K. (1970). Cleavage of structural proteins during the assembly of the head of bacteriophage T4. *Nature* 227: 680 – 685

[Lapuente-Brun et al, 2013] E. Lapuente-Brun, R.Moreno-Loshuertos, R. Acín-Peréz, A. Latorre-Pellicer, C. Colás, E. Balsa, E. Perales-Clemente, P.M. Quirós, E. Calvo, M.A. Rodríguez-Hernández, P. Navas, R. Cruz, Á. Carracedo, C. López-Otín, A. Pérez-Martos, P. Fernández-Silva, E. Fernández-Vizarra, J.A. Enríquez, Supercomplex assembly determines electron flux in themitochondrial electron transport chain, Science 340 (2013) 1567–1570.

[Lasic, 1988] Lasic, D.D. (1988). The mechanism of vesicle formation. *Biochem J* 256: 1 – 11

[Layne, 1957] Layne, E. (1957). Spectrophotometric and turbidimetric methods for measuring proteins. *Methods Enzymol* 3: 447 - 454

[Lazarou et al, 2007] Lazarou, M.; McKenzie, M.; Ohtake, A.; Thorburn, D. R.; Ryan, M. T. (2007) Analysis of the assembly profiles for mitochondrial- and nuclear-DNA-encoded subunits into complex I. *Mol Cell Biol* 27: 4228 – 4237

[Lehninger, 1959] Lehninger A (1959) Respiratory-energy transformation. *Rev Mod Phys* 31: 136-146

[Leif et al, 1995] Leif, H.; Sled, V.D.; Ohnishi, T.; Weiss, H.; Friedrich,T. (1995). Isolation and characterization of the proton-translocating NADH: ubiquinone oxidoreductase from *Escherichia coli. Eur J Biochem* 230: 538 - 548

[Lenaz, 1988] Lenaz G (1988). Role of mobility of redox components in the inner mitochondrial membrane. *J Membr Biol* 104: 193-209

[Lenaz and Genova, 2007] Lenaz G, Genova ML (2007). Kinetics of integrated electron transfer in the mitochondrial respiratory chain: random collision vs. solid state electron channeling. *Am J Physiol Cell Physiol* 292: C1221-C1239

[Lenaz and Genova, 2009a] Lenaz G, Genova ML (2009). Structural and functional organization of the mitochondrial respiratory chain: A dynamic super-assembly. *Int J Biochem Cell Biol* 41: 1750-1772

[Lenaz and Genova, 2009b] Lenaz, G.; Genova, M.L. (2009). Mobility and function of coenzyme Q (ubiquinone) in the mitochondrial respiratory chain. *Biochim Biophys Acta* 1787: 563-573

[Lenaz and Genova, 2010] Lenaz G, Genova ML.(2010). Structure and organization of mitochondrial respiratory complexes: a new understanding of an old subject. Antioxid Redox Signal. 2010 Apr 15;12(8):961-1008.

[Lenaz and Genova, 2012] Lenaz, G.; Genova, M.L. (2012). Supramolecular organisation of mitochondrial respiratory chain: A new challenge for the mechanism and control of oxidative phosphorylation. *Adv Exp Med Biol* 748: 107-144

[Lenaz *et al*, 1999] Lenaz G, Fato R, Di Bernardo S, Jarreta D, Costa A, Genova ML, Parenti Castelli G (1999). Localization and mobility of coenzyme Q in lipid bilayers and membranes. *Biofactors* 9: 87-93

[Lenaz *et al*, 2004] Lenaz, G.; Fato, R.; Baracca, A.; Genova, M.L. (2004). Mitochondria quinone reductases: Complex I. *Methods Enzymol* 382: 3 - 20

[Lenaz *et al*, 2006] Lenaz, G.; Fato, R.; Genova, M.L.; Bergamini, C.; Bianchi, C.; Biondi, A. (2006). Mitochondrial complex I: structural and functional aspects. *Biochim Biophys Acta* 1757: 1406 - 1420

[Lenaz *et al*, 2007] Lenaz, G.; Bergamini, C.; Leoni, S.; Fato, R. (2007). Oxygen radical generation by mitochondrial complex I: from the molecular mechanism of electron transfer to pathophysiological implications. In: Complex I and alternative dehydrogenases, edited by Gonzalez Siso MI. Kerala, India: Transworld Research Network, 2007, pp. 119 - 156.

[Lenaz *et al*, 2010] Lenaz, G.; Baracca, A.; Barbero, G.; Bergamini, C.; Dalmonte, M.E.; Del Sole, M.; Faccioli, M.; Falasca, A.; Fato, R.; Genova, M.L.; Sgarbi, G.; Solaini, G. (2010). Mitochondrial respiratory chain super-complex I-III in physiology and pathology. *Biochim Biophys Acta* 1797: 633-640

[Li et al, 2007a] Li, G.; Chen, S.; Thompson, M.N.; Greenberg, M.L. (2007). New insights into the regulation of cardiolipin biosynthesis in yeast: implications for Barth syndrome. *Biochim Biophys Acta* 1771: 432-441

[Li et al, 2007b] Li, Y.; D'Aurelio, M.; Deng, J.H.; Park, J.S.; Manfredi, G.; Hu, P.; Lu, J.; Bai, Y. (2007). An assembled complex IV maintains the stability and activity of complex I in mammalian mitochondria. *J Biol Chem* 282: 17557 – 17562

[Lin and Beal, 2006] Mitochondrial dysfunction and oxidative stress in neurodegenerative diseases. *Nature* 443: 787 – 795

[Lowry et al, 1951] Lowry, O.H.; Rosebrough, N.J.; Farr, A.L.; Randall, R.J. (1951). Protein measurement with the Folin phenol reagent. *J Biol Chem* 193: 265 - 275

[Lümmen, 1998] Lümmen, P. (1998). Complex I inhibitors as insecticides and acaricides. *Biochim Biophys Acta* 1364: 287 – 296

[Ma et al 2004] Ma, L.; Vaz, F.M.; Gu, Z.; Wanders, R.J.; Greenberg, M.L. (2004). The human TAZ gene complements mitochondrial dysfunction in the yeast *taz1Δ* mutant. Implications for Barth syndrome. *J Biol Chem* 279: 44394 - 44399

[Maas et al, 2009] Maas, M.F.; Krause, F.; Dencher, N.A.; Sainsard-Chanet, A. (2009). Respiratory complexes III and IV are not essential for the assembly/stability of complex I in fungi. *J Mol Biol* 387:259-269

[Magalon *et al*, 2012] Magalon A, Arias-Cartin R, Walburger A (2012). Supramolecular organization in prokaryotic respiratory systems. *Adv Microb Physiol* 61: 217-266

[Majander et al, 1994] Majander, A.; Finel, M.; Wikström, M. (1994) Diphenyleneiodonium inhibits reduction of iron-sulfur clusters in the mitochondrial NADH-ubiquinone oxidoreductase (complex I). *J Biol Chem* 269: 21037 – 21042

[Makhatadze and Privalov, 1992] Makhatadze, G.I.; Privalov, P.L. (1992). Protein interactions with urea and guanidinium chloride. A calorimetric study. J Mol Biol 226: 491 – 505

[Maranzana et al, 2013] Maranzana, E.; Barbero, G.; Falasca, A.I.; Lenaz, G.; Genova, M. L. (2013). Mitochondrial respiratory supercomplexes association limits production of reactive oxygen species from Complex I. *Antioxid Redox Signal* 19: 1469 - 1480

[Marques et al, 2007] Marques, I.; Dencher, N.A.; Videira, A.; Krause, F. (2007). Supramolecular organization of the respiratory chain in *Neurospora crassa* mitochondria. *Eukaryot Cell* 6: 2391-2405

[Mathiesen and Hägerhäll, 2002] Mathiesen, C.; Hägerhäll, C. (2002). Transmembrane topology of the NuoL, M and N subunits of NADH:quinone oxidoreductase and their homologues among membrane-bound hydrogenases and bona fide antiporters. *Biochim Biophys Acta* 1556: 121 - 132

[Mathiesen and Hägerhäll, 2003] Mathiesen, C.; Hagerhall, C. (2003). The 'antiporter module' of respiratory chain complex I includes the MrpC/NuoK subunit – a revision of the modular evolution scheme. *FEBS Lett* 549: 7 – 13

[McKenzie and Ryan, 2010] McKenzie, M.; Ryan, M.T. (2010). Assembly factors of human mitochondrial complex I and their defects in disease, *IUBMB Life* 62: 497 – 502

[McKenzie et al 2006] McKenzie, M.; Lazarou, M.; Thorburn, D.R.; Ryan, M.T. (2006). Mitochondrial respiratory chain supercomplexes are destabilized in Barth syndrome patients. *J Mol Biol* 361: 462-469

[McLellan, 1982] McLellan, T. (1982). Electrophoresis buffers for polyacrylamide gels at various pH. *Anal Biochem* 126: 94 - 99

[Megehee et al, 2006] Megehee, J.A.; Hosler, J.P.; Lundrigan, M.D. (2006). Evidence for a cytochrome bcc-aa3 interaction in the respiratory chain of *Mycobacterium smegmatis*. *Microbiology* 152: 823-829

[Mileykovskaya et al, 2012] Mileykovskaya, E.; Penczek, P.A.; Fang, J.; Mallampalli, V.K.; Sparagna, G.C.; Dowhan, W. (2012). Arrangement of the respiratory chain complexes in *Saccharomyces cerevisiae* supercomplex III_2IV_2 revealed by single particle cryo-electron microscopy. *J Biol Chem* 287: 23095-23103

[Mimaki et al, 2012] Mimaki, M.; Wang, X.; McKenzie, M.; Thorburn, D.R.; Ryan, M.T. (2012). Understanding mitochondrial complex I assembly in health and disease. *Biochim Biophys Acta* 1817: 851 – 862

[Möglich et al, 2005] Möglich, A.; Krieger, F.; Kiefhaber, T. (2005). Molecular basis for the effect of urea and guanidinium chloride on the dynamics of unfolded polypeptide chains. *J Mol Biol* 345: 153 - 62

[Moparthi and Hagerhall, 2011] Moparthi, V.K.; Hagerhall, C. (2011). The evolution of respiratory chain complex I from a smaller last common ancestor consisting of 11 protein subunits. *J Mol Evol* 72:484 – 497

[Moparthi et al, 2011] Moparthi, V.K.; Kumar, B.; Mathiesen, C.; Hägerhäll, C. (2011). Homologous protein subunits from Escherichia coli NADH:quinone oxidoreductases can

functionally replace MrpA and MrpD in Bacillus subtilis. Biochim Biophys Acta 1807: 427 - 436

[Moreno-Lastres et al, 2012] Moreno-Lastres, D.; Fontanesi, F.; García-Consuegra, I.; Martín, M.A.; Arenas, J.; Barrientos, A.; Ugalde, C. (2012). Mitochondrial complex I plays an essential role in human respirasome assembly. *Cell Metab* 15: 324 - 335

[Moser *et al*, 2005] Moser CC, Page, CC, Leslie Dutton P (2005). Tunneling in PSII. *Photochem Photobiol Sci.*4: 933 – 939

[Moser *et al*, 2006] Moser, C, Farid TA, Chobot SE, Dutton PL (2006). Electron tunneling chains of mitochondria. *Biochim Biophys Acta* 1757: 1096 – 1109

[Murphy, 2009] Murphy, M.P. (2009). How mitochondria produce reactive oxygen species*. Biochem J* 417: 1 - 13

[Muster et al, 2010] Muster, B.; Kohl, W.; Wittig, I.; Strecker, V.; Joos, F.; Haase, W.; Bereiter-Hahn, J.; Busch, K. (2010). Respiratory chain complexes in dynamic mitochondria display a patchy distribution in life cells. *PLoS ONE 5*, e11910

[Niebisch and Bott, 2003] Niebisch, A.; Bott, M. (2003). Purification of a cytochrome bc-aa$_3$ supercomplex with quinol oxidase activity from *Corynebacterium glutamicum*. Identification of a fourth subunity of cytochrome aa$_3$ oxidase and mutational analysis of diheme cytochrome c1. *J Biol Chem* 278: 4339-4346

[Niepmann, 2007] Niepmann, M. (2007). Discontinuous native protein gel electrophoresis: pros and cons. *Expert Rev Proteomics* 4: 355 - 361

[Nouws et al, 2010] Nouws, J.; Nijtmans, L.; Houten, S.M.; van den Brand, M.; Huynen, M.; Venselaar, H.; Hoefs, S.; Gloerich, J.; Kronick, J.; Hutchin, T.; Willems, P.; Rodenburg, R.; Wanders, R.; van den Heuvel, L.; Smeitink, J.; Vogel, R.O. (2010). Acyl-CoA dehydrogenase 9 is required for the biogenesis of oxidative phosphorylation complex I. *Cell Metab* 12: 283 - 294

[Nubel et al, 2009] Nubel, E.; Wittig, I.; Kerscher, S.; Brandt, U. Schägger, H. (2009). Two-dimensional native electrophoresis analysis of respiratory supercomplexes from *Yarrowia lipolytica*. *Proteomics* 9: 2408-2418

[Ohnishi, 1998] Ohnishi, T. (1998). Iron-sulfur clusters/semiquinones in complex I. *Biochim Biophys Acta* 1364:186 – 206

[Ohnishi and Salerno, 2005] Ohnishi, T.; Salerno, J. C. (2005). Conformation-driven and semiquinone-gated proton-pump mechanism in the NADH-ubiquinone oxidoreductase (complex I). FEBS Lett 579: 4555 – 4561

[Ohnishi et al, 1998] Ohnishi, T.; Sled, V.D.; Yano, T.; Yagi, T.; Burbaev,D. S. ; Vinogradov, A. D. (1998). Structure-function studies of iron-sulfur clusters and semiquinones in the

NADH-Q oxidoreductase segment of the respiratory chain. *Biochim Biophys Acta* 1365:301–308

[Ohnishi et al 2005] Ohnishi, S.T.; Ohnishi, T.; Muranaka, S.; Fujita, H.; Kimura, H.; Uemura, K.; Yoshida, K.; Utsumi, K. (2005). A possible site of superoxide generation in the complex I segment of rat heart mitochondria. *J Bioenerg Biomembr* 37: 1 - 15

[Ohnishi et al 2010a] Ohnishi, S. T.; Salerno, J. C.; Ohnishi, T. (2010). Possible roles of two quinone molecules in direct and indirect proton pumps of bovine heart NADH-quinone oxidoreductase (complex I). Biochim Biophys Acta 1797: 1891 – 1893

[Ohnishi et al 2010b] Ohnishi, T.; Nakamaru-Ogiso, E.; Ohnishi, S. T. (2010). A new hypothesis on the simultaneous direct and indirect proton pump mechanisms in NADH-quinone oxidoreductase (complex I). *FEBS Lett* 584: 4131 – 4137

[Ohnishi et al, 2010c] Ohnishi, S.T.; Shinzawa-Itoh, K.; Ohta, K.; Yoshikawa, S.; Ohnishi, T. (2010) New insights into the superoxide generation sites in bovine heart NADH-ubiquinone oxidoreductase (Complex I): the significance of protein-associated ubiquinone and the dynamic shifting of generation sites between semiflavin and semiquinone radicals. *Biochim Biophys Acta* 1797:1901–1909

[Ornstein, 1964] Ornstein, L. (1964). Disc electrophoresis I: background and theory. *Ann NY Acad Sci* 121: 321–349

[Osman et al 2011] Osman, C.; Voelker, D.; Langer, T. (2011). Making heads or tails of phospholipids in mitochondria. *J Cell Biol* 192: 7-16

[Ovandi, 1991] Ovandi, J. (1991). Physiological significance of metabolic channelling. *J Theor Biol* 152: 135 – 141

[Ozawa, 1997] Ozawa, T. (1997). Genetic and functional changes in mitochondria associated with aging. *Physiol Rev* 77: 425 – 464

[Page et al, 1999] Page, C.C.; Moser, C.C.; Chen, X.; Dutton, P.L. (1999). Natural engineering principles of electron tunnelling in biological oxidation-reduction. *Nature* 402: 47 - 52

[Palmisano et al, 2007] Palmisano, G.; Sardanelli, A. M.; Signorile, A.; Papa, S.; Larsen, M. R. (2007). The phosphorylation pattern of bovine heart complex I subunits. *Proteomics* 7:1575 - 1583

[Palsdottir and Hunte, 2004] Palsdottir, H.; Hunte, C. (2004). Lipids in membrane protein structures. *Biochim Biophys Acta* 1666: 2-18

[Panov et al, 2007] Panov, A.; Dikalov, S.; Shalbuyera, N.; Hemendinger, R.; Greenamyere, J.T.; Rosenfeld, J. (2007). Species- and tissue-specific relationships between mitochondrial

permeability transition and generation of ROS in brain and liver mitochondria of rats and mice. *Am J Physiol Cell Physiol* 292: C708-C718

[Papahadjopoulos and Miller, 1967] Papahadjopoulos, D.; Miller, N. (1967). Phospholipid model membranes I. Structural characteristic of hydrated liquid crystals. *Biochim Biophys Acta* 135: 624 - 638

[Papahadjopoulos and Watkins, 1967] Papahadjopoulos, D.; Watkins, J.C. (1967). Phospholipid model membranes II. Permeability properties of hydrated liquid crystals. *Biochim Biophys Acta* 135: 639 – 652

[Paradies et al, 2011] Paradies, G.; Petrosillo, G.; Paradies, V.; Ruggiero, F.M. (2011). Mitochondrial dysfunction in brain aging: role of oxidative stress and cardiolipin. *Neurochem Int* 58: 447-457

[Peng et al, 2003] Peng, G.; Fritzsch, G.; Zickermann, V.; Schägger, H.; Mentele, R. Lottspeich, F.; Bostina, M.; Radermacher,M.; Huber, R.; Stetter, K.O.; Michel, H. (2003). Isolation, characterization and electron microscopic single particle analysis of the NADH:ubiquinone oxidoreductase (complex I) from the hyperthermophilic eubacterium *Aquifex aeolicus. Biochemistry* 42: 3032 – 3039

[Perales-Clemente et al, 2010] Perales-Clemente, E.; Fernandez-Vizarra, E.; Acin-Perez, R.; Movilla, N.; Bayona-Bafaluy, M. P.; Moreno-Loshuertos, R.; Perez-Martos, A.; Fernandez-Silva, P.; Enriquez, J. A. (2010) Five entry points of the mitochondrially encoded subunits in mammalian complex I assembly. *Mol Cell Biol* 30: 3038 - 3047

[Peterson, 1977] Peterson, G.L. (1977). A simplification of the reaction of the protein assay method of Lowry *et al.* which is more generally applicable. *Anal Biochem* 83: 346 - 356

[Peterson, 1979] Peterson, G.L. (1979). Review of the Folin phenol protein quantitation method of Lowry, Rosebrough, Farr and Randall. *Anal Biochem* 100: 201 - 220

[Pfeiffer et al, 2003] Pfeiffer, K.; Gohil, V.; Stuart, R.A.; Hunte, C.; Brandt, U.; Greenberg, M.L.; Schägger, H. (2003). Cardiolipin stabilizes respiratory chain supercomplexes. *J Biol Chem* 278: 52873-52880

[Pineau et al, 2005] Pineau, B.; Mathieu, C.; Gerard-Hirne, C.; De Paepe, R.; Chetrit, P. (2005). Targeting the NAD7 subunit to mitochondria restores a functional complex I and a wild type phenotype in the Nicotiana sylvestris CMS II mutant lacking nad7. *J Biol Chem* 280: 25994-26001

[Prunetti et al, 2010] Prunetti, L.; Infossi, P.; Brugna, M.; Ebel, C.; Giudici-Orticoni, M.T.; Guiral, M. (2010). New functional sulfide oxidase-oxygen reductase supercomplex in the membrane of the hyperthermophilic bacterium *Aquifex aeolicus. J Biol Chem* 285: 41815-41826

[Rabilloud, 2009] Rabilloud, T. (2009). Detergents and chaotropes for protein solubilization before two-dimensional electrophoresis. *Methods Mol Biol* 528: 259-267

[Racker et al, 1979] Racker, E.; Violand, B.; O'Neal, S.; Alfonzo, M.; Telford, J. (1979) Reconstitution, a way of biochemical research; some new approaches to membrane-bound enzymes. *Arch Biochem Biophys* 198: 470 - 477

[Ragan and Heron, 1978] Ragan CI, Heron C (1978). The interaction betweenmitochondrialNADH-ubiquinone oxidoreductase and ubiquinol-cytochrome c oxidoreductase—evidence for stoicheiometric association. *Biochem. J.* 174: 783–790

[Raha and Robinson, 2000] Raha, S.; Robinson, B.H. (2000). Mitochondria, oxygen free radicals, disease and ageing. *Trends Biochem Sci* 25: 502 - 508

[Rasmussen et al, 2001] Rasmussen, T.; Scheide, D.; Brors, B.; Kintscher, L.; Weiss, H.; Friedrich, T. (2001) Identification of two tetranuclear FeS clusters on the ferredoxin-type subunit of NADH:ubiquinone oxidoreductase (complex I). *Biochemistry* 40: 6124 – 6131

[Ray et al, 2012] Ray, P.D.; Huang, B.W.; Tsuji, Y. (2012). Reactive oxygen species (ROS) homeostasis and redox regulation in cellular signaling. *Cell Signal* 24: 981–990

[Refojo et al, 2010a] Refojo, P.N.; Sousa, F.L.; Teixeira, M.; Pereira, M.M. (2010). The alternative complex III: A different architecture using known building modules. *Biochim Biophys Acta*: 1797: 1869-1876

[Refojo et al, 2010b] Refojo, P.N.; Teixeira, M.; Pereira, M.M. (2010). The alternative complex III of *Rhodothermus marinus* and its structural and functional association with caa3 oxygen reductase. *Biochim Biophys Acta* 1797: 1477-1482

[Rich, 1984] Rich PR (1984). Electron and proton transfer through quinones and cytochrome bc complexes. *Biochim Biophys Acta* 768: 53-79

[Richardson 2000] Richardson, D.J. (2000). Bacterial respiration a flexible process for a changing environment. *Microbiology* 146: 551-571

[Rigaud and Levy, 2003] Rigaud, J.L.; Levy, D. (2003). Reconstitution of membrane proteins into liposomes. *Methods Enzymol* 372: 65 - 86

[Rigaud et al, 1995] Rigaud, J. L.; Pitard, B.; Levy, D. (1995). Reconstitution of membrane proteins into liposomes: application to energy-transducing membrane proteins. *Biochim Biophys Acta* 1231: 223 – 246

[Rosca and Hoppel, 2009] Rosca, M.G.; Hoppel, C.L. (2009). New aspects of impaired mitochondrial function in heart failure. *J Bioenerg Biomembr* 41: 107-712

[Rosca and Hoppel, 2010] Rosca, M.G.; Hoppel, C.L. (2010). Mitochondria in heart failure. *Cardiovasc Res* 88: 40-50

[Rosca et al, 2008] Rosca, M.G.; Vazquez, E.J.; Kerner, J.; Parland, W.; Chandler, M.P.; Stanley, W.; Sbbah, H.N.; Hoppel, C.L. (2008). Cardiac mitochondria in heart failure: decrease in respirasomes and oxidative phosphorylation. *Cardiovasc Res* 80: 30-39

[Rose, 1853] Rose, F. (1853). Über die Verbindungen des Eiweiss mit Metalloxygen. *Poggendorf Annalen der Physik und Chemie* 104: 132 - 142

[Saada et al, 2009] Saada, A.; Vogel, R.O.; Hoefs, S.J.; van den Brand, M.A.; Wessels, H.J.; Willems, P.H.; Venselaar, H.; Shaag, A.; Barghuti, F.; Reish, O.; Shohat, M.; Huynen, M.A.; Smeitink, J.A.; van den Heuvel, L.P.; Nijtmans, L.G. (2009) Mutations in NDUFAF3 (C3ORF60), encoding an NDUFAF4 (C6ORF66)-interacting complex I assembly protein, cause fatal neonatal mitochondrial disease, *Am J Hum Genet* 84: 718 - 727.

[Sabar et al, 2005] Sabar, M.; Balk, J.; Leaver, C.J. (2005). Histochemical staining and quantification of plant mitochondrial respiratory chain complexes using blue-native polyacrylamide gel electrophoresis. *Plant J* 44: 893-901

[Santiago et al 1973] Santiago, E.; López-Moratalla, N.; Segovia, J.F. (1973). Correlation between losses of mitochondrial ATPase activity and cardiolipin degradation. *Biochem Biophys Res Commun* 53: 439-445

[Saunders et al, 1962] Saunders, L.; Perrin, J.; Gammack, D. (1962). Ultrasonic irradiation of some phospholipid sols. *J Pharm Pharmacol* 14: 567 - 572

[Sazanov, 2007] Sazanov, L. A. (2007). Respiratory complex I: mechanistic and structural insights provided by the crystal structure of the hydrophilic domain. *Biochemistry* 46: 2275 – 2288

[Sazanov and Hinchliffe, 2006] Sazanov, L. A. & Hinchliffe, P. (2006). Structure of the hydrophilic domain of respiratory complex I from Thermus thermophilus. Science 311, 1430-1436.

[Schäfer et al, 2006] Schäfer, E.; Seelert, H.; Reifschneider, N.H.; Krause, F.; Dencher, N.A.; Vonck, J. (2006) Architecture of active mammalian respiratory chain supercomplexes. *J Biol Chem* 281:15370 –15375

[Schäfer et al, 2007] Schäfer, E.; Dencher, N.A.; Vonck, J.; Parcej, D.N. (2007) Three-dimensional structure of the respiratory chain supercomplex $I_1III_2IV_1$ from bovine heart mitochondria. *Biochemistry* 44:12579–12585

[Schägger, 1995] Schägger H (1995). Quantification of oxidative phosphorylation enzymes after blue native electrophoresis and two-dimensional resolution: normal complex I protein amounts in Parkinson's disease conflict with reduced catalytic activities. *Electrophoresis* 16: 763-770

[Schägger, 2001] Schägger H (2001). Blue-native gels to isolate protein complexes from mitochondria. *Methods Cell Biol* 65: 231 – 244

[Schägger and von Jagow, 1991] Schägger H, von Jagow G (1991). Blue native electrophoresis for isolation of membrane protein complexes in enzymatically active form. *Anal Biochem* 199: 223-231

[Schägger and Ohm, 1995] Schägger H, Ohm TG (1995). Human diseases with defects in oxidative phosphorylation. 2. F_1F_0 ATP-synthase defects in Alzheimer disease revealed by blue native polyacrylamide gel electrophoresis. *Eur J Biochem* 227: 916-921

[Schägger and Pfeiffer, 2000] Schägger H, Pfeiffer K (2000). Supercomplexes in the respiratory chains of yeast and mammalian mitochondria. *EMBO J* 19: 1777 – 1783

[Schägger and Pfeiffer, 2001] Schägger H, Pfeiffer K (2001). The ratio of oxidative phosphorylation complexes I-V in bovine heart mitochondria and the composition of respiratory chain supercomplexes. *J Biol Chem* 276: 37861 - 37867

[Schägger *et al*, 1994] Schägger H, Cramer WA, von Jagow G (1994). Analysis of molecular masses and oligomeric states of protein complexes by blue native electrophoresis and isolation of membrane protein complexes by two-dimensional native electrophoresis. *Anal Biochem* 217: 223-231

[Schägger *et al*, 2004] Schägger,H.; de Coo, R.; Bauer, M.F.; Hofmann, S.; Godinot, C.; Brandt, U. (2004). Significance of respirasomes for the assembly/stability of human respiratory chain complex I. *J Biol Chem* 279: 36349-36353

[Schalame and Ren, 2006] Schalame, M.; Ren, M. (2006). Barth syndrome, a human disorder of cardiolipin metabolism, *FEBS Lett* 580: 5450-5455

[Schapira, 1998] Schapira, A.H. (1998). Human complex I defects in neurodegenerative diseases. *Biochim Biophys Acta* 1364: 261 – 270

[Schilling et al, 2005] Schilling, B.; Aggeler, R.; Schulenberg, B.; Murray, J.; Row, R. H.; Capaldi, R. A.; Gibson, B. W. (2005) Mass spectrometric identification of a novel phosphorylation site in subunit NDUFA10 of bovine mitochondrial complex I. *FEBS Lett* 579: 2485 - 2490

[Schwerzmann *et al*, 1986] Schwerzmann, K.; Cruz-Orive, L.M.; Eggman, R.; Sänger, A.; Weibel, E.R. (1986). Molecular architecture of the inner membrane of mitochondria from rat liver: a combined biochemical and sterological study. *J Cell Biol* 102: 97-103

[Seelert et al, 2009] Seelert, H.; Dani, D.N.; Dante, S.; Hauss, T.; Krause, F.; Schäfer, E.; Frenzel, M.; Poetsch, A.; Rexroth, S.; Schwassmann, H.J.; Suhai, T.; Vonck, J.; Dencher, N.A. (2009). From protons to OXPHOS supercomplexes and Alzheimer's disease: structure-

dynamics-function relationships of energy-transducing membranes. *Biochim Biophys Acta* 1787: 657-671

[Sekiguchi et al, 2009] Sekiguchi, K.; Murai, M.; Miyoshi, H. (2009). Exploring the binding site of acetogenin in the ND1 subunit of bovine mitochondrial complex I. *Biochim Biophys Acta 1787*: 1106 – 1111

[Shi and Jackowski, 1998] Shi, Q.; Jackowski, G. (1998). One-dimensional polyacrylamide gel electrophoresis. From: *Gel Electrophoresis of proteins. A practical approach.* 3rd ed. pp 1 - 50. Edited by: Hames, B.D. Oxford University Press. New York, NY (USA)

[Shinzawa-Itho et al 2007] Shinzawa-Itho, K.; Aoyama, H.; Muramoto, K.; Terada, H.; Kurauchi, T.; Tadehara, Y.; Yamasaki, A.; Sugimura, T.; Kurono, S.; Tsujimoto, K.; Mizushima, T.; Yamashita, E.; Tsukihara, T.; Yoshikawa, S. (2007). Structures and physiological roles of 13 integral lipids of bovine heart cytochrome *c* oxidase. *EMBO J* 26: 1713-1725

[Sled et al, 1994] Sled, V. D.; Rudnitzky, N. I.; Hatefi, Y.; Ohnishi, T. (1994) Thermodynamic analysis of flavinin mitochondrial NADH:ubiquinone oxidoreductase (complex I). *Biochemistry* 33: 10069 – 10075

[Smith, 1967] Smith, A.L. (1967). Preparation, properties, and conditions for assay of mitochondria: Slaughterhouse material, small-scale. *Methods Enzymol* 10: 81 - 86

[Solmaz and Hunte, 2008] Solmaz, S.R.; Hunte, C. (2008) Structure of complex III with bound cytochrome c in reduced state and definition of a minimal core interface for electron transfer. *J Biol Chem* 283: 17542-17549

[Sone *et al*, 1987] Sone N, Sekimachi M, Kutoh E (1987). Identification and propertiies of a quinol oxidase super-complex composed of a bc_1 complex and cytochrome oxidase in the thermophilic bacterium PS3. *J Biol Chem* 262: 15386-15391

[Souza et al, 2012] Sousa, P.M.F.; Videira, M.A.M.; Bohn, A.; Hood, B.L.; Conrads, T.P.; Goulao, L.F.: Melo, A.M.P. (2012). The aerobic respiratory chain of *Escherichia coli*: from genes to supercomplexes. *Microbiology* 158: 2408-2418

[Souza et al, 2013a] Sousa, P.M.F. ; Videira, M.A.M.; Santos, F.A.; Hood, B.L.; Conrads, T.P.; Melo, A.M.P. (2013). The $bc:caa_3$ supercomplexes from the Gran positive bacterium *Bacillus subtilis* respiratory chain: a megacomplex organization?. *Arch Biochem Biophys* 537: 153-160

[Souza et al, 2013b] Sousa, P.M.F.; Videira, M.A.M.; Melo, A.M.P. (2013). The formate:oxygen oxidoreductase supercomplex of *Escherichia coli* aerobic respiratory chain. FEBS *Lett* 587: 2559-2564

[Strecker et al 2010] Strecker, V.; Wumaier, Z.; Wittig, I.; Schägger, H. (2010). Large pore gels to separate mega protein complexes larger than 10 MDa by blue native electrophoresis: Isolation of putative respiratory strings or patches. *Proteomics* 10: 3379-3387

[Strogolova et al, 2012] Strogolova, V.; Furness, A.; Robb-McGrath, M.; Garlich, J.; Stuart, R.A (2012). Rcf1 and Rcf2, members of the hypoxia-induced gene 1 protein family, are critical components of the mitochondrial cytochrome bc_1-cytochrome *c* oxidase supercomplex. *Mol Cell Biol* 32: 1363–1373

[Stroh et al, 2004] Stroh, A.; Anderkas, O.; Pfeiffer, K.; Yagi, T.; Finel, M.; Ludwing, B.;Schägger, H. (2004). Assembly of respiratory complexes I, III, and IV into NADH oxidase supercomplex stabilizes complex I in Paracoccus dinitrificans. *J Biol Chem* 279: 5000-5007

[Sugiana et al, 2008] Sugiana, C.; D.J. Pagliarini, D.J.; McKenzie, M.; Kirby, D.M.; Salemi, R.; Abu-Amero, K.K.; Dahl, H.H.; Hutchison, W.M.; Vascotto, K.A.; Smith, S.M.; Newbold, R.F.; Christodoulou, J.; Calvo, S.; Mootha, V. K.; Ryan, M.T.; Thorburn, D. R. (2008). Mutation of C20orf7 disrupts complex I assembly and causes lethal neonatal mitochondrial disease. *Am J Hum Genet* 83: 468 - 478

[Sunderhaus et al, 2010] Sunderhaus, S.; Klodmann, J.; Lenz, C.; Braun, H.P. (2010). Supramolecular structure of the OXPHOS system in highly thermogenic tissue of *Arum maculatum. Plant Physiol Biochem* 48: 265-272

[Suthammarak et al, 2009] Suthammarak, W.; Yang, Y.Y.; Morgan, P.G.; Sedensky, M.M. (2009). Complex I function is defective in complex IV-deficient *Caenorhabditis elegans. J Biol Chem* 284: 6425 – 6435

[Suthammarak et al, 2010] Suthammarak, W.; Morgan, P.G.; Sedensky, M.M. (2010). Mutations in mitochondrial complex III uniquely affect complex I in *Caenorhabditis elegans. J Biol Chem* 285: 40724 – 40731

[Swartz et al, 2005] Swartz, T.H.; Ikewada, S.; Ishikawa, O.; Ito, M.; Krulwich, T. A. (2005) The Mrp system: a giant among monovalent cation/proton antiporters? *Extremophiles* 9: 345 - 354

[Takeshige and Minakami, 1979]. Takeshige, K., Minakami, S. (1979). NADH and NADPH-dependent formation of superoxide anions by bovine heart submitochondrial particles and NADH-ubiquinone reductase preparation. *Biochem J* 180:129–135

[Taylor et al, 2005] Taylor, N.L.; Heazlewood, J.L.; Day, D.A.; Millar, A.H. (2005). Differential impact of environmental stress on the pea mitochondrial proteome. *Mol Cell Proteomics* 4: 1122-1133

[Tian et al, 2005] Tian, F.; Too, O. B.; Pavlov, A. A.; De Sterck, H. (2005) A hydrogen-rich early earth atmosphere. *Science* 308: 1014 - 1017

[Tisdale, 1967] Tisdale HD (1967). Preparation and properties of succinic-cytochrome *c* reductase (complex II-III). *Methods Enzymol* 10: 213-216

[Towin et al, 1979] Towin, H.; Staehelin, T.; Gordon, J. (1979). Electrophoretic transfer of proteins from polyacrylamide gels to nitrocellulose sheets: procedure and some applications. *Proc Natl Acad Sci USA* 76: 4350 - 4354

[Tran-Betcke et al, 1990] Tran-Betcke, A.; Warnecke, U.; Böcker, C.; Zaborosch, C.; Friedrich, B. (1990). Cloning and nucleotide sequences of the genes for the subunits of NAD-reducing hydrogenase of *Alcaligenes eutrophus* H16. *J Bacteriol* 172: 2920 – 2929

[Treberg et al, 2011] Treberg,J.R.; Quinlan, C.L.; Brand, M.D. (2011). Evidence for two sites of superoxide production by mitochondrial NADH-ubiquinone oxidoreductase (complex I). J Biol Chem 286: 27103 - 27110

[Turrens, 1997] Turrens, J. F. (1997). Superoxide production by the mitochondrial respiratory chain. *Biosci Rep* 17: 3 - 8

[Turrens, 2003] Turrens, J. F. (2003). Mitochondrial formation of reactive oxygen species. *J Physiol* 552: 355 – 344

[Turrens and Boveris, 1980] Turrens, J.F.; Boveris, A. (1980). Generation of superoxide anion by the NADH dehydrogenase of bovine heart mitochondria. *Biochem J* 191: 421 - 427

[Ugalde et al, 2004a] Ugalde, C.; Janssen, R.J.; van den Heuvel, L.P.; Smeitink, J.A.; Nijtmans, L.G. (2004). Differences in the assembly and stability of complex I and other OXPHOS complexes in inherited complex I deficiency. *Hum Mol Genet* 13: 659 – 667

[Ugalde et al, 2004b] Ugalde, C.; Vogel, R.; Huijbens, R.; Van den Heuvel, B.; Smeitink, J.; Nijtmans, L. (2004) Human mitochondrial complex I assembles through the combination of evolutionary conserved modules: a framework to interpret complex I deficiencies. *Hum Mol Genet* 13: 2461 – 2472

[Updyke and Engelhorn, 2004] Updyke, T.V.; Engelhorn, S.C. (2004). System for pH-neutral stable electrophoresis gel. U.S. patent 6,783,651. August 31, 2004

[Vanderkooi, 1978] Vanderkooi G(1978). Organization of protein and lipid components in membranes, in: Fleisher, S.; Hatefi, Y.; MacLennan, D.; Tzagoloff, A. (Eds.) Molecular Biology of Membranes. *Plenum Publishing Corp.* New York, NY, pp 25-55

[Van Lis et al, 2003] Van Lis, R.; Atteia, A.; Mendoza-Hernandez, G; Gonzalez-Halpen, D. (2003). Identification of novel mitochondrial protein components of *Chlamydomonas reinhardtii*. A proteomic approach. *Plant Physiol* 132: 318-330

[Vavricka et al, 2009] Vavricka, S.R.; Burri, E.; Beglinger, C.; Degen, L.; Manz, M. (2009). Serum protein electrophoresis: an underused but very useful test. *Digestion* 79: 203 - 210

[Vempati et al, 2009] Vempati, U.D.; Han, X.; Moraes, C.T. (2009). Lack of cytochrome c in mouse fibroblasts disrupts assembly / stability of respiratory complexes I and IV. *J Biol Chem* 284: 4383 – 4391

[Ventura et al, 2002] Ventura, B.; Genova, M. L.; Bovina, C.; Formiggini, G.; Lenaz, G. (2002). Control of oxidative phosphorylation by Complex I in rat liver mitochondria: implications for aging. *Biochim Biophys Acta* 1563: 249 - 260

[Verkhovskaya et al, 2008] Verkhovskaya, M. L.; Belevich, N.; Euro, L.; Wikström, M.; Verkhovsky, M. I. (2008). Real-time electron transfer in respiratory complex I. *Proc Natl Acad Sci USA* 105: 3763 - 3767

[Vignais et al, 2001] Vignais, P. M.; Billoud, B.; Meyer, J. (2001). Classification and phylogeny of hydrogenases. *FEMS Microbiol Rev* 25: 455 - 501

[Vinogradov et al, 1995] Vinogradov, A.D.; Sled, V.D.; Burbaev, D.S.; Grivennikova, V.G.; Moroz, I.A.; Ohnishi, T. (1995). Energy-dependent Complex I-associated ubisemiquinones in submitochondrial particles. *FEBS Lett* 370: 83 – 87

[Vogel et al, 2007] Vogel, R. O.; Dieteren, C. E.; van den Heuvel, L. P.; Willems, P. H.; Smeitink, J. A.; Koopman, W. J.; Nijtmans, L. G. (2007). Identification of mitochondrial complex I assembly intermediates by tracing tagged NDUFS3 demonstrates the entry point of mitochondrial subunits. *J Biol Chem* 282: 7582 – 7590

[Vonck and Schäfer, 2009] Vonck J, Schäfer E (2009) Supramolecular organization of protein complexes in the mitochondrial inner membrane. *Biochim Biophys Acta Mol Cell Res* 1793:117–124

[Vukotic et al, 2012] Vukotic, M.; Oeljeklaus, S.; Wiese, S.; Vögtle, F.N.; Meisinger, C.; Meyer, H.E.; Zieseniss, A.; Katschinski, D.M.; Jans, D.C.; Jakobs, S.; Warscheid, B.; Rehling, P.; Deckers, M. (2012). Rcf1 mediates cytochrome oxidase assembly and respirasome formation, revealing heterogeneity of the enzyme complex. *Cell Metab* 15: 336–347

[Walker, 1992] Walker, J.E. (1992). The NADH – ubiquinone oxidoreductase (complex I) of respiratory chains. *Q Rev Biophys* 25: 253 – 324

[Wallace, 2005] Wallace, D.C. (2005). A mitochondrial paradigm of metabolic and degenerative diseases, aging, and cancer: a dawn for evolutionary medicine. *Annu Rev Genet* 39: 359 – 407

[Warburg and Christian, 1942] Warburg, O.; Christian, W. (1942). Isoloerung und kristallisation des Garungsferments Enolase. *Biochem Z* 310: 384 -421

[Wheeler et al, 2004] Wheeler, D.; Chrambach, A.; Ashburn, P.; Jovin T.M. (2004). Discontinuous buffer systems operative at pH 2.5 - 11.0, 0 degrees C and 25 degrees C, available on the Internet. *Electrophoresis* 7-8: 973-974

[Wenz et al 2009] Wenz, T.; Hielscher, R.; Hellwig, P.; Schägger, H.; Richers, S.; Hunte, C. (2009). Role of phospholipids in respiratory cytochrome bc1 complex catalysis and supercomplex formation. *Biochim Biophys Acta* 1787: 609-616

[Wessels et al, 2009] Wessels, H. J.; Vogel, R. O; van den Heuvel, L.; Smeitink, J. A.; Rodenburg, R. J.; Nijtmans, L. G.; Farhoud, M. H.(2009). LC-MS/MS as an alternative for SDS-PAGE in blue native analysis of protein complexes. *Proteomics* 9: 4221 - 4228

[Wittig et al, 2006a] Wittig, I.; Carrozo, R.; Santorelli, F.; Schägger, H. (2006). Supercomplexes and subcomplexes of mitochondrial oxidative phosphorylation. *Biochim Biophys Acta* 1757: 1066-1072

[Wittig et al, 2006b] Wittig, I.; Braun, H.P.; Schägger, H. (2006). Blue native PAGE. *Nat Protocol* 1: 418 - 428

[Yagi and Matsuno-Yagi, 2003] Yagi, T.; Matsuno-Yagi, A. (2003). The proton-translocating NADH-Quinone oxidoreductase in the respiratory chain: the secret unlocked. *Biochemistry* 42: 2266 – 2274

[Yagi et al, 1998] Yagi, T.; Yano, T.; Di Bernardo, S.; Matsuno-Yagi, A. (1998). Procaryotic complex I (NDH-1), an overview. Biochim Biophys Acta 1364: 125 – 133

[Yano, 2002] Yano, T. (2002) The energy-transducing NADH: quinone oxidoreductase, complex I, *Mol Aspects Med* 23: 345 - 368

[Yano et al, 1996] Yano, T.; Sled, V.D.; Ohnishi, T.; Yagi, T. (1996). Expression and characterization of the flavoprotein subcomplex composed of 50-kDa (NQO1) and 25-kDa (NQO2) subunits of the proton-translocating NADH-quinone oxidoreductase of *Paracoccus denitrificans*. *J Biol Chem* 271: 5907 – 5913

[Yano et al, 2003] Yano, T.; Sklar, J.; Nakamaru-Ogiso, E.; Yagi, T.; Ohnishi,T. (2003). Characterization of cluster N5 as a fast-relaxing [4Fe-4S] cluster in the Nqo3 subunit of the proton-translocating NADH-ubiquinone oxidoreductase from *Paracoccus denitrificans*. *J Biol Chem* 278: 15514 – 15522

[Yano et al, 2005] Yano, T.; Dunham, W.R.; Ohnishi, T. (2005). Characterization of the delta muH+-sensitive ubisemiquinone species (SQ(Nf)) and the interaction with cluster N2: new insight into the energy-coupled electron transfer in complex I. *Biochemistry* 44:1744 -1754

[Yip et al, 2011] Yip, C.Y.; Harbour, M.E.; Jayawardena, K.; Fearnley, I.M.; Sazanov, L.A. (2011) Evolution of respiratory complex I: "supernumerary" subunits are present in the alpha-proteobacterial enzyme. *J Biol Chem* 286: 5023 - 5033

[Zhong et al, 2004] Zhong, Q.; Gohil, V.M.; Ma, L.; Greenberg, M.L. (2004). Absence of cardiolipin results in temperature sensitivity, respiratory defects, and mitochondrial DNA instability independent of pet56. *J Biol Chem* 279: 32294-32300

[Ziegler and Doeg, 1961] Ziegler DM, Doeg KA (1961). The isolation and properties of a soluble succinic coenzyme Q reductase from beef heart mitochondria. *Biochim Biophys Res Commun* 1: 344-349